

The $SL(2, \mathbb{Z})$ dualization algorithm at work

Riccardo Comi,^{a,b} Chiung Hwang,^{c,d,e,f} Fabio Marino,^{a,b,g} Sara Pasquetti,^{a,b} Matteo Sacchi^h

^a*Dipartimento di Fisica, Università di Milano-Bicocca, Piazza della Scienza 3, I-20126 Milano, Italy*

^b*INFN, sezione di Milano-Bicocca, Piazza della Scienza 3, I-20126 Milano, Italy*

^c*Interdisciplinary Center for Theoretical Study, University of Science and Technology of China, Hefei, Anhui 230026, China*

^d*Peng Huanwu Center for Fundamental Theory, Hefei, Anhui 230026, China*

^e*Center for Theoretical Physics of the Universe, Institute for Basic Science (IBS), Daejeon 34126, Korea*

^f*Department of Applied Mathematics and Theoretical Physics, University of Cambridge, Cambridge CB3 0WA, United Kingdom*

^g*Department of Mathematics, University of Surrey, Guildford, GU2 7XH, UK*

^h*Mathematical Institute, University of Oxford, Woodstock Road, Oxford, OX2 6GG, United Kingdom*

E-mail: r.comi2@campus.unimib.it, chiung@ustc.edu.cn,
f.marino25@campus.unimib.it, sara.pasquetti@gmail.com,
matteo.sacchi@maths.ox.ac.uk

ABSTRACT: Recently an algorithm to dualize a theory into its mirror dual has been proposed, both for $3d \mathcal{N} = 4$ linear quivers and for their $4d \mathcal{N} = 1$ uplift. This mimics the manipulations done at the level of the Type IIB brane setup that engineers the $3d$ theories, where mirror symmetry is realized as S -duality, but it is entirely field-theoretic and based on the application of genuine infra-red dualities that implement the local action of S -duality on the quiver. In this paper, we generalize the algorithm to the full duality group, which is $SL(2, \mathbb{Z})$ in $3d$ and $PSL(2, \mathbb{Z})$ in $4d$. This also produces dualities for $3d \mathcal{N} = 3$ theories with Chern–Simons couplings, some of which have enhanced $\mathcal{N} = 4$ supersymmetry, and their new $4d \mathcal{N} = 1$ counterpart. In addition, we propose three ways to study the RG flows triggered by possible VEVs appearing at the last step of the algorithm, one of which uses a new duality that implements the Hanany–Witten move in field theory.

Contents

1	Introduction	2
2	$PSL(2, \mathbb{Z})$ walls, QFT blocks and duality moves	6
2.1	$PSL(2, \mathbb{Z})$ operators	6
2.2	QFT building blocks	17
2.3	Basic duality moves	21
2.3.1	S-dualization	21
2.3.2	T-dualization	24
2.3.3	\mathbb{T}^T -dualization	28
3	Dualization algorithm, VEVs, RG flows and HW moves	30
3.1	S-dualization of SQCD	31
3.2	Method I: VEV propagation via sequential Higgsing	34
3.3	Method II: VEV propagation via the IP duality	38
3.4	Method III: VEV propagation via the HW duality move	42
4	Algorithm in $3d$	45
4.1	$SL(2, \mathbb{Z})$ operators	45
4.2	QFT building blocks	49
4.3	Basic duality moves	52
4.3.1	\mathcal{S} -dualization	52
4.3.2	\mathcal{T} -dualization	55
4.3.3	\mathcal{T}^T -dualization	56
4.4	The Hanany–Witten duality move	59
5	Duality webs	61
5.1	$4d$ $PSL(2, \mathbb{Z})$ duality web	62
5.2	$4d$ operators map	69
5.3	$3d$ $SL(2, \mathbb{Z})$ duality web	75
5.4	$3d$ operators map	79
A	The $FE[USp(2N)]$ theory, the S-wall	83
B	Asymmetric S-walls	85
C	Derivations of basic duality moves	93
D	Proof of the Hanany–Witten duality move	97
E	Limits of the $FE[USp(2N)]$ theory for $c = 1$ and $c = t^{\frac{1}{2}}$	101

1 Introduction

Infra-red (IR) dualities among supersymmetric gauge theories are interesting phenomena that have been extensively studied over the years. These correspond to the situation in which distinct microscopic theories flow to the same fixed point in the IR. The first example due to Seiberg [1] concerns four-dimensional SQCDs with minimal supersymmetry relating those with different gauge groups. After the discovery of the Seiberg duality, many others have been found not only in four dimensions but also in other dimensions. For instance in $3d$ we have analogues of the Seiberg duality (so-called *Seiberg-like dualities*) as well as *mirror symmetry* [2], which is another class of three-dimensional dualities looking completely different from the former. The $3d$ mirror symmetry can be neatly understood in terms of type IIB brane set-ups [3] as the action of S -duality, which makes it possible to extend it to a larger class of dualities reflecting more general $SL(2, \mathbb{Z})$ transformations.

Given this proliferation of IR dualities, there are various fundamental questions that one can ask purely from the field theory perspective. For example, among other things, one may ask if we can derive all $3d$ and lower dimensional IR dualities from $4d$ dualities.¹ The program of obtaining $3d$ dualities from $4d$ dualities was initiated in [4] in the more general context of studying dualities across dimensions (see for example [5–10] for the derivation of $2d$ dualities from higher dimensions) and it was continued in many subsequent works (see [11–23] for a partial list of references). For a long time, the answer to this question was regarded as negative, especially because of $3d$ mirror symmetry, considered an inherently three-dimensional phenomenon. However, recently, $4d$ avatars of $3d$ mirror dualities have been discovered [24]. These new $4d$ dualities reduce to $3d$ mirror dualities after circle reduction and suitable deformations, strengthening the expectation that indeed the physics of $3d$ dualities can be derived from $4d$.

Another intriguing question is whether there is a fundamental set of dualities in terms of which other dualities can be derived. This second question was addressed in various dimensions by using the notion of *sequential deconfinement* [25–38], which can be used to derive non-trivial dualities for theories with matter fields in tensor representations by only assuming a small set of fundamental dualities. This has a nice counterpart in Mathematics, where various integral identities that can be interpreted as matchings of partition functions of dual theories were derived with a similar strategy [39–42].

Furthermore, interestingly, it has recently been shown in [43] (see also [22]) that mirror dualities, both in $3d$ and in $4d$, can be derived by an algorithmic procedure based on the iteration of a single fundamental duality, the Aharony duality [44] in $3d$ and the Intriligator–Pouliot duality [45] in $4d$, revealing a hidden relation between mirror dualities and Seiberg-like

¹Four dimensions are in some sense the critical number of dimensions for IR dualities because $d > 4$ dimensional gauge theories are free in the IR. Instead, one may consider UV dualities in higher dimensions.

dualities. While the result of [43] only discussed mirror dualities, which as we mentioned are related to the S -duality of Type IIB string theory, in this paper we extend the algorithm to the full set of dualities that are inherited from the entire $SL(2, \mathbb{Z})$ duality group of Type IIB string theory.

These dualities typically involve more general (p, q) 5-branes rather than just NS5- and D5-branes. Consequently, the $3d$ theories that are engineered with these brane systems will have Chern–Simons couplings, which a priori preserve only $\mathcal{N} = 3$ supersymmetry. However with specific matter contents and superpotentials the amount of supersymmetry can be enhanced to $\mathcal{N} = 4$ [46–49] and up to $\mathcal{N} = 8$ [50, 51].² For example, as shown in [60] the more general $SL(2, \mathbb{Z})$ dualities can map Yang–Mills fixed points to Chern–Simons theories coupled to matter. In the former $\mathcal{N} = 4$ supersymmetry is manifest, meaning that this should be enhanced from the apparent $\mathcal{N} = 3$ in the latter.

Our first main result is to uplift these more general dualities for linear quiver theories to $4d$, where we will see that the actual duality group is $PSL(2, \mathbb{Z})$ rather than $SL(2, \mathbb{Z})$ as in the $3d$ case. In this paper, the generators of the $PSL(2, \mathbb{Z})$ in $4d$ will be denoted by \mathbf{S} and \mathbf{T} , while those of the $SL(2, \mathbb{Z})$ in $3d$ will be denoted by \mathcal{S} and \mathcal{T} . These generators satisfy slightly different relations: $\mathbf{S}^2 = I$ and $(\mathbf{ST})^3 = I$ in $PSL(2, \mathbb{Z})$, while $\mathcal{S}^2 = -I$ and $(\mathcal{ST})^3 = I$ in $SL(2, \mathbb{Z})$, which basically distinguish these two groups. The second result is to extend the analysis of [43] showing that also the entire $SL(2, \mathbb{Z})$ (in $3d$) and $PSL(2, \mathbb{Z})$ (in $4d$) actions can be defined in field theory as local operations on the quiver theory. The result will lead to an algorithm to derive systematically all of these dualities from a set of fundamental duality moves, which generalizes the idea of [61] for the abelian mirror symmetry to the non-abelian case and beyond mirror dualities.

Our results build on some recent ones of [24], where a family of $4d$ $\mathcal{N} = 1$ theories labelled by partitions σ and ρ of N , the $E_\rho^\sigma[USp(2N)]$ linear quiver theories sketched in Figure 1, have been introduced. These theories, upon compactification to $3d$ and suitable real mass and Coulomb branch VEV deformations, reduce to the $3d$ $\mathcal{N} = 4$ $T_\rho^\sigma[U(N)]$ linear quiver theories [62], which we also depict in Figure 1. The $E_\rho^\sigma[USp(2N)]$ quiver theories were shown to enjoy, like their $3d$ counterpart, a mirror duality relating pairs of theories with partitions ρ and σ swapped.

The $3d$ $T_\rho^\sigma[U(N)]$ linear quiver can be realized on an Hanany–Witten brane set-up [3] with N D3-branes suspended between K D5-branes and L NS5-branes, where K and L are the lengths of the partitions σ and ρ respectively. The entries of the partitions correspond to the net number of D3-branes ending on the D5 and the NS5-branes, respectively, going from the interior to the exterior of the configuration. On the other hand, no brane construction is known for its $4d$ uplift, the $E_\rho^\sigma[USp(2N)]$ quiver.

The idea of the local dualization approach arises from such brane realization of the $3d$ quiver theories, where the dualities follow from the $SL(2, \mathbb{Z})$ action on the brane set-up. As suggested in [62], such $SL(2, \mathbb{Z})$ actions can be implemented on each 5-brane separately by dualizing that brane only and creating $SL(2, \mathbb{Z})$ duality domain walls on its right and on its

²Such enhancements of supersymmetry can be easily detected using the superconformal index, see for example [52–59].

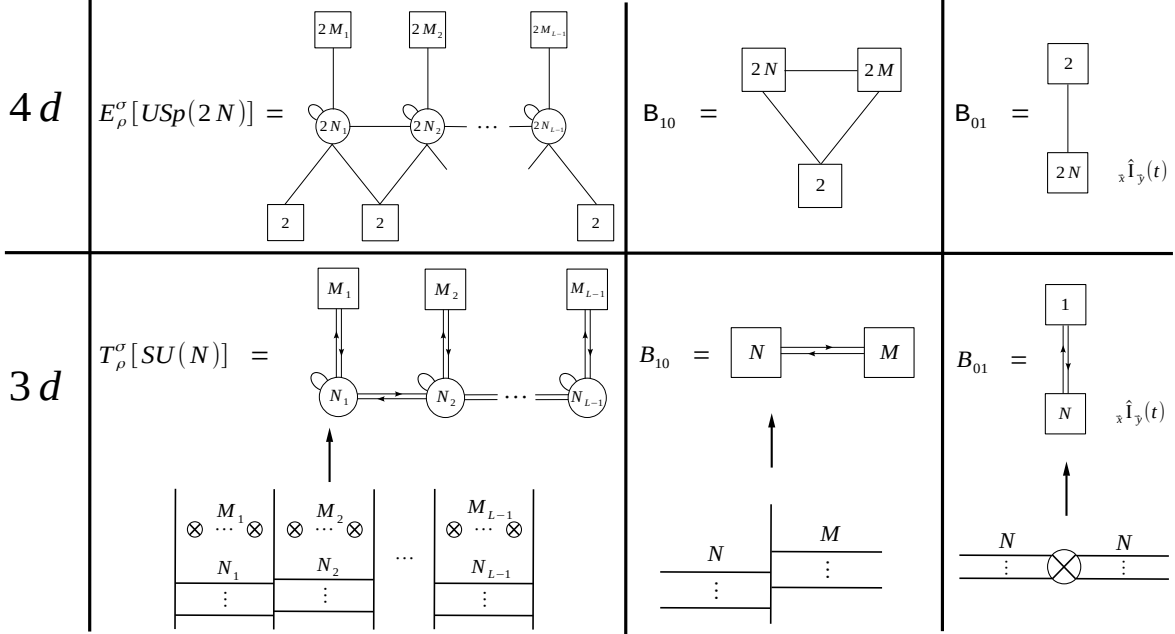


Figure 1. The $E_\rho^\sigma[USp(2N)]$ and the $T_\rho^\sigma[U(N)]$ theories with the brane realization of the latter are given in the first column. The partitions $\rho = [N^{l_N}, \dots, 1^{l_1}]$ and $\sigma = [N^{k_N}, \dots, 1^{k_1}]$ with l_n, k_m satisfying the conditions $\sum_{n=1}^N n \times l_n = \sum_{m=1}^N m \times k_m = N$, $L = l_1 + \dots + l_N$ and $K = k_1 + \dots + k_N$ encode the gauge and flavor ranks as $M_{L-i} = k_i$ and $N_{L-i} = \sum_{j=i+1}^L \rho_j - \sum_{j=i+1}^N (j-i)k_j$. In 3d all nodes are of unitary type, and each line is an $\mathcal{N} = 2$ chiral, with arcs corresponding to adjoint representations and straight lines to bifundamental representations related by the standard $\mathcal{N} = 4$ superpotential. In 4d all nodes are of symplectic type, and each arc is now an antisymmetric chiral, which couples to the bifundamental chirals on its left and right, while the fields in the “saw” are in a cubic superpotential. There are also singlets which we omit in the drawing, see [24] for the details. In the second and third columns the 3d and 4d QFT blocks associated to NS5 and D5-branes are shown.

left. A QFT analogue of such a local action corresponding to $\mathcal{S} \in SL(2, \mathbb{Z})$ was recently formulated in [43], and we will extend this to the full $SL(2, \mathbb{Z})$ duality group in this paper.³

In order to state the algorithm, first of all, we need to define the notion of QFT blocks to be *associated* to each type of 5-brane. As sketched in Figure 1 and discussed in detail in the next section, we can associate QFT blocks $\mathcal{B}_{10}, \mathcal{B}_{01}, \mathcal{B}_{11}$ to NS5 (or (1,0)), D5 (or (0,1)) and (1,1)-branes, where the first two were already discussed in [43] while the last one is newly discussed in this paper. We stress the fact that in 4d there is no brane realization, so our 4d QFT blocks are defined as the *uplift* of the 3d QFT blocks $\mathcal{B}_{10}, \mathcal{B}_{01}, \mathcal{B}_{11}$, in the sense that the former reduces to the latter in the suitable 3d limit that we previously mentioned. Notice that the low energy theories of brane set-ups containing (1, k)-branes with $k > 1$ are captured by 3d theories with Chern–Simons couplings, whose 4d uplift will be introduced by generalizing the results of [24].⁴

³See [63, 64] for previous work at the level of the three-sphere partition function.

⁴As pointed out already in [64], the field theory associated to a brane set-up containing more general

We then define the QFT realization of the duality walls. In $3d$ each $SL(2, \mathbb{Z})$ element, corresponding to a duality wall for the $4d$ $\mathcal{N} = 4$ SYM, is associated to a certain $3d$ $\mathcal{N} = 4$ quiver theory. For example, the \mathcal{S} generator of $SL(2, \mathbb{Z})$ is associated with the $T[SU(N)]$ theory of Gaiotto and Witten [62], which is the case with trivial partitions $\rho = \sigma = [1^N]$ of the $T_\rho^\sigma[SU(N)]$ family. In analogy with the three-dimensional case, we call “walls” also in $4d$ the QFT objects associated to the $PSL(2, \mathbb{Z})$ elements, although we do not have their realization as walls in a $5d$ theory. For example, in [22], the \mathcal{S} generator of $PSL(2, \mathbb{Z})$ was associated to the $FE[USp(2N)]$ quiver theory of [21].⁵ This theory is related to the $E[USp(2N)]$ theory by the addition of some singlet flipping fields. Here we will introduce the QFT objects associated to the T-wall and to the \mathbb{T}^T -wall as well.

Finally, we define the action of the duality walls on the QFT blocks. In [43] two basic duality moves were defined. The first one is associated to the action of the S-wall on a (1,0) block, which turns it into a (0,1) block. The second one is associated to the action of the S-wall on a (0,1) block, which turns it into a (1,0) block. Crucially in [22, 43] it was shown that these basic moves are genuine IR dualities which can be derived by iterative applications of Seiberg-like dualities (Intriligator–Pouliot [45] in $4d$ and Aharony [44] in $3d$). We will complete this list by defining the action of the S-wall and of the T-wall on the (1,0), (0,1) and (1,1) blocks. Importantly, these new duality moves will also be consequences of Seiberg-like dualities.

Having defined the QFT blocks, the $(P)SL(2, \mathbb{Z})$ generators and the basic duality moves, we can implement the dualization algorithm generating the dual theory of any linear quiver theory that is associated to a given $(P)SL(2, \mathbb{Z})$ generator.⁶ The algorithm consists of the following steps:

1. Chop a $4d$ or $3d$ quiver into QFT blocks by ungauging every gauge node.
2. Dualize each QFT block using the basic duality moves corresponding to the chosen $(P)SL(2, \mathbb{Z})$ generator.
3. Glue back the dualized blocks by restoring the original gauge nodes.
4. Follow the RG flow triggered by VEVs that can be generated in the previous step.

We will illustrate these steps in the case of $4d$ SQCD. In particular, we will show that the last step can be implemented in three different ways, one of which consists of another genuine IR duality that is the QFT analogue of the Hanany–Witten move swapping different types of 5-branes [3].

(p, q) -branes with $p > 1$ are non-Lagrangian.

⁵The $FE[USp(2N)]$ theory was first introduced in [21] in the context of the compactifications of the $6d$ $\mathcal{N} = (1, 0)$ rank N E-string theory to $4d$ $\mathcal{N} = 1$ on Riemann surfaces with flux, and it is also related to various theories enjoying non-trivial symmetry enhancements, see for example [65–67]. This origin of the theory suggests that it should be possible to interpret it as a duality domain wall in a $5d$ $\mathcal{N} = 1$ gauge theory similar to those studied in [68–73].

⁶We remark that starting from these dualities for linear quivers one can algorithmically generate more dualities as done for example in [74, 75].

Lastly, we would like to emphasise that, as mentioned above, all the basic moves can be derived by Seiberg-like dualities. Therefore, our algorithm demonstrates that the full $(P)SL(2, \mathbb{Z})$ group of dualities can be derived by Seiberg-like dualities, either Intriligator–Pouliot in $4d$ or Aharony in $3d$.

The rest of the paper is organized as follows. In Section 2 we discuss the basic ingredients needed in the dualization algorithm in $4d$, namely the $PSL(2, \mathbb{Z})$ walls, the QFT blocks and the duality moves. In Section 3 we present an example of application of the dualization algorithm in the case of the SQCD. Here we show three equivalent ways to study the RG flow triggered by the VEVs for some operators that can appear at the last step of the algorithm, which consist respectively in studying explicitly the Higgsing with the index, applying sequentially the Intriligator–Pouliot duality or applying iteratively a new duality move that mimics the Hanany–Witten move in the brane setup. In Section 4 we state the basic ingredient for applying the dualization algorithm in $3d$, which are obtained as a limit of the $4d$ ones. In Section 5 we discuss a web of dualities for the SQCD that is obtained with $PSL(2, \mathbb{Z})$ dualizations in $4d$ and $SL(2, \mathbb{Z})$ dualizations in $3d$. Finally, in various appendices we summarize some definitions and give derivations for some results used in the main text.

In this paper we will consider only *good* theories in the Gaiotto–Witten sense [62], which for the SQCD case implies restricting to $N_f \geq 2N_c$. *Bad* theories, containing operators falling below the unitarity bound, will be studied in [76] using the dualization algorithm. Various properties of bad theories have been already studied in [77–85]. Moreover, it has been observed for example in [86–90] that they can arise from the compactification of higher dimensional theories, which makes their study important in the context of understanding the Higgs branch of theories with eight supercharges.

2 $PSL(2, \mathbb{Z})$ walls, QFT blocks and duality moves

In this section we introduce several ingredients involved in the dualization algorithm: the duality-walls, the QFT blocks, and the basic duality moves.

2.1 $PSL(2, \mathbb{Z})$ operators

We first introduce the field theory objects, the duality-walls, associated to the generators S and T of $PSL(2, \mathbb{Z})$. We will also introduce the Identity-wall and the wall associated to the T^T generator as it produces interesting dualities although it is not an independent element of $PSL(2, \mathbb{Z})$. As we will see in Section 4, the $SL(2, \mathbb{Z})$ group structure in $3d$ can be derived from the $PSL(2, \mathbb{Z})$ structure in $4d$ by taking suitable circle reduction and real mass/Coulomb branch (CB) VEV deformations.

The S-wall. In $3d$, the S generator of $SL(2, \mathbb{Z})$ is associated with the $T[SU(N)]$ theory of Gaiotto and Witten [62]. Indeed, the way this theory was originally constructed is as a duality domain wall between two copies of the $4d$ $\mathcal{N} = 4$ $SU(N)$ SYM theory at values of the coupling τ and $-\frac{1}{\tau}$, respectively. As it was shown in [21], the $T[SU(N)]$ theory can be obtained from a dimensional reduction of the $4d$ $\mathcal{N} = 1$ theory called $E[USp(2N)]$ supplemented by suitable real mass deformations and CB VEVs. Following [22, 43], in $4d$ we identify S with a slight

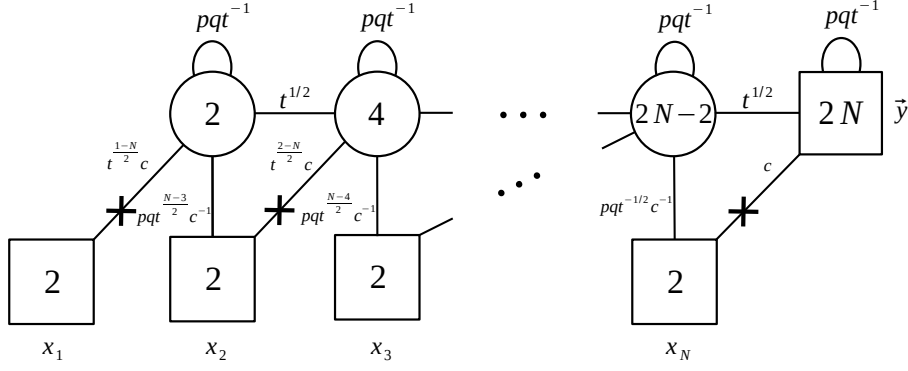


Figure 2. The $FE[USp(2N)]$ quiver theory. In the drawing we are also specifying our conventions for the fugacities for the global symmetries that we will turn on in the index. Specifically, p and q are fugacities for combinations of the trial R-charge and angular momenta, and the power of pq represents a half of the R-charge. Similarly, t and c are the fugacities for the other abelian symmetries, whose powers encode the corresponding charges of the fields.

variant of this theory which includes additional gauge singlet chiral fields, and that is called the $FE[USp(2N)]$ theory shown in Figure 2. We refer the reader for example to [22] for the explicit definition of this theory and to Appendix A for a brief review, while here we only review some of its properties that are relevant for our discussion. The $FE[USp(2N)]$ theory has a $USp(2N)_x \times USp(2N)_y \times U(1)_t \times U(1)_c$ global symmetry in the IR, and we will represent it schematically as in Figure 3, where we are explicitly displaying its two $USp(2N)$ symmetries.

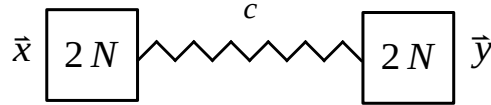


Figure 3. Schematic representation of the 4d S-wall. Here \vec{x} are the $USp(2N)_x$ fugacities, while \vec{y} the $USp(2N)_y$ fugacities. We also specify the fugacity c but not t .

The index of the S-wall theory has the following recursive definition:

$$\begin{aligned}
\mathcal{I}_S^{(N)}(\vec{x}; \vec{y}; t; c) &= \Gamma_e(pqc^{-2}) \Gamma_e(pqt^{-1})^N \prod_{i < j}^N \Gamma_e(pqt^{-1}x_i^{\pm 1}x_j^{\pm 1}) \prod_{i=1}^N \Gamma_e(cy_N^{\pm 1}x_i^{\pm 1}) \\
&\times \oint d\vec{z}_{N-1} \Delta_{N-1}(\vec{z}_{N-1}) \prod_{a=1}^{N-1} \prod_{i=1}^N \Gamma_e(t^{1/2}z_a^{\pm 1}x_i^{\pm 1}) \Gamma_e(pqt^{-1/2}c^{-1}y_N^{\pm 1}z_a^{\pm 1}) \\
&\times \mathcal{I}_S^{(N-1)}(z_1, \dots, z_{N-1}; y_1, \dots, y_{N-1}; t; t^{-1/2}c), \tag{2.1}
\end{aligned}$$

where we defined the contribution of the vector multiplet and the integration measure as

$$\Delta_n(\vec{z}_n) = \frac{[(p; p)_\infty (q; q)_\infty]^n}{\prod_{i=1}^n \Gamma_e(x_i^{\pm 2}) \prod_{i < j}^n \Gamma_e(x_i^{\pm 1} x_j^{\pm 1})}, \quad d\vec{z}_n = \frac{1}{n!} \frac{\prod_{i=1}^n dz_i}{2\pi i z_i}. \quad (2.2)$$

This integral function coincides with the *interpolation kernel* of Rains [91] and it enjoys various remarkable identities, some of which were interpreted as properties of the $FE[USp(2N)]$ theory in [21].

It is also useful to consider, following [22, 43], an asymmetric version of the S-wall, in the sense that it displays two non-abelian symmetries of unequal ranks $USp(2N)$ and $USp(2M)$ with $M < N$. We will represent such an asymmetric S-wall schematically as in Figure 4.

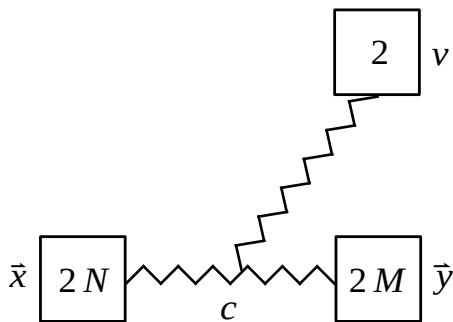


Figure 4. The 4d asymmetric S-wall.

This can be easily obtained from the $FE[USp(2N)]$ theory by turning on a deformation associated with an operator transforming in the antisymmetric representation of one of the two $USp(2N)$ symmetries, with the effect of breaking it down to $USp(2M) \times SU(2)$ for $M < N$. The details of this deformation can be found in [22, 24]. At the level of the index, the pattern of breaking of the global symmetry due to the deformation is encoded in a specific specialization of some of the flavor fugacities

$$\mathcal{I}_S^{(N)}(\vec{x}; \vec{y}, t^{\frac{N-M-1}{2}} v, \dots, t^{-\frac{N-M-1}{2}} v; t; c). \quad (2.3)$$

More details regarding the asymmetric S-wall can be found in Appendix B.

The Identity-wall. One property of the S-wall theory proven in [22] is that concatenating two of them, which in field theory amounts to gauging a diagonal combination of a $USp(2N)$ symmetry from each S-wall, these annihilate each other giving an Identity-wall as shown in the first quiver in Figure 5.

We can make this statement more precise at the level of the index, which, as shown in [22], is given by a distribution

$$\oint d\vec{z}_N \Delta_N(\vec{z}; t) \mathcal{I}_S^{(N)}(\vec{x}; \vec{z}; t; c) \mathcal{I}_S^{(N)}(\vec{z}; \vec{y}; t; c^{-1}) = \hat{x} \hat{y}(t), \quad (2.4)$$

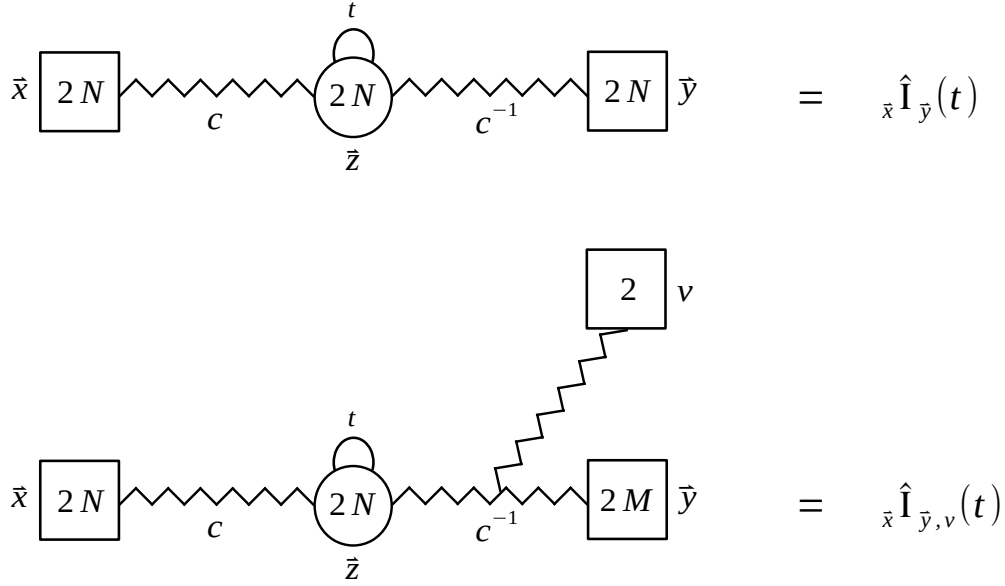


Figure 5. The symmetric and the asymmetric Identity-walls.

with

$$\hat{x}\hat{y}(t) = \frac{\prod_{j=1}^N 2\pi i x_j}{\Delta_N(\vec{x}; t)} \sum_{\sigma \in S_N} \sum_{\pm} \prod_{j=1}^N \delta(x_j - y_{\sigma(j)}^{\pm}). \quad (2.5)$$

The sum over elements of the permutation group S_N and over signs \pm corresponds to a sum over the transformation actions of the Weyl group of $USp(2N)$. In the denominator we have the contribution of the $USp(2N)$ vector multiplet $\Delta_N(\vec{x})$, defined in (2.2), and the antisymmetric chiral multiplet $A_N(\vec{x}; t)$:

$$\Delta_N(\vec{x}; t) = \Delta_N(\vec{x}) A_N(\vec{x}; t), \quad A_N(\vec{x}; t) = \Gamma_e(t)^N \prod_{i < j}^N \Gamma_e(tx_i^{\pm 1} x_j^{\pm 1}). \quad (2.6)$$

Notice that the l.h.s. of the relation of Figure 5 for $N = 1$ coincides, up to flipping fields, with the $SU(2)$ theory with four chirals, which is known to have a quantum deformed moduli space of vacua [92] and an index given by a delta distribution [93].

A similar property holds also for the asymmetric S-wall; namely an ordinary S-wall glued to an asymmetric S-wall results in an asymmetric Identity-wall as shown at the bottom of Figure 5. In the index we simply implement the specialization of fugacities (2.3) into (2.4)

$$\oint d\vec{z}_N \Delta_N(\vec{z}; t) \mathcal{I}_S^{(N)}(\vec{x}; \vec{z}; t; c) \mathcal{I}_S^{(N)}(\vec{z}; \vec{y}; t^{\frac{N-M-1}{2}} v, \dots, t^{-\frac{N-M-1}{2}} v; t; c^{-1}) = \hat{x}\hat{y}, v(t), \quad (2.7)$$

where the index of the asymmetric Identity-wall is given by

$$\hat{\mathbb{I}}_{\vec{x}, v}(t) = \frac{\prod_{i=1}^N 2\pi i x_i}{\Delta_N(\vec{x}; t)} \sum_{\sigma \in S_N, \pm} \prod_{i=1}^N \delta\left(x_i - y_{\sigma(i)}^{\pm 1}\right) \Bigg|_{y_{M+j} = t^{\frac{N-M+1-2j}{2}} v}. \quad (2.8)$$

The T-wall. In $3d$, the \mathcal{T} generator of $SL(2, \mathbb{Z})$ is associated with the addition of a Chern–Simons (CS) coupling at level one. We propose that the $4d$ analogue denoted by \mathbb{T} is a pair of $USp(2N)$ fundamental chiral fields and for convenience we also attach to it an Identity-wall, as shown in Figure 6. Indeed, in the $3d$ limit, after giving a CB VEV deformation that breaks the symplectic group to a unitary one, we consider a real mass deformation for the $U(1)_d$ symmetry which integrates out all the fields and produces a CS level 1 for the $U(N)$ group. We will come back to the connection to $3d$ in Section 4.

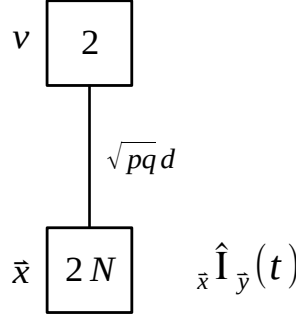


Figure 6. The $4d$ T-wall. In the drawing \vec{x} are the $USp(2N)$ fugacities, v the $SU(2)$ fugacity and d the fugacity for an abelian symmetry.

The index expression for the T-wall in $4d$ is simply

$$\mathcal{I}_{\mathbb{T}}^{(N)}(\vec{x}; \vec{y}; v; t; d) = \prod_{j=1}^N \Gamma((pq)^{\frac{1}{2}} dx_j^{\pm} v^{\pm})_{\vec{x} \hat{\mathbb{I}}_{\vec{y}}(t)}. \quad (2.9)$$

Group multiplication and $PSL(2, \mathbb{Z})$ relations. The objects we have introduced can be associated with the corresponding elements of the $PSL(2, \mathbb{Z})$ group. To see if those objects respect the group structure, we need to define the group multiplication acting on them. Let us recall eq. (2.4). Here, we glue two S-walls by gauging the diagonal $USp(2N)_z$ of two $USp(2N)$ symmetries groups, one from each S-wall, to obtain the Identity-wall. Moreover, we add an additional antisymmetric chiral field Φ with the superpotential

$$\text{Tr}_z [\Phi \cdot (\mathcal{O}_{\mathbb{H}}^L - \mathcal{O}_{\mathbb{H}}^R)], \quad (2.10)$$

where $\mathcal{O}_{\mathbb{H}}^{L/R}$ are the antisymmetric operators defined in eq. (A.2) of two glued $USp(2N)$ symmetries of the S-walls. This superpotential as well as the anomaly-free condition of the

gauged $USp(2N)_z$ group completely determine the abelian charges of the second S-wall in terms of those of the first S-wall, as shown in (2.4). Therefore, once we define the group multiplication in this way, the property in Figure 5 can be interpreted as

$$SS = 1, \quad (2.11)$$

indicating that the inverse of the S-wall is the S-wall itself. This is one of the defining relations of $PSL(2, \mathbb{Z})$.

Next, let us examine the multiplication property of the T-wall as a group element in $PSL(2, \mathbb{Z})$. The group multiplication of two T-walls is defined in the same way as that of the S-wall explained above. We introduce an additional chiral Φ in the antisymmetric representation of the diagonal $USp(2N)_z$ of two $USp(2N)$ symmetries, one from each T-wall, with the superpotential (2.10) and then gauge this diagonal $USp(2N)_z$. The generalization to \mathbb{T}^k is straightforward and shown in Figure 7.

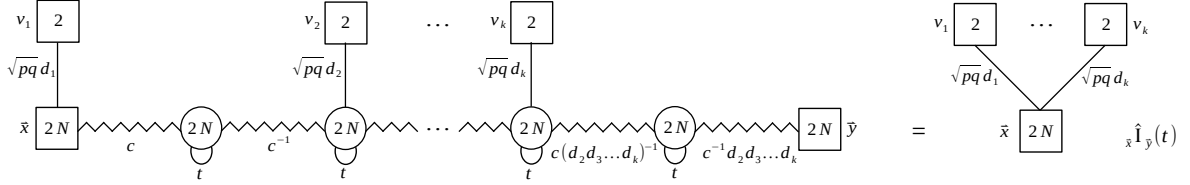


Figure 7. The \mathbb{T}^k -wall. On the r.h.s. we used the fact that two glued S-walls give an Identity-wall.

For $k = 2$, the corresponding index is given by

$$\begin{aligned} & \oint d\vec{z}_N \Delta_N(\vec{z}; t) \mathcal{I}_T^{(N)}(\vec{x}; \vec{z}; v; t; d_1) \mathcal{I}_T^{(N)}(\vec{z}; \vec{y}; u; t; d_2) \\ &= \oint d\vec{z}_N \Delta_N(\vec{z}; t) \prod_{i=1}^N \Gamma((pq)^{\frac{1}{2}} d_1 x_i^\pm v^\pm)_{\vec{x} \hat{\mathbb{I}}_{\vec{z}}(t)} \prod_{j=1}^N \Gamma((pq)^{\frac{1}{2}} d_2 z_j^\pm u^\pm)_{\vec{z} \hat{\mathbb{I}}_{\vec{y}}(t)} \\ &= \prod_{i=1}^N \Gamma((pq)^{\frac{1}{2}} d_1 x_i^\pm v^\pm) \prod_{j=1}^N \Gamma((pq)^{\frac{1}{2}} d_2 x_j^\pm u^\pm)_{\vec{x} \hat{\mathbb{I}}_{\vec{y}}(t)} = \prod_{i=1}^N \prod_{a=1}^4 \Gamma((pq)^{\frac{1}{2}} d x_i^\pm u_a)_{\vec{x} \hat{\mathbb{I}}_{\vec{y}}(t)}, \quad (2.12) \end{aligned}$$

where we defined

$$d_1 = d s, \quad d_2 = d s^{-1}, \quad u_a = \begin{cases} s v^{\pm 1} & a = 1, 2 \\ s^{-1} u^{\pm 1} & a = 3, 4 \end{cases} \quad (2.13)$$

so that the fugacities u_a satisfying $\prod_{a=1}^4 u_a = 1$ can be interpreted as $SU(4)$ fugacities. Similarly, for \mathbb{T}^k we get

$$\prod_{i=1}^N \prod_{j=1}^{2k} \Gamma((pq)^{\frac{1}{2}} d x_i^\pm v_j)_{\vec{x} \hat{\mathbb{I}}_{\vec{y}}(t)}, \quad (2.14)$$

where v_j are the $SU(2k)$ fugacities satisfying $\prod_{j=1}^{2k} v_j = 1$, and $d^k = \prod_{i=1}^k d_i$.

So far, we have defined the group multiplication between the same elements, either S or T. To complete the definition of the group multiplication, we need to address the multiplication between S and T. For this purpose, a crucial role will be played by the so-called *braid move*, which is a duality that was proposed in [21] and summarize in Figure 8 (we refer the reader to Section 3.4 of [21] for more details). This will also allow us to derive many of the duality moves later needed in the algorithm.

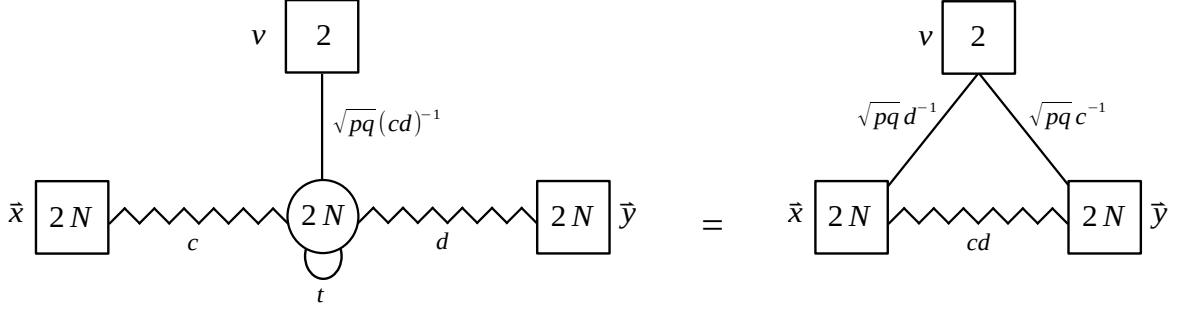


Figure 8. The braid duality move.

At the level of the index the braid duality is encoded in the following integral identity:

$$\begin{aligned} & \oint d\vec{w}_N \Delta_N(\vec{w}; t) \mathcal{I}_S^{(N)}(\vec{x}; \vec{w}; t; c) \prod_{j=1}^N \Gamma((pq)^{\frac{1}{2}} c^{-1} d^{-1} w_j^{\pm} v^{\pm}) \mathcal{I}_S^{(N)}(\vec{w}; \vec{y}; t; d) \\ &= \prod_{j=1}^N \Gamma((pq)^{\frac{1}{2}} d^{-1} x_j^{\pm} v^{\pm}) \mathcal{I}_S^{(N)}(\vec{x}; \vec{y}; t; cd) \prod_{j=1}^N \Gamma((pq)^{\frac{1}{2}} c^{-1} y_j^{\pm} v^{\pm}), \end{aligned} \quad (2.15)$$

which was proven in Proposition 2.12 of [91]. It was later understood as a sort of generalization of Seiberg duality [1] and derived from the perspective of the $4d$ compactification of the $6d$ E-string theory on a torus with flux in [21]. It turns out that this duality can be derived by assuming only the Intriligator–Pouliot (IP) duality [45] and applying it iteratively, as it will be shown in [94].

For the multiplication between S and T, the operation is basically defined in the almost same way as that of S or T alone. We introduce an additional antisymmetric chiral Φ with the superpotential (2.10) and gauge the diagonal $USp(2N)$, but there is one additional ingredient: if a group element contains S sandwiched between two T elements, we introduce an extra superpotential

$$\text{Tr} P_1 \Pi P_2, \quad (2.16)$$

where P_1 and P_2 are two fundamental chirals in the T-walls, and Π is a bifundamental operator between two $USp(2N)$ in the S-wall (see Table 8 for its charges under the global symmetries). It will shortly become clear that this prescription ensures the group structure of $PSL(2, \mathbb{Z})$.

As we have seen above, the inverse element of S is S itself. Namely, once two S -walls are glued, they give rise to the Identity-wall as shown in (2.4). On the other hand, the inverse element of T is rather non-trivial and is given by $T^{-1} = STSTS$, as shown in Figure 9.

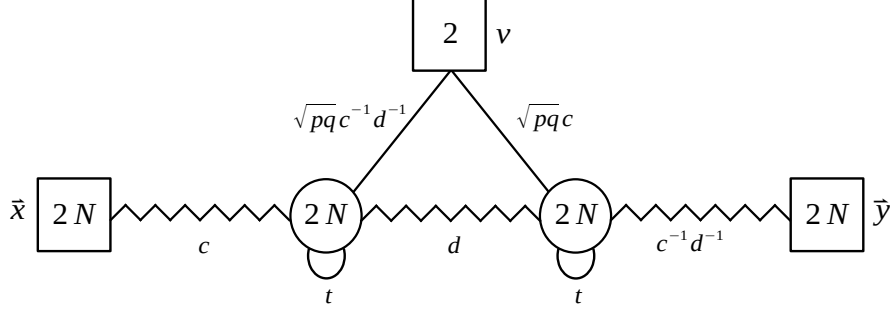


Figure 9. The T^{-1} -wall given by $T^{-1} = STSTS$ after getting rid of all the Identity-walls in the definition of each T -wall.

Note that all the abelian charges of the walls are fixed by the anomaly-free condition and the cubic superpotential (2.16); in this case, P_1 and P_2 in the superpotential are the two fundamental chirals in the two T -walls, and Π is the bifundamental operator of the S -wall in the middle. The index of the T^{-1} -wall is expressed compactly in terms of those of the S and T components as follows:

$$\begin{aligned} \mathcal{I}_{T^{-1}}^{(N)}(\vec{x}; \vec{y}; v; t; d) &= \oint \left(\prod_{i=1}^4 d\vec{z}_N^{(i)} \Delta_N(\vec{z}^{(i)}; t) \right) \mathcal{I}_S^{(N)}(\vec{x}; \vec{z}^{(1)}; t; c) \mathcal{I}_T^{(N)}(\vec{z}^{(1)}; \vec{z}^{(2)}; v; t; c^{-1}d^{-1}) \\ &\times \mathcal{I}_S^{(N)}(\vec{z}^{(2)}; \vec{z}^{(3)}; t; d) \mathcal{I}_T^{(N)}(\vec{z}^{(3)}; \vec{z}^{(4)}; v; t; c) \mathcal{I}_S^{(N)}(\vec{z}^{(4)}; \vec{y}; t; c^{-1}d^{-1}). \end{aligned} \quad (2.17)$$

Now we want to check that $TT^{-1} = 1$. According to the rule we gave above, we gauge the diagonal $USp(2N)$ in the presence of an extra antisymmetric chiral Φ and two types of the superpotential terms, one from (2.10) and the other from (2.16) as shown in the first diagram of Figure 10.

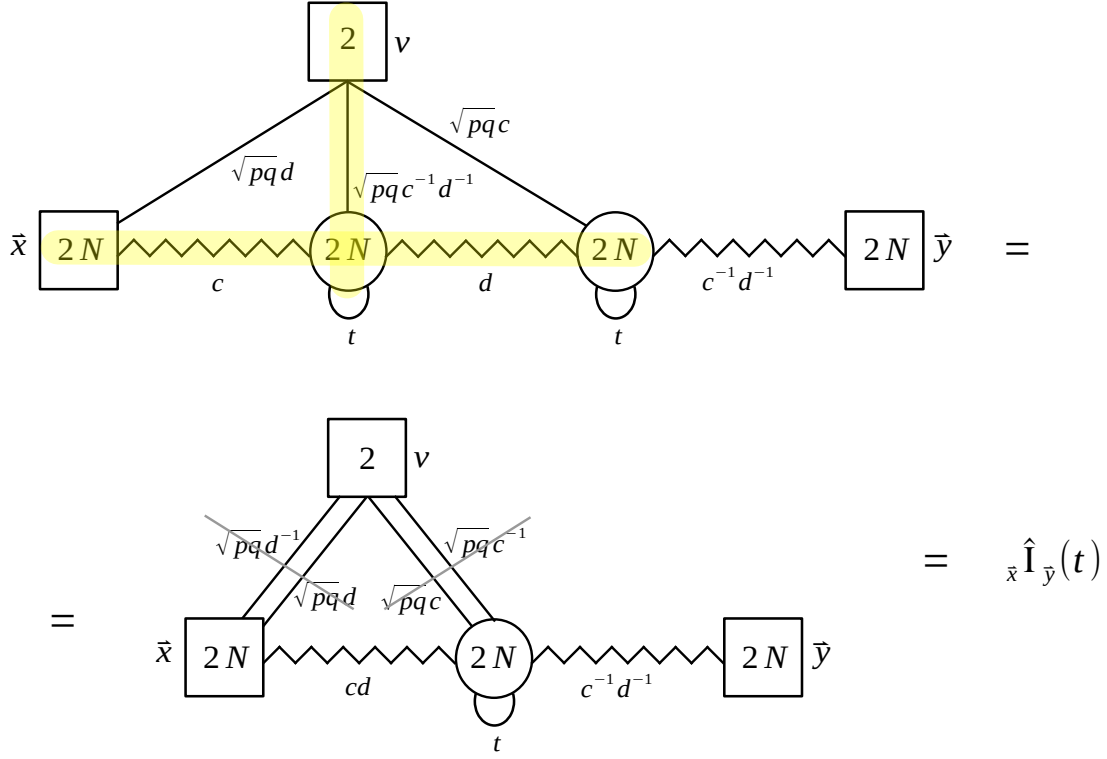


Figure 10. The field theory realization of the relation $\mathbb{T}\mathbb{T}^{-1} = \mathbb{T}\mathbb{S}\mathbb{T}\mathbb{S}\mathbb{T}\mathbb{S} = I$, the other $PSL(2, \mathbb{Z})$ defining relation. Notice it also encodes $\mathbb{T}^T(\mathbb{T}^T)^{-1} = I$. The grey lines are traced over massive fields which can be integrated out.

The corresponding index can then be written as follows:

$$\begin{aligned}
& \oint d\vec{w}_N \Delta_N(\vec{w}; t) \mathcal{I}_{\mathbb{T}}^{(N)}(\vec{x}; \vec{w}; v; t; d) \mathcal{I}_{\mathbb{T}^{-1}}^{(N)}(\vec{w}; \vec{y}; v; t; d) \\
&= \oint d\vec{w}_N \Delta_N(\vec{w}; t) \left(\prod_{i=1}^4 d\vec{z}_N^{(i)} \Delta_N(\vec{z}^{(i)}; t) \right) \mathcal{I}_{\mathbb{T}}^{(N)}(\vec{x}; \vec{w}; v; t; d) \mathcal{I}_{\mathbb{S}}^{(N)}(\vec{w}; \vec{z}^{(1)}; t; c) \\
&\quad \times \mathcal{I}_{\mathbb{T}}^{(N)}(\vec{z}^{(1)}; \vec{z}^{(2)}; v; t; c^{-1}d^{-1}) \mathcal{I}_{\mathbb{S}}^{(N)}(\vec{z}^{(2)}; \vec{z}^{(3)}; t; d) \mathcal{I}_{\mathbb{T}}^{(N)}(\vec{z}^{(3)}; \vec{z}^{(4)}; v; t; c) \mathcal{I}_{\mathbb{S}}^{(N)}(\vec{z}^{(4)}; \vec{y}; t; c^{-1}d^{-1}) \\
&= \oint \left(\prod_{i=2}^3 d\vec{z}_N^{(i)} \Delta_N(\vec{z}^{(i)}; t) \right) \prod_{j=1}^N \Gamma((pq)^{\frac{1}{2}} dx_j^{\pm} v^{\pm}) \mathcal{I}_{\mathbb{S}}^{(N)}(\vec{x}; \vec{z}^{(2)}; t; c) \\
&\quad \times \prod_{j=1}^N \Gamma((pq)^{\frac{1}{2}} c^{-1}d^{-1} z_j^{(2)\pm} v^{\pm}) \mathcal{I}_{\mathbb{S}}^{(N)}(\vec{z}^{(2)}; \vec{z}^{(3)}; t; d) \prod_{j=1}^N \Gamma((pq)^{\frac{1}{2}} cz_j^{(3)\pm} v^{\pm}) \mathcal{I}_{\mathbb{S}}^{(N)}(\vec{z}^{(3)}; \vec{y}; t; c^{-1}d^{-1}).
\end{aligned} \tag{2.18}$$

In the last equality we wrote explicitly the contribution of the T-walls in terms of doublets and Identity-walls using (2.9), and we also used the delta functions inside the Identity-walls

to get rid of some of the integrations. The final result is what is represented on the top of Figure 10.

Note that each triangle in the first quiver in Figure 10 makes a superpotential of the form (2.16). Because of the constraints on the fugacities imposed by this superpotential, we can apply the braid move of Figure 8 as highlighted in Figure 10 to obtain the second quiver, where, after removing the massive fields, we find two consecutive S-walls which are equivalent to a single Identity-wall. This gives us the index identity

$$\oint d\vec{w}_N \Delta_N(\vec{w}; t) \mathcal{I}_T^{(N)}(\vec{x}; \vec{w}; v; t; d) \mathcal{I}_{T^{-1}}^{(N)}(\vec{w}; \vec{y}; v; t; d) = \vec{x} \hat{\mathbb{I}}_{\vec{y}}(t). \quad (2.19)$$

We comment in passing that while on the l.h.s. we have an explicit dependence on the fugacity v , the r.h.s. doesn't depend on it. Nevertheless, the identity holds for any value of v . This tells us that also the l.h.s. is actually independent of v . While here it is just a comment about the mathematical identity, we will see this phenomenon many times and later comment on its physical implications when discussing identities that are associated with genuine IR dualities.

As we have seen so far, a cubic superpotential (2.16) must be turned on when an S-wall sits between two T-walls. What about if we have multiple T-walls? For example, if we have a single T-wall on the left and two T-walls on the right of an S-wall, two natural choices of the superpotential would be

$$\text{Tr} Q \Pi P_1, \quad \text{or} \quad \text{Tr} Q \Pi (P_1 + P_2), \quad (2.20)$$

where Q is the chiral from the left T-wall and P_1, P_2 are the chirals from the two right T-walls. In fact, those two choices are equivalent up to a field redefinition. Therefore, a quiver associated with TST^2 would be as in Figure 11.

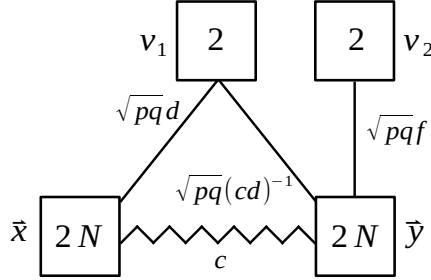


Figure 11. The field theory realization of the combination TST^2 .

Moreover, we can also consider TST^2ST . In this case, we have the two candidates depicted in Figure 12. One can find the correct choice by multiplying TS from the left and ST from the right, which is supposed to give 1. As shown in Figure 13 only the first choice gives the expected Identity-wall. Thus, we conclude that the first quiver in Figure 12 is the correct implementation of TST^2ST . Generalizing this observation, we can also find the quiver corresponding to TST^kST , which we give in Figure 14.

In conclusion, with our gluing prescriptions, the S and T-walls satisfy two conditions $\text{SS} = 1$ and $(\text{ST})^3 = 1$, which generate the $PSL(2, \mathbb{Z})$ group. Furthermore, as we will see in

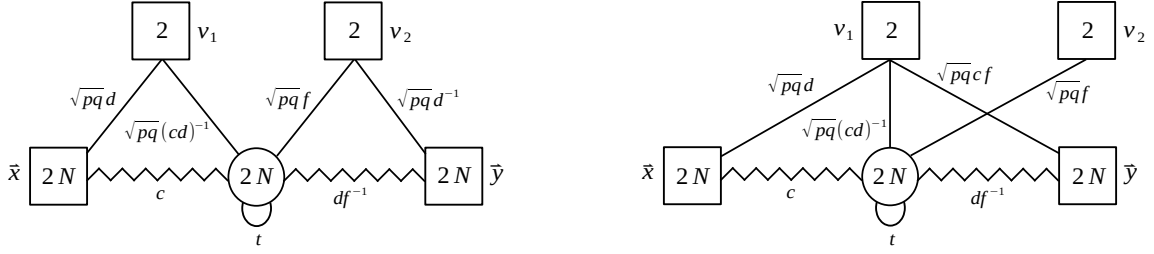


Figure 12. Two options for TST^2ST . As we explain in the text, only the first one is correct.

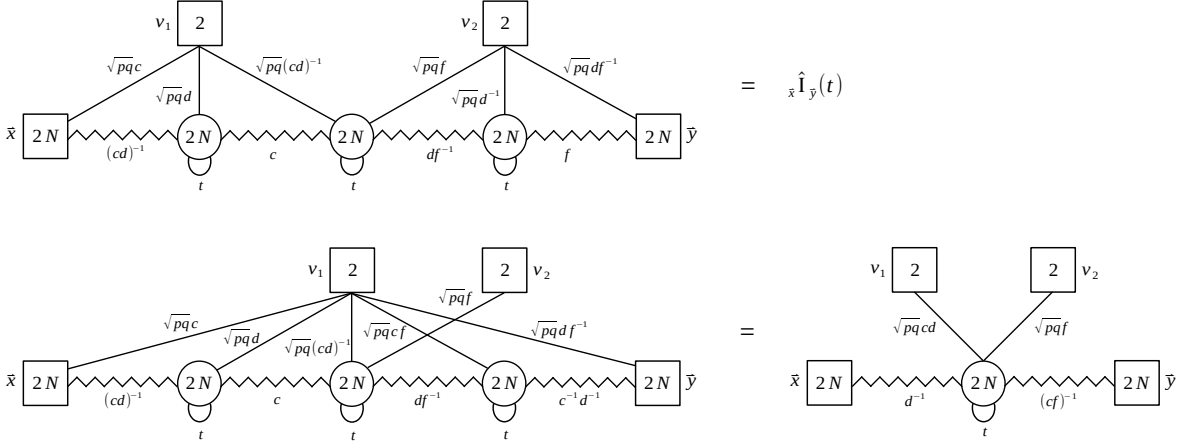


Figure 13. Two possible realizations of the combination $(TS)TST^2ST(ST)$. Only the first one is correct, since the second doesn't reproduce the Identity-wall expected from the relation $(TS)TST^2ST(ST) = I$.

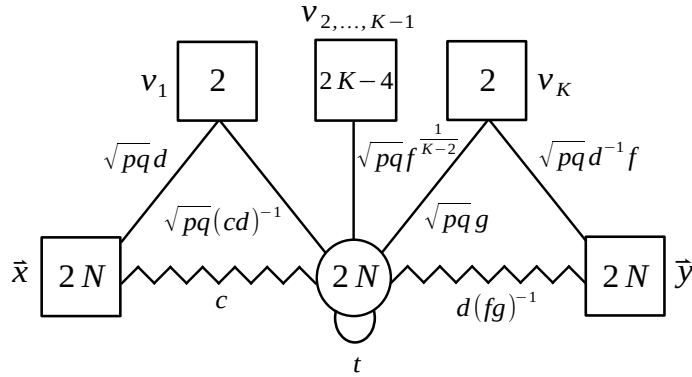


Figure 14. The field theory realization of the combination TST^kST .

the next section, the S and T-walls act on the QFT blocks consistently with the $PSL(2, \mathbb{Z})$ structure.

The \mathbb{T}^T -wall. Finally, for later convenience, we would like to discuss another element of $PSL(2, \mathbb{Z})$: $\mathbb{T}^T = \text{TST}$.⁷ Although this is not an independent operation, it is interesting to consider it on its own, especially since we will consider the \mathbb{T}^T -dual of some quivers later on. Its QFT realization consists of two sets of the $USp(2N) \times SU(2)$ bifundamental fields coupled to one copy of the $FE[USp(2N)]$ theory to form a triangle as depicted in Figure 15, consistently with our previous discussion on the multiplication rules for the $PSL(2, \mathbb{Z})$ operators.

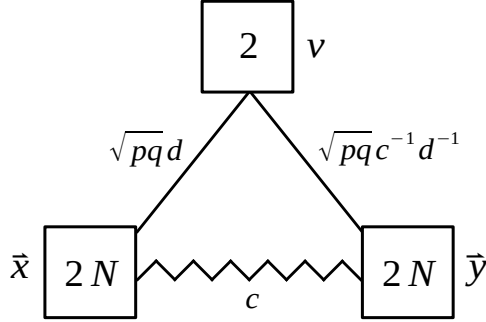


Figure 15. The 4d \mathbb{T}^T -wall.

The index expression associated to the \mathbb{T}^T -wall is

$$\begin{aligned} \mathcal{I}_{\mathbb{T}^T}^{(N)}(\vec{x}; \vec{y}; v; t; c; d) &= \oint d\vec{z}_N^{(1)} d\vec{z}_N^{(2)} \Delta_N(\vec{z}^{(1)}) \Delta_N(\vec{z}^{(2)}) \mathcal{I}_{\mathbb{T}}^{(N)}(\vec{x}; \vec{z}^{(1)}; t; d) \\ &\quad \times \mathcal{I}_{\mathbb{S}}^{(N)}(\vec{z}^{(1)}; \vec{z}^{(2)}; t; c) \mathcal{I}_{\mathbb{T}}^{(N)}(\vec{z}^{(2)}; \vec{y}; t; (cd)^{-1}) \\ &= \mathcal{I}_{\mathbb{S}}^{(N)}(\vec{x}; \vec{y}; t; c) \prod_{j=1}^N \Gamma_e \left((pq)^{\frac{1}{2}} dx_j^{\pm} v^{\pm} \right) \Gamma_e \left((pq)^{\frac{1}{2}} (cd)^{-1} y_j^{\pm} v^{\pm} \right), \end{aligned} \quad (2.21)$$

where in the last equality we wrote explicitly the contribution of the T-walls in terms of doublets and Identity-walls using (2.9) and we also used the delta functions inside the Identity-walls to get rid of some of the integrations.

From the $PSL(2, \mathbb{Z})$ relation in Figure 10 we can easily determine the inverse $(\mathbb{T}^T)^{-1} = \text{STS}$, whose associated quiver is given in Figure 16.

2.2 QFT building blocks

In this section we introduce the three fundamental 4d QFT building blocks. By the way the $PSL(2, \mathbb{Z})$ operators in the previous subsection act on them, we can think of those QFT building blocks as being labelled by vectors (1,0), (0,1) and (1,1) on which $PSL(2, \mathbb{Z})$ elements

⁷The name \mathbb{T}^T originates from the fact that the matrix representation of $\mathbb{T}^T = \text{TST}$ is actually the transpose of the matrix associated with T.

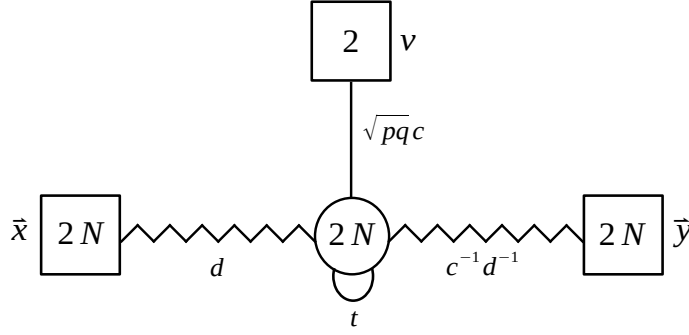


Figure 16. The $(T^T)^{-1} = \text{STS}$ wall.

act as matrix multiplications. We will then see in Section 4 that they reduce in $3d$ to the QFT building blocks that are associated to the NS5, D5 and (1,1)-branes. For these reasons, we will call them \mathbf{B}_{10} , \mathbf{B}_{01} and \mathbf{B}_{11} blocks.

The \mathbf{B}_{10} block. The first block is associated to an NS5 or (1,0)-brane. In $3d$ this would simply be a $U(N) \times U(M)$ bifundamental hypermultiplet. As proposed in [43], its $4d$ uplift, the \mathbf{B}_{10} block, is a $USp(2N) \times USp(2M)$ bifundamental chiral multiplet plus four chirals, each two of which are in the fundamental representation of $USp(2N)$ or that of $USp(2M)$, respectively. These interact with a cubic superpotential, so they can be represented as in Figure 17.

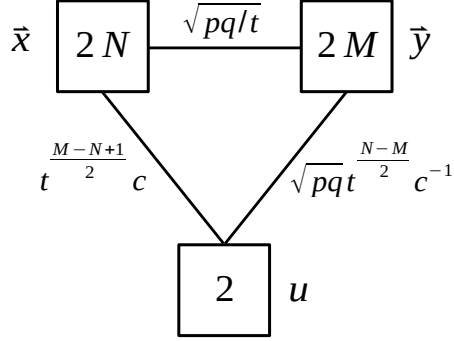


Figure 17. The \mathbf{B}_{10} block.

The index of the \mathbf{B}_{10} block is given by

$$\begin{aligned}
\mathcal{I}_{(1,0)}^{(N,M)}(\vec{x}; \vec{y}; u; t; c) &= \prod_{i=1}^N \prod_{j=1}^M \Gamma_e \left((pq/t)^{\frac{1}{2}} x_i^{\pm} y_j^{\pm} \right) \prod_{i=1}^N \Gamma_e \left(t^{\frac{M-N+1}{2}} c x_j^{\pm} u^{\pm} \right) \\
&\times \prod_{j=1}^M \Gamma_e \left((pq)^{\frac{1}{2}} t^{\frac{N-M}{2}} c^{-1} y_j^{\pm} u^{\pm} \right). \tag{2.22}
\end{aligned}$$

In the $3d$ limit we consider a real mass deformation that breaks the USp groups down to U and also a real mass deformation for $U(1)_c$ that gives mass to the two $SU(2)$ chiral doublets, thus leaving a $U(N) \times U(M)$ bifundamental hyper only. The process of integrating out these fields also produces background CS levels ± 1 and ∓ 1 for the $U(N)$ and $U(M)$ gauge nodes, respectively, where the signs depend on that of the real mass for $U(1)_c$. Nevertheless, these CS couplings always cancel out when gluing several building blocks together to form quivers. We will give more details on the $3d$ limit in Section 4.

The B_{01} block. The second block is the one that we associate to a D5 or (0,1)-brane. In $3d$ this is just a single fundamental hypermultiplet, while its $4d$ uplift, the B_{01} block, is a pair of $USp(2N)$ fundamental chirals. Let us first consider the situation in which a D5 is suspended between the same number N of D3-branes on the left and on the right so that these yield two $USp(2N)$ symmetries of the same rank. In order to give this QFT building block a structure with two $USp(2N)$ symmetries, we also attach to it an Identity-wall. Thus, we define the B_{01} block as in Figure 18.

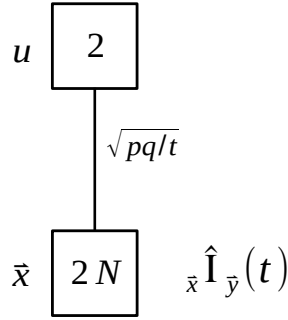


Figure 18. The B_{01} block.

To the B_{01} block we can associate the index expression

$$\mathcal{I}_{(0,1)}^{(N,N)}(\vec{x}; \vec{y}; u; t) = \prod_{j=1}^N \Gamma_e \left((pq/t)^{\frac{1}{2}} x_j^{\pm} u^{\pm} \right) \hat{x} \hat{\mathbb{I}}_{\vec{y}}(t). \quad (2.23)$$

We can generalize this to the case corresponding to a D5-brane suspended between different numbers of D3-branes, say N D3's on the left and M D3's on the right as shown in Figure 19.

The associated index is given by

$$\mathcal{I}_{(0,1)}^{(N,M)}(\vec{x}; \vec{y}; u; t) = \prod_{j=1}^M \Gamma_e \left((pq/t)^{\frac{N-M+1}{2}} y_j^{\pm} u^{\pm} \right) \hat{x} \hat{\mathbb{I}}_{\vec{y},u}(t), \quad (2.24)$$

where $\hat{x} \hat{\mathbb{I}}_{\vec{y},v}(t)$ is the asymmetric Identity-wall defined in (2.8).

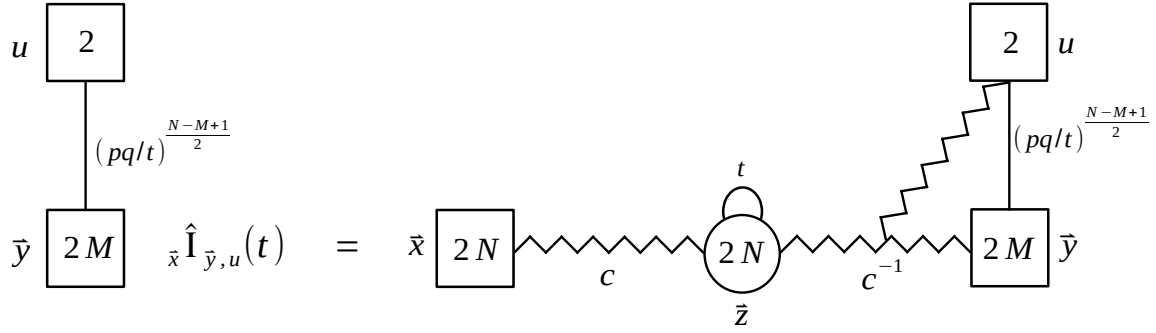


Figure 19. The asymmetric B_{01} block.

The B_{11} block. Finally, we consider the QFT building block associated to a $(1, 1)$ -brane. This wasn't considered in [43] and we propose it here to be a $USp(2N) \times USp(2M)$ bifundamental plus additional chiral fields that form a double triangle structure as in Figure 20.⁸

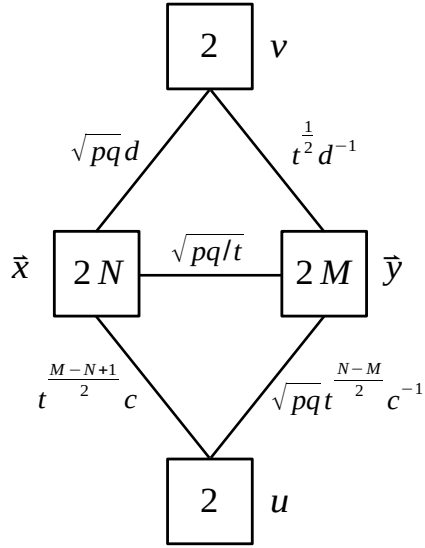


Figure 20. The B_{11} block.

⁸The two triangles can actually be combined to form a single triangle with an $SU(4)$ flavor node. Nevertheless, we will split the flavors into the two triangles so that only the $SU(2)^2 \times U(1)$ subgroup is manifest because the two triangles and the associated $SU(2)$ symmetries will play different roles in the dualization algorithm.

The corresponding index is

$$\begin{aligned} \mathcal{I}_{(1,1)}^{(N,M)}(\vec{x}; \vec{y}; v; u; t; c; s) &= \prod_{i,j=1}^N \Gamma_e \left((pq/t)^{\frac{1}{2}} x_i^\pm y_j^\pm \right) \prod_{j=1}^N \Gamma_e \left((pq)^{\frac{1}{2}} dx_j^\pm v^\pm \right) \Gamma_e \left(t^{\frac{1}{2}} d^{-1} y_j^\pm v^\pm \right) \\ &\times \Gamma_e \left(t^{\frac{M-N+1}{2}} cx_j^\pm u^\pm \right) \Gamma_e \left((pq)^{\frac{1}{2}} t^{\frac{N-M}{2}} c^{-1} y_j^\pm u^\pm \right). \end{aligned} \quad (2.25)$$

When we consider the $3d$ limit, similarly to the case of the NS5-brane, the real mass deformation for $U(1)_c$ produces background CS levels for the two $U(N)$ nodes, which cancel out when considering a quiver. The real mass deformation for $U(1)_d$ also produces CS levels, but when considering a quiver these only cancel out if we have a stack of $(1, 1)$ -branes, while they remain if we have adjacent $(1, 0)$ and $(1, 1)$ -branes. In such a case, they become dynamical CS couplings for the $U(N)$ gauge field arising from the D3's suspended between the $(1, 0)$ and $(1, 1)$ -branes, as expected. One can also obtain the QFT building block corresponding to the $(1, -1)$ -brane, which can be obtained as the \mathcal{S} -dualization of $(1, 1)$. As we will see, both the $(1, 1)$ and $(1, -1)$ -branes correspond to double triangle building blocks with some relative charge difference, leading to the opposite CS levels in the $3d$ limit. Again, we postpone a more detailed discussion of the $3d$ counterpart to Section 4.

2.3 Basic duality moves

In this section, we present the basic duality moves involved in the dualization algorithm, which utilize all the ingredients we have introduced in the previous subsections. We will first review the \mathcal{S} -dualizations of the \mathbf{B}_{10} and the \mathbf{B}_{01} building blocks proposed in [43]. Then we will discuss new duality moves involving the other field theory ingredients we introduced.

2.3.1 \mathcal{S} -dualization

Let us first consider dualities for the QFT building blocks generated by the \mathcal{S} operator.

The $\mathbf{B}_{10} = \mathbf{S}\mathbf{B}_{01}\mathbf{S}^{-1}$ duality move. We first consider the $4d$ QFT analogue of the \mathcal{S} -dualization of a D5-brane into an NS5-brane, which relates a \mathbf{B}_{01} and a \mathbf{B}_{10} block [43]. This can be associated with a genuine field theory duality relating the quiver theories in Figure 21.

This is a non-trivial IR duality that was derived by iteratively applying the Intriligator–Pouliot (IP) duality in [22]. At the level of the index, this dualization translates into the following integral identity:

$$\begin{aligned} \mathcal{I}_{(1,0)}^{(N,M)}(\vec{x}; \vec{y}; u; t; ct^{\frac{M-N}{2}}) &= \prod_{i=1}^{N-M} \frac{\Gamma_e(t^{1-i}c^2)}{\Gamma_e(pqt^{-i})} \oint d\vec{z}_N^{(1)} d\vec{z}_M^{(2)} \Delta_N(\vec{z}^{(1)}; t) \Delta_M(\vec{z}^{(2)}; t) \\ &\times \mathcal{I}_{\mathcal{S}}^{(N)}(\vec{x}; \vec{z}^{(1)}; t; c) \mathcal{I}_{(0,1)}^{(N,M)}(\vec{z}^{(1)}; \vec{z}^{(2)}; u; t) \mathcal{I}_{\mathcal{S}}^{(M)}(\vec{z}^{(2)}; \vec{y}; t; (pq/t)^{\frac{1}{2}}c^{-1}), \end{aligned} \quad (2.26)$$

where we recall that the index of the \mathbf{B}_{10} and the \mathbf{B}_{01} blocks were defined in (2.22) and (2.24) respectively.

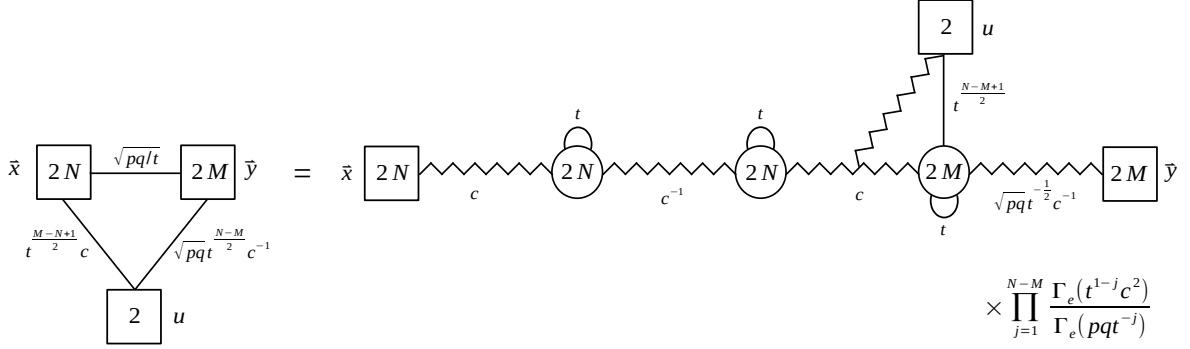


Figure 21. The $B_{10} = SB_{01}S^{-1}$ duality move. Notice that for $N \neq M$ we have on the r.h.s. the asymmetric B_{01} block, which is associated with a D5 with a different number N and M of D3's on each side. We represent the gauge singlet fields that are charged only under the abelian global symmetries and not the non-abelian ones by writing explicitly their index contribution.

The $B_{01} = SB_{10}S^{-1}$ duality move. We next consider the QFT analogue of the S-dualization of an NS5-brane into a D5-brane. The quiver corresponding to this duality move is given in Figure 22.

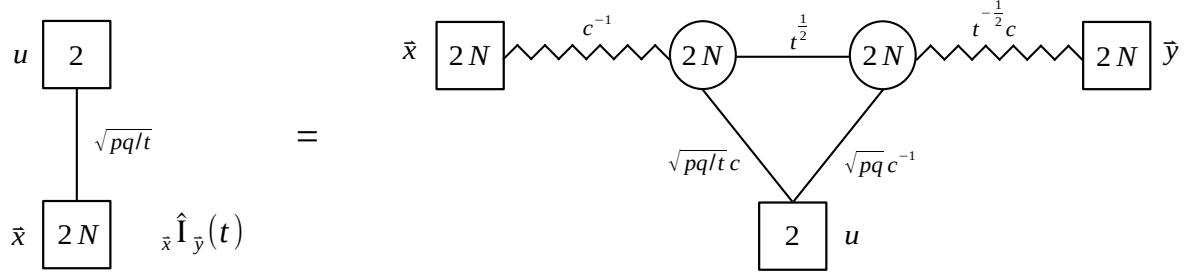


Figure 22. The $B_{01} = SB_{10}S^{-1}$ duality move.

At the level of the index we have

$$\begin{aligned} \mathcal{I}_{(0,1)}^{(N,N)}(\vec{x}; \vec{y}; u; t) &= \oint dw_N^{(0)} dw_N^{(1)} \Delta_N(\vec{w}^{(0)}) \Delta_N(\vec{w}^{(1)}) \\ &\times \mathcal{I}_S^{(N)}(\vec{x}; \vec{w}^{(0)}; t; c^{-1}) \mathcal{I}_{(1,0)}^{(N,N)}(\vec{w}^{(0)}; \vec{w}^{(1)}; u; pq/t; c) \mathcal{I}_S^{(N)}(\vec{w}^{(1)}; \vec{y}; t; t^{-\frac{1}{2}}c). \end{aligned} \quad (2.27)$$

For convenience, we also give the dualization of L D5-branes as L NS5-branes between S and $S^{-1} = S$, shown in Figure 23.

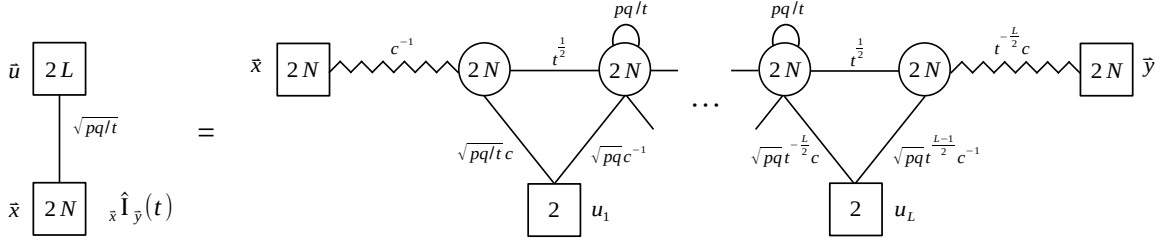


Figure 23. The $(\mathbf{B}_{01})^L = \mathbf{S}(\mathbf{B}_{10})^L \mathbf{S}^{-1}$ duality move.

The index identity associated to this duality is explicitly

$$\begin{aligned}
\hat{x} \hat{\mathbb{I}}_{\hat{y}}(t) \prod_{i=1}^N \prod_{j=1}^L \Gamma_e \left((pq/t)^{\frac{1}{2}} u_j^{\pm 1} x_i^{\pm 1} \right) &= \oint \prod_{k=0}^L dw_N^{(k)} \Delta_N(\vec{w}^{(0)}) \\
&\times \mathcal{I}_{\mathbf{S}}^{(N)}(\vec{x}; \vec{w}^{(0)}; t; c^{-1}) \prod_{i=1}^L \mathcal{I}_{(1,0)}^{(N,N)} \left(\vec{w}^{(i-1)}; \vec{w}^{(i)}; u_i; pq/t; ct^{\frac{1-i}{2}} \right) \\
&\times \prod_{k=1}^{L-1} \Delta_N(\vec{w}^{(k)}; pq/t) \mathcal{I}_{\mathbf{S}}^{(N)}(\vec{w}^{(L)}; \vec{y}; t; t^{-\frac{L}{2}}c) \Delta_N(\vec{w}^{(L)}). \tag{2.28}
\end{aligned}$$

Also this result can be derived by iterating the IP duality as shown in [22, 43]. Alternatively, it can be derived from the S-dualization of a D5 into an NS5 by applying \mathbf{S} on the left and $\mathbf{S}^{-1} = \mathbf{S}$ on the right and using the property we reviewed in the previous subsection that two concatenated S-walls give an Identity-wall.

The $\mathbf{B}_{11} = \mathbf{S}\mathbf{B}_{1-1}\mathbf{S}^{-1}$ duality move. The last S-dualization we consider is that of a (1,-1) into a (1,1)-brane, which can be represented as in Figure 24.

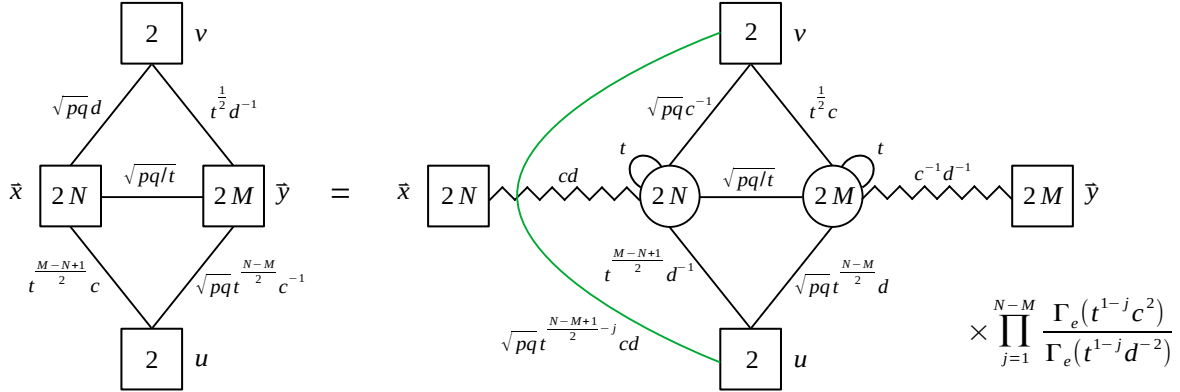


Figure 24. The $\mathbf{B}_{11} = \mathbf{S}\mathbf{B}_{1-1}\mathbf{S}^{-1}$ duality move. The green line denotes a set of gauge singlet fields labelled $j = 1, \dots, N - M$.

This duality move was not considered in [43]. We provide its derivation in Appendix C, where the main ingredient is the braid duality of Figure 8. The corresponding index identity

is

$$\begin{aligned}
& \mathcal{I}_{(1,1)}^{(N,M)}(\vec{x}; \vec{y}; v; u; t; c; d) \\
&= \prod_{j=1}^{N-M} \frac{\Gamma_e(t^{1-j}c^2)}{\Gamma_e(t^{1-j}d^{-2})} \Gamma_e\left(\sqrt{pqt}^{\frac{N-M+1}{2}-j} cdu^\pm v^\pm\right) \oint d\vec{z}_N d\vec{w}_M \Delta_N(\vec{z}; t) \Delta_M(\vec{w}; t) \\
&\quad \times \mathcal{I}_{\mathcal{S}}^{(N)}(\vec{x}; \vec{z}; t; cd) \mathcal{I}_{(1,-1)}^{(N,M)}(\vec{z}; \vec{w}; v; u; t; c; d) \mathcal{I}_{\mathcal{S}}^{(M)}(\vec{w}; \vec{y}; t; c^{-1}d^{-1}), \tag{2.29}
\end{aligned}$$

where the index contribution of the \mathbf{B}_{1-1} block is

$$\mathcal{I}_{(1,-1)}^{(N,M)}(\vec{z}; \vec{w}; v; u; t; c; d) = \mathcal{I}_{(1,1)}^{(N,M)}(\vec{z}; \vec{w}; v; u; t; d^{-1}; c^{-1}), \tag{2.30}$$

with $\mathcal{I}_{(1,1)}^{(N,M)}$ being defined in (2.25).

Indeed, since the difference between the (1,1)-brane and the (1,-1)-brane is only a relative notion compared to other types of branes such as NS5 and D5, it is not surprising that they correspond to the same type of QFT building blocks with different charges. Assuming the 3d limit prescription involving the real mass deformation implemented by sending $\log c \rightarrow -\infty$, $\log d \rightarrow +\infty$ with hierarchy $\log(cd) \rightarrow -\infty$, one can distinguish the two branes by looking at the sign of the $U(1)_d$ charges of each block. For example, the left and right edges of the upper triangle of the \mathbf{B}_{11} block that appears on the l.h.s. of Figure 24 have $U(1)_d$ charges +1 and -1, leading to CS levels +1 and -1 in the 3d limit, respectively. This is consistent with the relation

$$\mathbf{B}_{11} = \mathbf{T}\mathbf{B}_{10}\mathbf{T}^{-1}, \tag{2.31}$$

which we will examine in the next subsection in detail. On the other hand, the edges of the lower triangle of the \mathbf{B}_{1-1} block that appears on the r.h.s. of Figure 24 have the $U(1)_d$ charges -1 and +1, leading to CS levels -1 and +1 in the 3d limit, respectively. One should remember that there are extra CS level contributions from $U(1)_c$ charged fields, but, as mentioned before, they turn out to be canceled when the blocks are glued to form an entire quiver theory.

2.3.2 T-dualization

We now consider dualities for the QFT building blocks generated by the T operator.

The $\mathbf{B}_{01} = \mathbf{T}\mathbf{B}_{01}\mathbf{T}^{-1}$ duality move. This move states that the \mathbf{B}_{01} block is transparent to the T-dualization. To show this, we first recall that $\mathbf{T}^{-1} = \mathbf{S}\mathbf{T}\mathbf{S}\mathbf{T}$. The quiver duality associated with this relation is then given in Figure 25, where according to our gluing prescription we turn on a cubic superpotential for each triangle. This duality trivially follows from the relation in Figure 10.

As an index identity we have

$$\mathcal{I}_{(0,1)}^{(N,N)}(\vec{x}; \vec{y}; u; t)$$

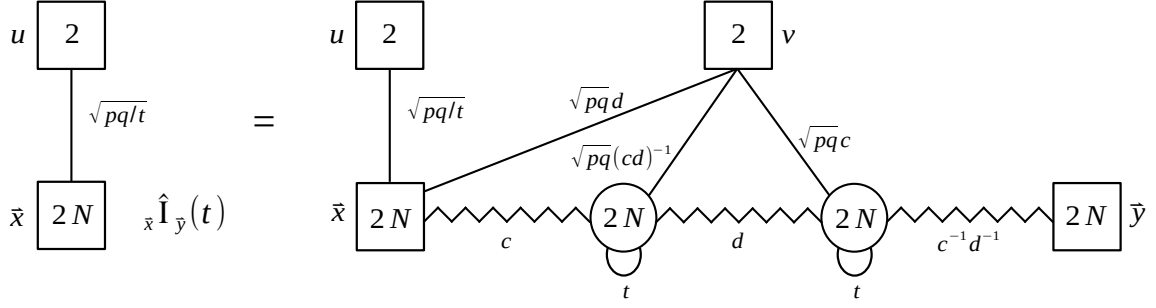


Figure 25. The $B_{01} = TB_{01}T^{-1} = TB_{01}STSTS$ duality move.

$$\begin{aligned}
&= \oint \left(\prod_{k=1}^6 dw_N^{(k)} \Delta_N(\vec{z}^{(k)}; t) \right) \mathcal{I}_T^{(N)}(\vec{x}; \vec{w}^{(1)}; v; t; d) \mathcal{I}_{(0,1)}^{(N,N)}(\vec{w}^{(1)}; \vec{w}^{(2)}; u; t) \\
&\quad \times \mathcal{I}_S^{(N)}(\vec{w}^{(2)}; \vec{w}^{(3)}; t; c) \mathcal{I}_T^{(N)}(\vec{w}^{(3)}; \vec{w}^{(4)}; v; t; c^{-1}d^{-1}) \mathcal{I}_S^{(N)}(\vec{w}^{(4)}; \vec{w}^{(5)}; t; d) \\
&\quad \times \mathcal{I}_T^{(N)}(\vec{w}^{(5)}; \vec{w}^{(6)}; v; t; c) \mathcal{I}_S^{(N)}(\vec{w}^{(6)}; \vec{y}; t; c^{-1}d^{-1}) \\
&= \oint \left(\prod_{i=1}^2 d\vec{z}_N^{(i)} \Delta_N(\vec{z}^{(i)}; t) \right) \prod_{j=1}^N \Gamma_e \left((pq/t)^{\frac{1}{2}} x_j^{\pm} u^{\pm} \right) \prod_{j=1}^N \Gamma \left((pq)^{\frac{1}{2}} dx_j^{\pm} v^{\pm} \right) \mathcal{I}_S^{(N)}(\vec{x}; \vec{z}^{(1)}; t; c) \\
&\quad \times \prod_{j=1}^N \Gamma \left((pq)^{\frac{1}{2}} c^{-1} d^{-1} z_j^{(1)\pm} v^{\pm} \right) \mathcal{I}_S^{(N)}(\vec{z}^{(1)}; \vec{z}^{(2)}; t; d) \prod_{j=1}^N \Gamma \left((pq)^{\frac{1}{2}} cz_j^{(2)\pm} v^{\pm} \right) \\
&\quad \times \mathcal{I}_S^{(N)}(\vec{z}^{(2)}; \vec{y}; t; c^{-1}d^{-1}). \tag{2.32}
\end{aligned}$$

The $B_{11} = TB_{10}T^{-1}$ duality move. The quiver representation of this duality move is given in Figure 26. We can convince ourselves that the superpotentials are consistent with our gluing rules by observing that since $B_{10} = SB_{01}S$, we have $B_{11} = TB_{10}STSTS = TSB_{01}TSTS$ which is shown (for simplicity for $N = M$) in Figure 27 and is clearly consistent with the rule of turning on the cubic superpotential in (2.16) whenever an S-wall is sandwiched between two T-walls.

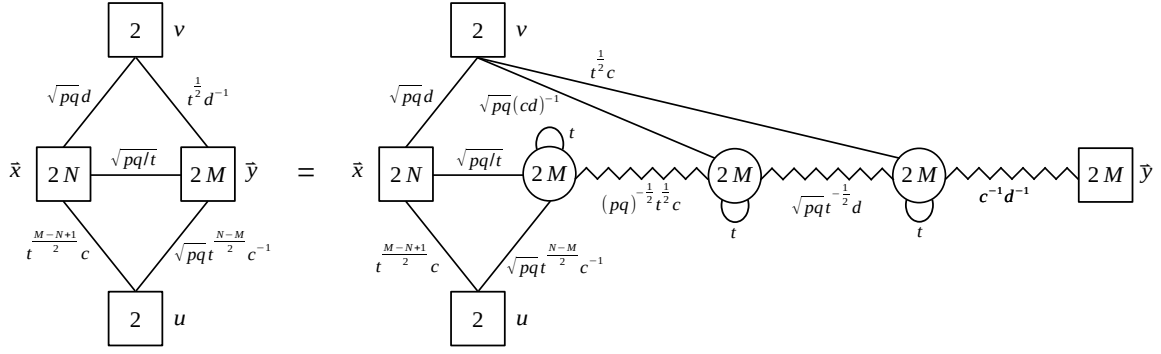


Figure 26. The $B_{11} = TB_{10}\Gamma^{-1} = TB_{10}STSTS$ duality move.

At the level of the index we have

$$\begin{aligned}
\mathcal{I}_{(1,1)}^{(N,M)}(\vec{x}; \vec{y}; v; u; t; c; d) &= \oint \left(\prod_{k=1}^6 dw_N^{(k)} \Delta_N(\vec{z}^{(k)}; t) \right) \mathcal{I}_{\Gamma}^{(N)}(\vec{x}; \vec{w}^{(1)}; v; t; d) \mathcal{I}_{(1,0)}^{(N,M)}(\vec{w}^{(1)}; \vec{w}^{(2)}; u; t; c) \\
&\quad \times \mathcal{I}_{\mathcal{S}}^{(M)}(\vec{w}^{(2)}; \vec{w}^{(3)}; t; (pq/t)^{-\frac{1}{2}}c) \mathcal{I}_{\Gamma}^{(M)}(\vec{w}^{(3)}; \vec{w}^{(4)}; v; t; c^{-1}d^{-1}) \mathcal{I}_{\mathcal{S}}^{(M)}(\vec{w}^{(4)}; \vec{w}^{(5)}; t; (pq/t)^{\frac{1}{2}}d) \\
&\quad \times \mathcal{I}_{\Gamma}^{(M)}(\vec{w}^{(5)}; \vec{w}^{(6)}; v; t; c) \mathcal{I}_{\mathcal{S}}^{(M)}(\vec{w}^{(6)}; \vec{y}; t; c^{-1}d^{-1}) \\
&= \oint \left(\prod_{i=1}^3 dz_M^{(i)} \Delta_M(\vec{z}^{(i)}; t) \right) \prod_{j=1}^N \Gamma((pq)^{\frac{1}{2}} dx_j^{\pm} v^{\pm}) \mathcal{I}_{(1,0)}^{(N,M)}(\vec{x}; \vec{z}^{(1)}; u; t; c) \\
&\quad \times \mathcal{I}_{\mathcal{S}}^{(M)}(\vec{z}^{(1)}; \vec{z}^{(2)}; t; (pq/t)^{-\frac{1}{2}}c) \prod_{j=1}^M \Gamma((pq)^{\frac{1}{2}} c^{-1} d^{-1} z_j^{(2)\pm} v^{\pm}) \mathcal{I}_{\mathcal{S}}^{(M)}(\vec{z}^{(2)}; \vec{z}^{(3)}; t; (pq/t)^{\frac{1}{2}}d) \\
&\quad \times \prod_{j=1}^M \Gamma(t^{\frac{1}{2}} cz_j^{(3)\pm} v^{\pm}) \mathcal{I}_{\mathcal{S}}^{(M)}(\vec{z}^{(3)}; \vec{y}; t; c^{-1}d^{-1}). \tag{2.33}
\end{aligned}$$

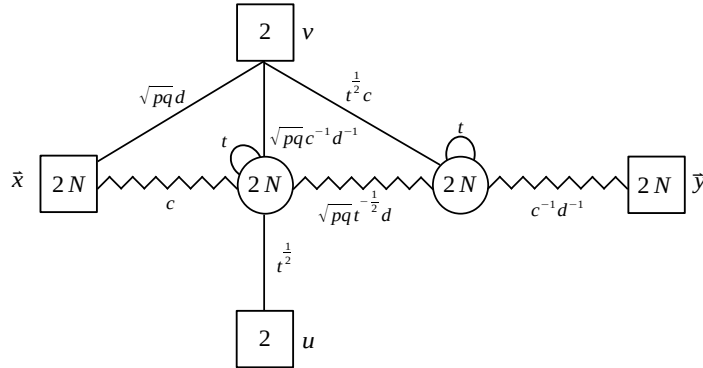


Figure 27. The quiver representation of $TSB_{01}TSTS$, which is equal to $B_{11} = TB_{10}STSTS$. To obtain this quiver from the one on the right of Figure 26, we use the duality move $B_{10} = SB_{01}S$ of Figure 21.

The duality move of Figure 26 can be easily proven by applying the braid duality move of Figure 8 to the second gauge node on the r.h.s., removing the massive fields and reconstructing an Identity-wall from the fusion of the last two S-walls.

The $\mathbf{B}_{10} = \mathbf{TB}_{1-1}\mathbf{T}^{-1}$ duality move. The quiver associated with this duality move is given in Figure 28, and the corresponding index identity is given by

$$\begin{aligned}
& \mathcal{I}_{(1,0)}^{(N,M)}(\vec{x}; \vec{y}; u; t; c) \\
&= \oint \left(\prod_{i=1}^3 dz_M^{(i)} \Delta_M(\vec{z}^{(i)}; t) \right) \prod_{j=1}^N \Gamma((pq)^{\frac{1}{2}} dx_j^{\pm} v^{\pm}) \mathcal{I}_{(1,1)}^{(N,M)}(\vec{x}; \vec{z}^{(1)}; v; u; t; c; d^{-1}) \\
&\quad \times \mathcal{I}_S^{(M)}(\vec{z}^{(1)}; \vec{z}^{(2)}; t; cd^{-1}) \prod_{j=1}^M \Gamma(pqt^{-\frac{1}{2}} c^{-1} z_j^{(2)\pm} v^{\pm}) \mathcal{I}_S^{(M)}(\vec{z}^{(2)}; \vec{z}^{(3)}; t; (pq/t)^{-\frac{1}{2}} d) \\
&\quad \times \prod_{j=1}^M \Gamma((pq)^{\frac{1}{2}} cd^{-1} z_j^{(3)\pm} v^{\pm}) \mathcal{I}_S^{(M)}(\vec{z}^{(3)}; \vec{y}; t; (pq/t)^{\frac{1}{2}} c^{-1}), \tag{2.34}
\end{aligned}$$

where from now on we will only give the expressions where we have already replaced the contribution of the T-walls and simplified all Identity-walls.

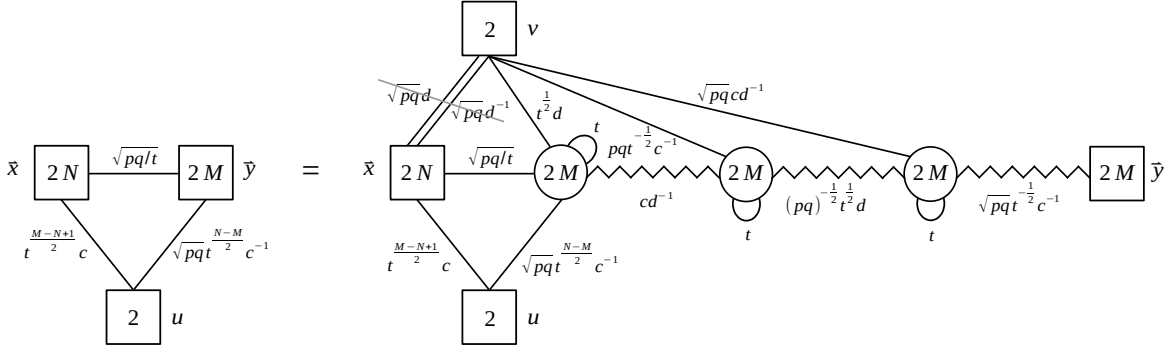


Figure 28. The $\mathbf{B}_{10} = \mathbf{TB}_{1-1}\mathbf{T}^{-1} = \mathbf{TB}_{1-1}\mathbf{STSTS}$ duality move. On the r.h.s. we included two massive fields (barred by the grey line) to explicitly display the \mathbf{B}_{1-1} block between the T and \mathbf{T}^{-1} operators.

Notice that on the r.h.s. there is an $SU(2)_v$ symmetry that instead doesn't appear on the l.h.s.. Related to this, we can see that in the index identity (2.34) the fugacity v appears on the r.h.s. but not on the l.h.s.. Nevertheless, the identity holds for any value of v , which tells us that also the r.h.s. is secretly independent of it. Remember that the index is counting operators in our theory graded by their quantum numbers, as one can see by expanding it as a power series. Each term of the expansion indeed corresponds to an operator in the theory whose quantum numbers are encoded in the powers of the corresponding fugacity that appear. We can then understand our observation as the fact that there is no operator in the spectrum of our theory that transforms under $SU(2)_v$, or in other words, the symmetry acts

trivially on the spectrum of the low energy theory. Consistently with this, we find that all the anomalies involving $SU(2)_v$ vanish. We will see many examples of this phenomenon in the rest of the paper.

Again this duality move can be easily proven by applying the braid duality move of Figure 8 to the second gauge node on the r.h.s., removing the massive fields and reconstructing an Identity-wall from the fusion of the last two S-walls.

2.3.3 \mathbf{T}^T -dualization

Finally, we consider dualities for the QFT building blocks generated by the \mathbf{T}^T operator.

The $\mathbf{B}_{11} = \mathbf{T}^T \mathbf{B}_{01} (\mathbf{T}^T)^{-1}$ duality move. Remembering that $(\mathbf{T}^T)^{-1} = \text{STS}$ we find that the duality move associated with this relation is as given in Figure 29.

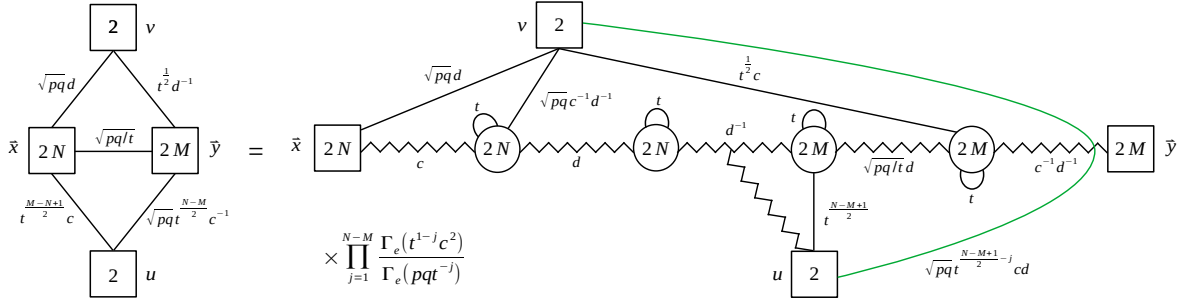


Figure 29. The $\mathbf{B}_{11} = \mathbf{T}^T \mathbf{B}_{01} (\mathbf{T}^T)^{-1}$ duality move. The green line denotes gauge singlet fields labelled by $j = 1, \dots, N - M$.

At the level of the index this translates into the identity

$$\begin{aligned}
& \mathcal{I}_{(1,1)}^{(N,M)}(\vec{x}; \vec{y}; v; u; t; c; d) \\
&= \prod_{j=1}^{N-M} \frac{\Gamma_e(t^{1-j}c^2)}{\Gamma_e(pqt^{-j})} \Gamma_e\left((pq)^{\frac{1}{2}} t^{\frac{N-M+1}{2}-j} cdv^{\pm} u^{\pm}\right) \\
&\quad \times \oint d\vec{z}_N \Delta_N(\vec{z}; t) \left(\prod_{i=1}^2 d\vec{w}_M^{(i)} \Delta_M(\vec{w}^{(i)}; t) \right) \prod_{j=1}^N \Gamma((pq)^{\frac{1}{2}} dx_j^{\pm} v^{\pm}) \\
&\quad \times \mathcal{I}_S^{(N)}(\vec{x}; \vec{z}; t; c) \prod_{j=1}^N \Gamma((pq)^{\frac{1}{2}} c^{-1} d^{-1} z_j^{\pm} v^{\pm}) \mathcal{I}_{(0,1)}^{(N,M)}(\vec{z}; \vec{w}^{(1)}; u; pq/t) \\
&\quad \times \mathcal{I}_S^{(M)}(\vec{w}^{(1)}; \vec{w}^{(2)}; t; (pq/t)^{\frac{1}{2}} d) \prod_{j=1}^M \Gamma(t^{\frac{1}{2}} cw_j^{\pm} v^{\pm}) \mathcal{I}_S^{(M)}(\vec{w}^{(2)}; \vec{y}; t; c^{-1} d^{-1}), \quad (2.35)
\end{aligned}$$

where $\mathcal{I}_{(0,1)}^{(N,M)}(\vec{x}; \vec{y}; u; t)$ is defined in (2.24). We give a proof of this duality in Appendix C.

The $\mathbf{B}_{10} = \mathbf{T}^T \mathbf{B}_{10} (\mathbf{T}^T)^{-1}$ duality move. This move states that the \mathbf{B}_{10} block is transparent to the \mathbf{T}^T -dualization. The corresponding duality move is represented in Figure 30.

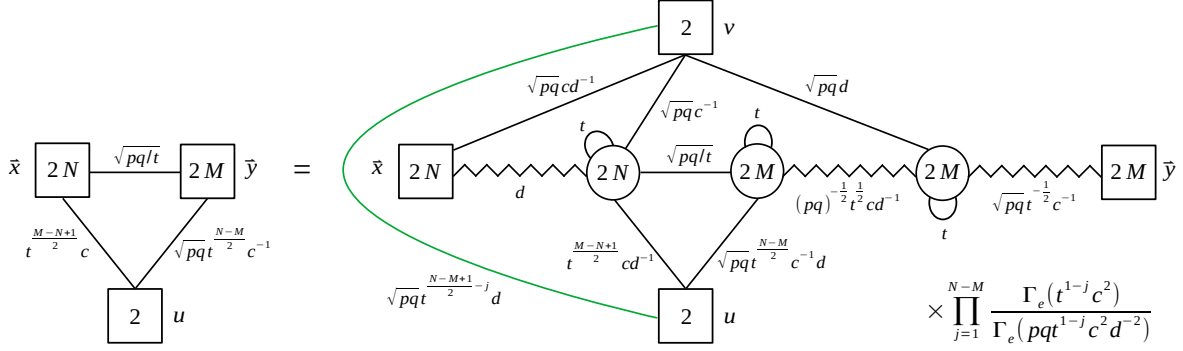


Figure 30. The $\mathbf{B}_{10} = \mathbf{T}^T \mathbf{B}_{10} (\mathbf{T}^T)^{-1}$ duality move. The green line denotes gauge singlet fields labelled by $j = 1, \dots, N - M$.

The index identity associated to this duality is

$$\begin{aligned}
& \mathcal{I}_{(1,0)}^{(N,M)}(\vec{x}; \vec{y}; u; t; c) \\
&= \prod_{j=1}^{N-M} \frac{\Gamma_e(t^{1-j} c^2)}{\Gamma_e(t^{1-j} c^2 d^{-2})} \Gamma_e\left((pq)^{\frac{1}{2}} t^{\frac{N-M+1}{2} - j} d\right) \\
&\quad \times \oint d\vec{z}_N \Delta_N(\vec{z}; t) \left(\prod_{i=1}^2 d\vec{w}_M^{(i)} \Delta_M(\vec{w}^{(i)}; t) \right) \prod_{j=1}^N \Gamma\left((pq)^{\frac{1}{2}} cd^{-1} x_j^{\pm} v^{\pm}\right) \mathcal{I}_S^{(N)}(\vec{x}; \vec{z}; t; d) \\
&\quad \times \prod_{j=1}^N \Gamma\left((pq)^{\frac{1}{2}} c^{-1} z_j^{\pm} v^{\pm}\right) \mathcal{I}_{(1,0)}^{(N,M)}(\vec{z}; \vec{w}^{(1)}; u; t; cd^{-1}) \mathcal{I}_S^{(M)}(\vec{w}^{(1)}; \vec{w}^{(2)}; t; (pq/t)^{-\frac{1}{2}} cd^{-1}) \\
&\quad \times \prod_{j=1}^M \Gamma\left((pq)^{\frac{1}{2}} dw_j^{(2)\pm} v^{\pm}\right) \mathcal{I}_S^{(M)}(\vec{w}^{(2)}; \vec{y}; t; (pq/t)^{\frac{1}{2}} c^{-1}). \tag{2.36}
\end{aligned}$$

We give a proof of this duality move in Appendix C.

The $\mathbf{B}_{01} = \mathbf{T}^T \mathbf{B}_{1-1} (\mathbf{T}^T)^{-1}$ duality move. Finally, we have the \mathbf{T}^T dual of a \mathbf{B}_{1-1} block giving a \mathbf{B}_{01} block, which we represent in Figure 31. The resulting index identity is given by

$$\begin{aligned}
& \prod_{j=1}^N \Gamma_e\left((pq/t)^{\frac{1}{2}} x_j^{\pm} u^{\pm}\right) \hat{\vec{x}} \hat{\vec{y}}(t) \\
&= \oint \left(\prod_{i=1}^3 d\vec{z}_N^{(i)} \Delta_N(\vec{z}^{(i)}; t) \right) \prod_{j=1}^N \Gamma\left((pq)^{\frac{1}{2}} cd^{-1} x_j^{\pm} v^{\pm}\right) \mathcal{I}_S^{(M)}(\vec{x}; \vec{z}^{(1)}; t; c^{-1}) \\
&\quad \times \prod_{j=1}^N \Gamma\left((pq)^{\frac{1}{2}} dz_j^{(1)\pm} v^{\pm}\right) \mathcal{I}_{(1,1)}^{(N)}(\vec{z}^{(1)}; \vec{z}^{(2)}; v; u; pq/t; c; d^{-1}) \mathcal{I}_S^{(N)}(\vec{z}^{(2)}; \vec{z}^{(3)}; t; cd^{-1}) \\
&\quad \times \prod_{j=1}^N \Gamma\left((pqt)^{\frac{1}{2}} c^{-1} z_j^{(3)\pm} v^{\pm}\right) \mathcal{I}_S^{(M)}(\vec{z}^{(3)}; \vec{y}; t; t^{-\frac{1}{2}} d). \tag{2.37}
\end{aligned}$$

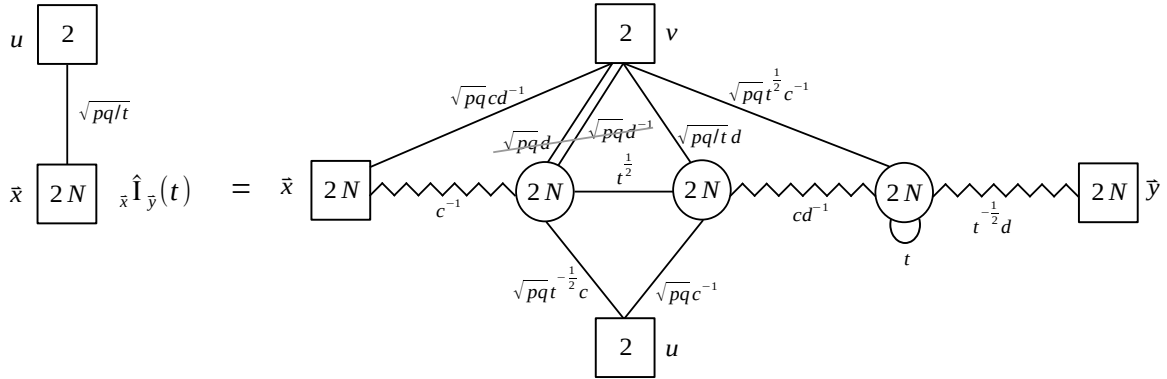


Figure 31. The $B_{01} = T^T B_{1-1} (T^T)^{-1}$ duality move. On the r.h.s. two massive fields are included to explicitly display the B_{1-1} block between the T^T and $(T^T)^{-1}$ operators.

We give a proof of this duality move in Appendix C.

3 Dualization algorithm, VEVs, RG flows and HW moves

In this section, we describe the local dualization algorithm using the ingredients we introduced in the previous section. Specifically, we illustrate the implementation of each step in the mirror-dualization of the SQCD.

The first step of the dualization algorithm consist in chopping a theory into QFT blocks by un-gauging each gauge node. This step produces several QFT blocks as well as non-dynamical vector multiplets and chiral fields in the antisymmetric representations of the frozen gauge symmetries. It is important to keep track of these fields to restore the correct gauging after the dualization.

In the second step, we dualize each QFT block by means of the basic duality moves.

In the third step, we restore the gauging of the original gauge nodes, which generates several Identity-walls. In case only symmetric Identity-walls are generated we just need to implement them to read out the dual theory. If asymmetric walls are generated instead, we need to take care of their effect since fields generically acquire VEVs when we implement the identifications that the asymmetric walls prescribe.

In the fourth step, when necessary, we study the RG flow triggered by these VEVs to obtain the final IR dual theory. There are various strategies we can follow at this point. We will see below how we can efficiently study the sequential Higgsing generated by these VEVs at the level of the index or alternatively we can reach the final IR configuration by a sequential applications of the IP duality, which basically trades VEVs for massive deformations.

We will also see a third strategy where the effect of this sequential Higgsing or the iteration of the IP duality is modularized into a new duality move shown in Figure 32, which we prove in Appendix D.

We call this duality move, which swaps a B_{01} with a B_{10} block, the Hanany–Witten (HW) duality move because, as we will see in Section 4, its $3d$ version exactly corresponds to the

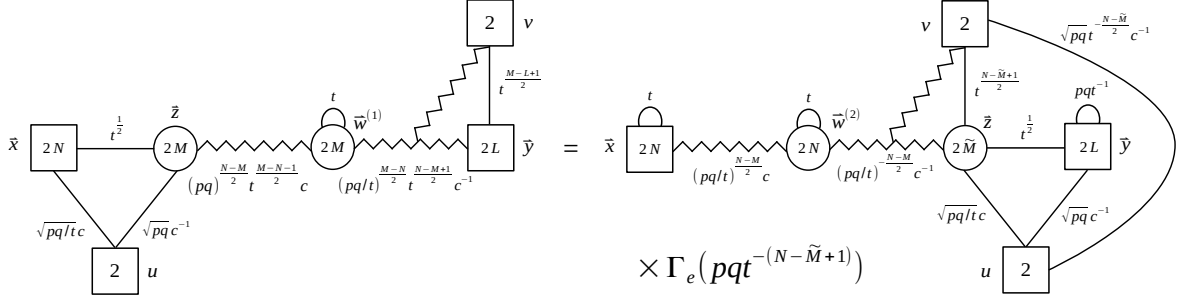


Figure 32. The Hanany–Witten duality move. Notice that on the r.h.s. the rank of the second gauge node is now $\widetilde{M} = N + L - M + 1$.

local effect of an HW brane move in the brane set-up realizing the 3d quiver theory. For $N \geq \widetilde{M} \geq 0$, the associated index identity is given by

$$\begin{aligned}
& \oint d\vec{z}_M \Delta_M(\vec{z}) \mathcal{I}_{(1,0)}^{(N,M)}(\vec{x}; \vec{z}; u; pqt^{-1}; c(pqt^{-1})^{\frac{N-M}{2}}) \hat{z}^{\pm} \hat{y}, v(t) \prod_{k=1}^L \Gamma_e\left(t^{\frac{M-L+1}{2}} y_k^{\pm} v^{\pm}\right) \\
&= \Gamma_e\left(pqt^{-(N-\widetilde{M}+1)}\right) \Gamma_e\left((pq)^{\frac{1}{2}} t^{-\frac{N-\widetilde{M}}{2}} c^{-1} u^{\pm} v^{\pm}\right) A_N(\vec{x}; t) A_L(\vec{y}; pq/t) \\
& \quad \times \oint d\vec{z}_{\widetilde{M}} \Delta_{\widetilde{M}}(\vec{z}) \hat{x}^{\pm} \hat{z}, v(t) \prod_{j=1}^{\widetilde{M}} \Gamma_e\left(t^{\frac{N-\widetilde{M}+1}{2}} z_j^{\pm} v^{\pm}\right) \mathcal{I}_{(1,0)}^{(\widetilde{M},L)}(\vec{z}; \vec{y}; u; pqt^{-1}; c(pqt^{-1})^{\frac{\widetilde{M}-L}{2}}).
\end{aligned} \tag{3.1}$$

With few manipulations, we can recombine the terms $\hat{z}^{\pm} \hat{y}, v(t) \prod_{k=1}^L \Gamma_e\left(t^{\frac{M-L+1}{2}} y_k^{\pm} v^{\pm}\right)$ in the first line into $\mathcal{I}_{(0,1)}^{(M,L)}(\vec{z}; \vec{y}; v; pq/t)$ (up to some factors) and similarly on the third line, to explicitly display the swap of a $\mathcal{B}_{(0,1)}$ with a $\mathcal{B}_{(1,0)}$ block. The manipulations involve performing flip-flip duality (see for example eq. (2.14) in [22]) on all the S-walls so to produce Identity-walls with fugacity pq/t . However we prefer to keep the formula as it is, since this is the most convenient form to implement the dualizations.

As we will see in Subsection 3.4, we can obtain the final configuration of the mirror dual theory by repeating this HW duality move, performing the field theory counterpart of the brane rearrangement that is needed to reach a configuration where there is a zero net number of D3-branes ending on the the D5-branes and so it is possible to read out the QFT.

Summarizing, if asymmetric Identity-walls are generated after the dualization of the QFT blocks, we can study their effect by using the sequential Higgsing, the IP iteration, or the HW duality move to obtain the final IR $PSL(2, \mathbb{Z})$ dual theory. We will illustrate these three strategies in the case of the SQCD in the following subsections.

3.1 S-dualization of SQCD

We will focus on the example of the 4d $\mathcal{N} = 1$ $USp(2N)$ SQCD with $2N_f + 4$ fundamental chirals and $N_f \geq 2N$, represented on the left of Figure 33. This theory corresponds to the

element $\rho = [N_f - N, N]$, $\sigma = [1^{N_f}]$ of the $E_\rho^\sigma[USp(2N)]$ family studied in [24] and reduces to the $U(N)$ SQCD with N_f flavors in the $3d$ limit.

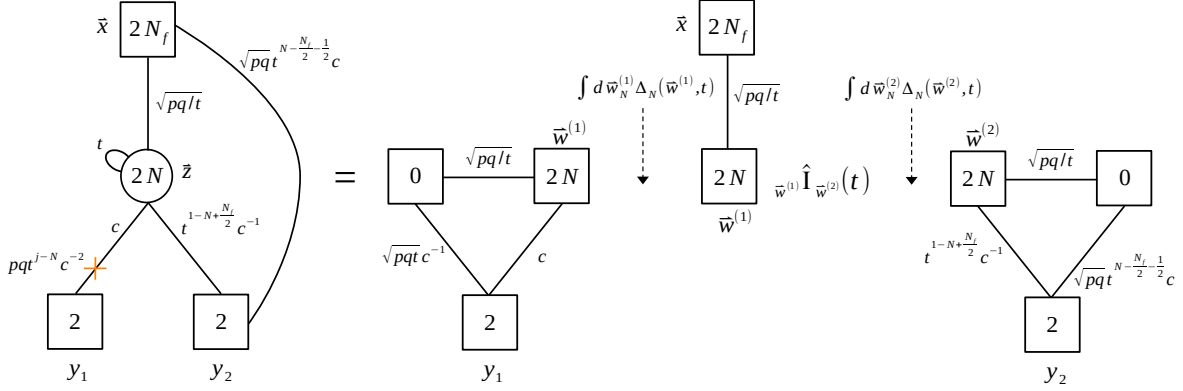


Figure 33. The SQCD and its block decomposition. The orange cross denotes a tower of singlets flipping the meson dressed with the j -th power of the antisymmetric with $j = 0, \dots, N - 1$. We also explicitly indicate the frozen integration measure containing vector and antisymmetric chiral fields. Notice that we add trivial lines to reconstruct the triangle structure that identifies the B_{10} blocks.

This theory can be decomposed into QFT blocks as shown on the right of Figure 33. When we chop it into the blocks, to avoid clutter, we remove the singlets of the original SQCD, the orange cross indicating a tower of singlets flipping the y_1 meson dressed up to the $(N - 1)$ th power of the antisymmetric field and the $SU(2)_{y_2} \times USp(2N_f)$ bifundamental. We will always adopt this convention of removing singlets before chopping theories into QFT blocks, then perform all the duality moves, and restore the original singlets after reaching the dual theory.

We now dualize each QFT block using the basic S-duality moves of Figures 21 and 22 and glue them back by restoring the original gauge symmetries. This results in the dualized quiver shown in Figure 34. The extra singlets we get from the dualization are denoted in the figure by their index contributions.

We can now implement the identifications of the asymmetric Identity-walls at the two sides of the quiver, which specialize the gauge fugacities $\bar{z}^{(0)}$ and $\bar{z}^{(N_f)}$ of the leftmost and rightmost nodes in a geometric progression as

$$z_j^{(0)} = t^{\frac{N+1-2j}{2}} y_1, \quad z_j^{(N_f)} = t^{\frac{N+1-2j}{2}} y_2, \quad j = 1, \dots, N, \quad (3.2)$$

to arrive at the quiver in Figure 35. The blue lines indicate two sets of N chirals in the bifundamental of $SU(2)_{y_1} \times USp(2N)_{z^{(1)}}$ and that of $SU(2)_{y_2} \times USp(2N)_{z^{(N_f-1)}}$, respectively. They contribute to the index by

$$\prod_{i=1}^N \Gamma_e \left(t^{a-\frac{N}{2}} z_i^{(1)\pm} y_1^\pm \right), \quad \prod_{i=1}^N \Gamma_e \left(t^{a-\frac{N}{2}} z_i^{(N_f-1)\pm} y_2^\pm \right) \quad a = 0, 1, \dots, N. \quad (3.3)$$

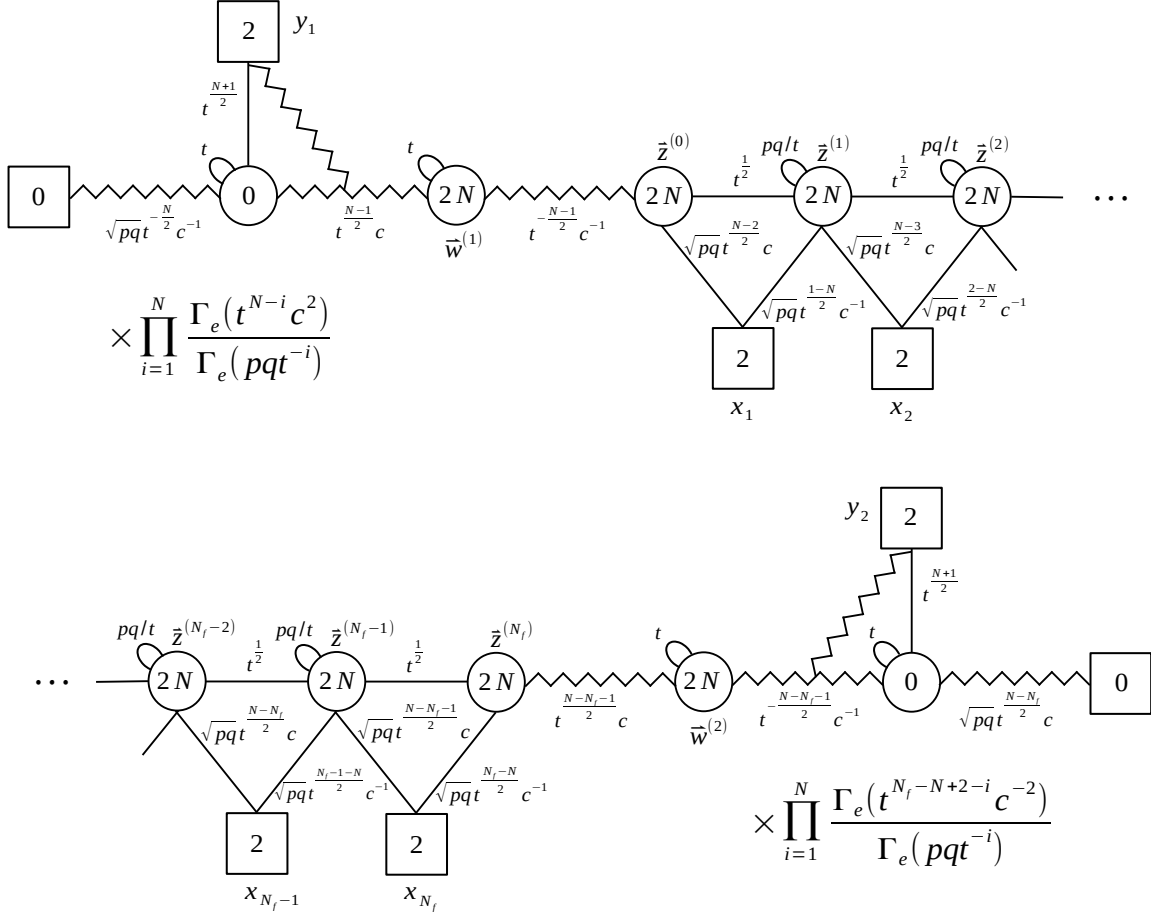


Figure 34. Result of the block dualization of the SQCD.

In addition, we have the following singlets coming from the dualization:

$$\begin{aligned}
& \widehat{A}_N(y_1; pq/t) \prod_{a=1}^N \Gamma_e \left(\sqrt{pqt}^{N-1/2-a} c x_1^\pm y_1^\pm \right) \frac{\Gamma_e(t^{N_c-a} c^2)}{\Gamma_e(pqt^{-a})} \\
& \times \widehat{A}_N(y_2; pq/t) \prod_{a=1}^N \Gamma_e \left(\sqrt{pqt}^{a-N+\frac{N_f-1}{2}} c^{-1} x_{N_f}^\pm y_2^\pm \right) \frac{\Gamma_e(t^{N_f-N_c+2-a} c^{-2})}{\Gamma_e(pqt^{-a})}, \quad (3.4)
\end{aligned}$$

where we defined

$$\widehat{A}_N(v; pq/t) = A_N \left(t^{\frac{N-1}{2}} v, \dots, t^{\frac{1-N}{2}} v; pq/t \right). \quad (3.5)$$

Now we have reached a quiver theory with no duality-walls left. As we are going to see shortly, there are some VEVs which trigger an RG flow, which we study in several ways in the following subsections.

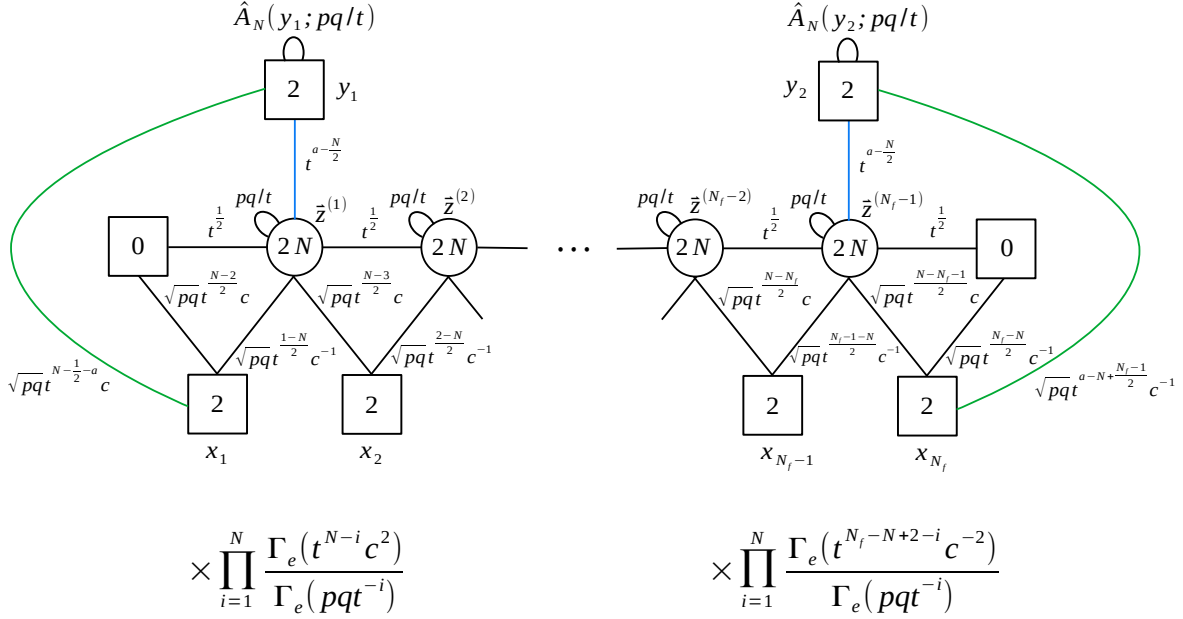


Figure 35. Result of the S-dualization of the SQCD. The blue and green legs denote sets of chirals labelled by $a = 1, \dots, N$. Mesons constructed with blue chirals acquire a VEV.

3.2 Method I: VEV propagation via sequential Higgsing

In the quiver in Figure 35, some of the mesons constructed with the chirals in blue acquire VEVs Higgsing the first and last node down to $SU(2)$. At the level of the index, following the strategy of [95], this can be seen by noticing that, for example, the $a = 1, N - 1$ chirals in the first set of eq. (3.3) can be paired up as

$$\prod_{i=1}^N \Gamma_e \left(t^{1-\frac{N}{2}} z_i^{(1)\pm} y_1^{\pm} \right) \Gamma_e \left(t^{\frac{N}{2}-1} z_i^{(1)\pm} y_1^{\pm} \right) = \prod_{i=1}^N \Gamma_e \left(z_i^{(1)\pm} (t^{1-\frac{N}{2}} y_1)^{\pm} \right) \Gamma_e \left(z_i^{(1)\pm} (t^{\frac{N}{2}-1} y_1)^{\pm} \right). \quad (3.6)$$

On the r.h.s., we have two gamma functions such that the product of their arguments is 1, signaling that the meson constructed from the corresponding chirals is uncharged under all the abelian symmetries including the R-symmetry and is thus taking a VEV. In that case, the location of the poles of these gamma functions collide and pinch the integration contour at two points, say at $z_1^{(1)} = t^{1-\frac{N}{2}} y_1$ and $z_{N-1}^{(1)} = t^{\frac{N}{2}-1} y_1$. Similarly, all the other chirals in

(3.3) but $a = 0$, N pair up producing colliding poles that pinch the integration contour at

$$\begin{cases} z_1^{(1)} = t^{1-\frac{N}{2}} y_1, \\ z_2^{(1)} = t^{2-\frac{N}{2}} y_1, \\ \vdots \\ z_{N-2}^{(1)} = t^{(N-2)-\frac{N}{2}} y_1, \\ z_{N-1}^{(1)} = t^{(N-1)-\frac{N}{2}} y_1, \\ z_N^{(1)} = \tilde{z}^{(1)}, \end{cases} \quad (3.7)$$

and an analogous freezing condition is imposed on the last $\tilde{z}^{(N_f-1)}$ node. The index after Higgsing is obtained by evaluating the residues at such points. Notice that when we evaluate the residues, there are pairs of poles and zeros canceling each other, coming from $\Gamma_e(1)$ contained in (3.3) and $\Gamma_e(pq)$ contained in $A_N(y_1, pq/t)$ and $A_N(y_2, pq/t)$, respectively.

Let's now focus on the left part of the quiver. Taking the residues at these poles, we obtain the theory after the Higgsing induced by the VEV shown in Figure 36. We now have $N - 1$ chirals (in blue) in the bifundamental of $SU(2)_{y_1} \times USp(2N)_{z^{(2)}}$ contributing to the index as

$$\prod_{i=1}^N \Gamma_e \left(t^{a-\frac{N-1}{2}} z_i^{(2)\pm} y_1^\pm \right) \quad a = 0, 1, \dots, N-1, \quad (3.8)$$

which now Higgs the leftmost $USp(2N)$ node, next to the $USp(2)$ node, down to $USp(4)$. Indeed we have $N - 2$ colliding poles and $N - 2$ zeros from the singlets $A_{N-1}(y_1, pq/t)$.

We can iterate this procedure N times creating a tail of nodes with increasing ranks as in Figure 37. Now there are no blue legs, the vertical chirals interact with a cubic superpotential with the antisymmetric

$$\prod_{i=1}^N \Gamma \left(t^{\frac{1}{2}} z_i^{(N)\pm} y_1^\pm \right), \quad \prod_{i=1}^N \Gamma \left(t^{\frac{1}{2}} z_i^{(N_f-N)\pm} y_2^\pm \right), \quad (3.9)$$

and there are no $A_k(y_1, pq/t)$ singlets, so no zeros. Therefore, there is no further VEV to implement. Repeating the procedure on the right part of the quiver and restoring the singlets of the original SQCD that we dropped when we chopped it into QFT blocks, we obtain the mirror dual shown in Figure 38. Notice that some of the singlets produced by the Higgsing cancel out with the original singlets, and we are left with the correct mirror dual of the $4d$ SQCD found in [24].

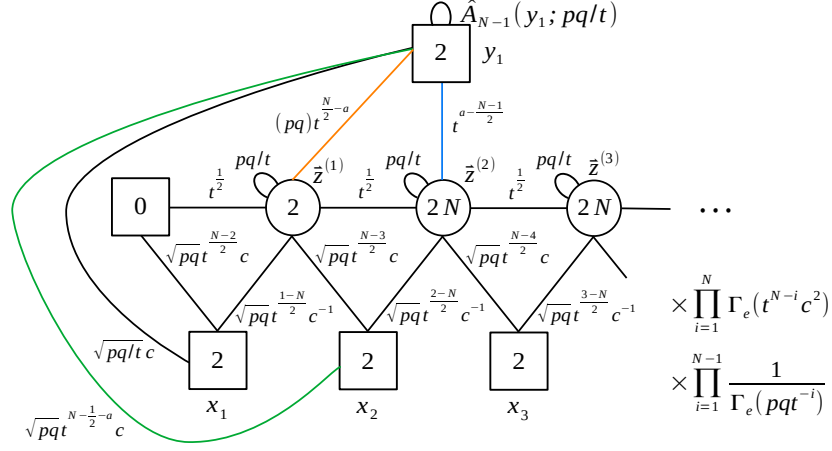


Figure 36. The result of the Higgsing of the leftmost $USp(2N)$ gauge node. The blue line denotes a set of chirals with $a = 1, \dots, N - 1$, the orange line denotes a set of chirals with $a = 2, \dots, N - 1$, while the green leg denotes a set of chirals with $a = 2, \dots, N$. Again the mesons constructed with the blue legs acquire a VEV.

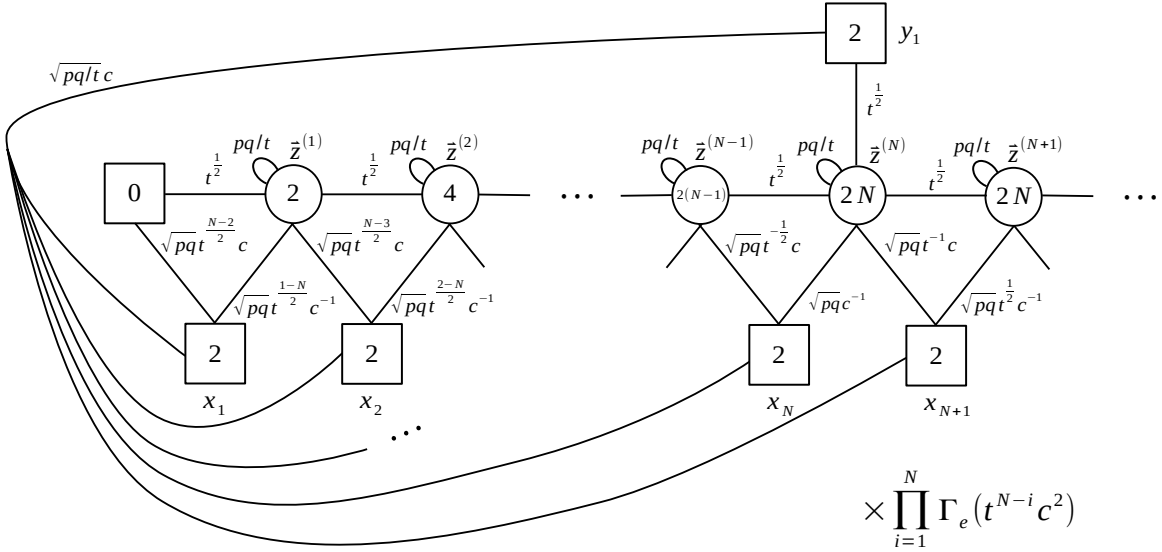


Figure 37. The final result of the sequential Higgsing. In this configuration there are no VEVs turned on.

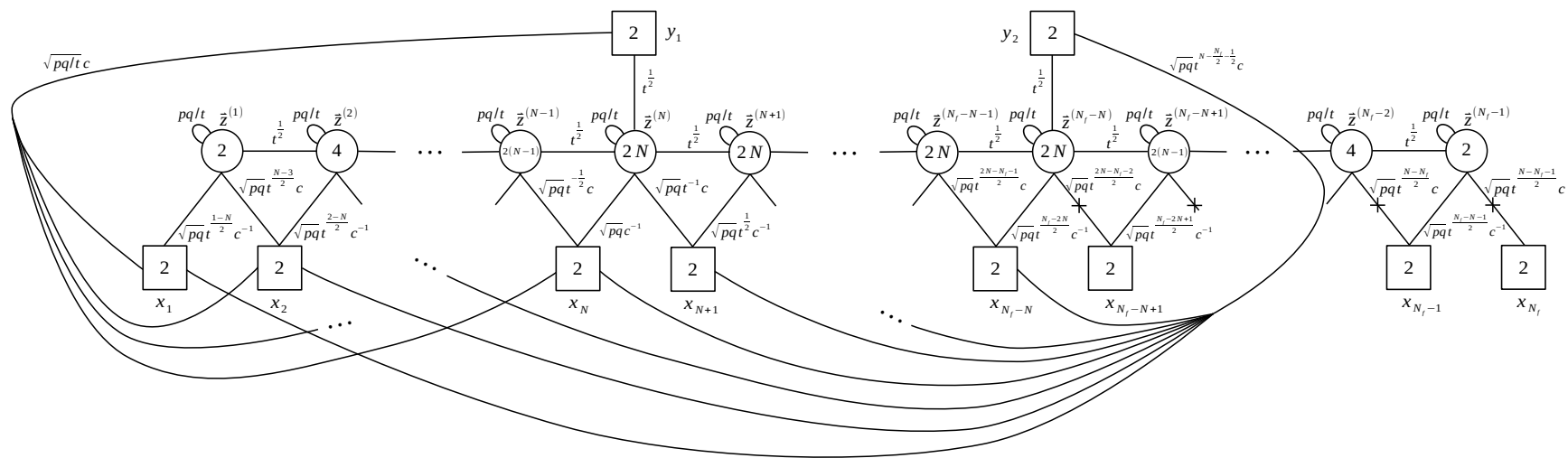


Figure 38. Mirror of the SQCD.

3.3 Method II: VEV propagation via the IP duality

The sequential Higgs mechanism due to the VEV propagation explained in the previous subsection can alternatively be implemented by iteratively applying the IP duality, basically trading VEVs for massive deformations. The idea is similar to the correspondence between the mass deformation and the Higgsing under the Seiberg duality [1].

Let's go back to the quiver in Figure 35. We focus again on the l.h.s. of the quiver and use the relation shown in Figure 39 and proved in Appendix F to trade the N bifundamentals chirals (in blue) for a single bifundamental.

$$\begin{aligned}
 \bar{x} \quad \boxed{2N} \xrightarrow[t^{1+\frac{N}{2}-j}]{} \boxed{2} \quad v \quad \hat{A}_N(v; pq/t) &= \bar{x} \quad \boxed{2N} \xrightarrow[t^{1-\frac{N}{2}}]{} \boxed{2} \quad v \\
 &\times \prod_{j=1}^N \Gamma_e(pqt^{j-2}) \Gamma_e(pqt^{-j})
 \end{aligned}$$

Figure 39. A relation between two WZ models. On the l.h.s. the blue leg denotes a set of chirals with $j = 1, \dots, N$.

The result is given by the first quiver in Figure 40. Notice that, since the first node $USp(2N)_{z(1)}$ (in orange) has no antisymmetric field, we can apply the IP duality to it, so to obtain the second quiver theory in Figure 40 where the dualized gauge node has now become $USp(2)_{z(1)}$. As an effect of the dualization, the y_1 flavor node has now *moved*: we have a y_1 flavor connected to the $USp(2N)_{z(2)}$ node with $U(1)_t$ charge increased by $1/2$, and a y_1 flavor connected to the $USp(2N)_{z(1)}$ node with charge $\sqrt{pqt}^{\frac{N}{2}-1}$. Also, some singlets are produced and some are cancelled. Consider, for example, the tower of N $SU(2)_{y_1} \times SU(2)_{x_1}$ bifundamental singlets: one of them is cancelled and instead one $SU(2)_{y_1} \times SU(2)_{x_2}$ bifundamental singlet is produced. Moreover, the legs of the saw are reorganized such that now x_1 is *swapped* with x_2 .

Another effect of the dualization was to give mass to the antisymmetric chiral of the adjacent $USp(2N)_{z(2)}$ (in red in the second quiver of Figure 40) so that we can apply again the IP duality to it and obtain the third quiver where the dualized gauge node is now $USp(4)_{z(2)}$. Notice that the y_1 flavor node keeps moving to the right. Also, x_1 keeps moving to the right.

It is clear that we can keep iterating this application of the IP duality, since at each step we remove the antisymmetric at the node on the right of the dualized one and restore the one at the node on the left. After $N-2$ steps, we reach the first quiver in the second line of Figure 40, where we have created a tail of gauge nodes with increasing ranks: $USp(2)$, $USp(4)$, and so on up to $USp(2N-4)$. Now the y_1 flavor node is attached to the $USp(2N)_{z(N-1)}$ gauge node with a chiral of charge t^0 , that is uncharged under all abelian symmetries. This indicates that the associated meson is taking a VEV, which triggers a Higgsing that we could implement by taking the residues at colliding poles as we did in the previous subsection. This is supported

by the fact that one of the singlets leads to a zero in the index since its index contribution is $\Gamma_e(pq)$. We then expect the rank of this node to be Higgsed by one unit.

Instead, we shall now employ a slightly different strategy which allows us to see the overall effect of the Higgsing using the IP duality twice. We hence apply the IP duality on the $USp(2N)_{z^{(N-1)}}$ node which becomes $USp(2N-2)_{z^{(N-1)}}$ to obtain the last quiver in Figure 40. Notice that the chirals connecting the $USp(2N-2)_{z^{(N-1)}}$ node to the y_1 flavor node have the charge of \sqrt{pq} , which means that they are massive and can be integrated out. This is due to the fact that this flavor had a VEV before the dualization, which turned the VEV into a complex mass deformation as usual in Seiberg-like dualities. After having integrated out the massive fields, we obtain the first quiver in Figure 41.

Now we have a tail with increasing ranks from $USp(2)$ to $USp(2N)$. Notice that the flavor node x_1 now sits between the $USp(2N-2)_{z^{(N-1)}}$ and $USp(2N)_{z^{(N)}}$ gauge nodes. Since the red $USp(2N-2)_{z^{(N-1)}}$ node has no antisymmetric, we can apply the IP duality on it. Notice that this doesn't simply revert the previous dualization that we did of the same node, since in between we integrated out the massive fields. We indeed obtain the second quiver in Figure 41. We then continue applying the IP duality moving towards the left until we reach the first $USp(2)_{z^{(1)}}$ node. At each step, we restore the antisymmetric on the previous node and remove the one at the subsequent node, which is what allows us to keep moving to the left with the application of the IP duality. Moreover, at each dualization the rank of the gauge node doesn't change, so that eventually we arrive at the same result as the end point of the VEV propagation studied in the previous subsection, which we show in Figure 37.

By repeating the same procedure also on the right side of the S-dualized SQCD quiver in Figure 34, we eventually arrive at the mirror dual drawn in Figure 38.

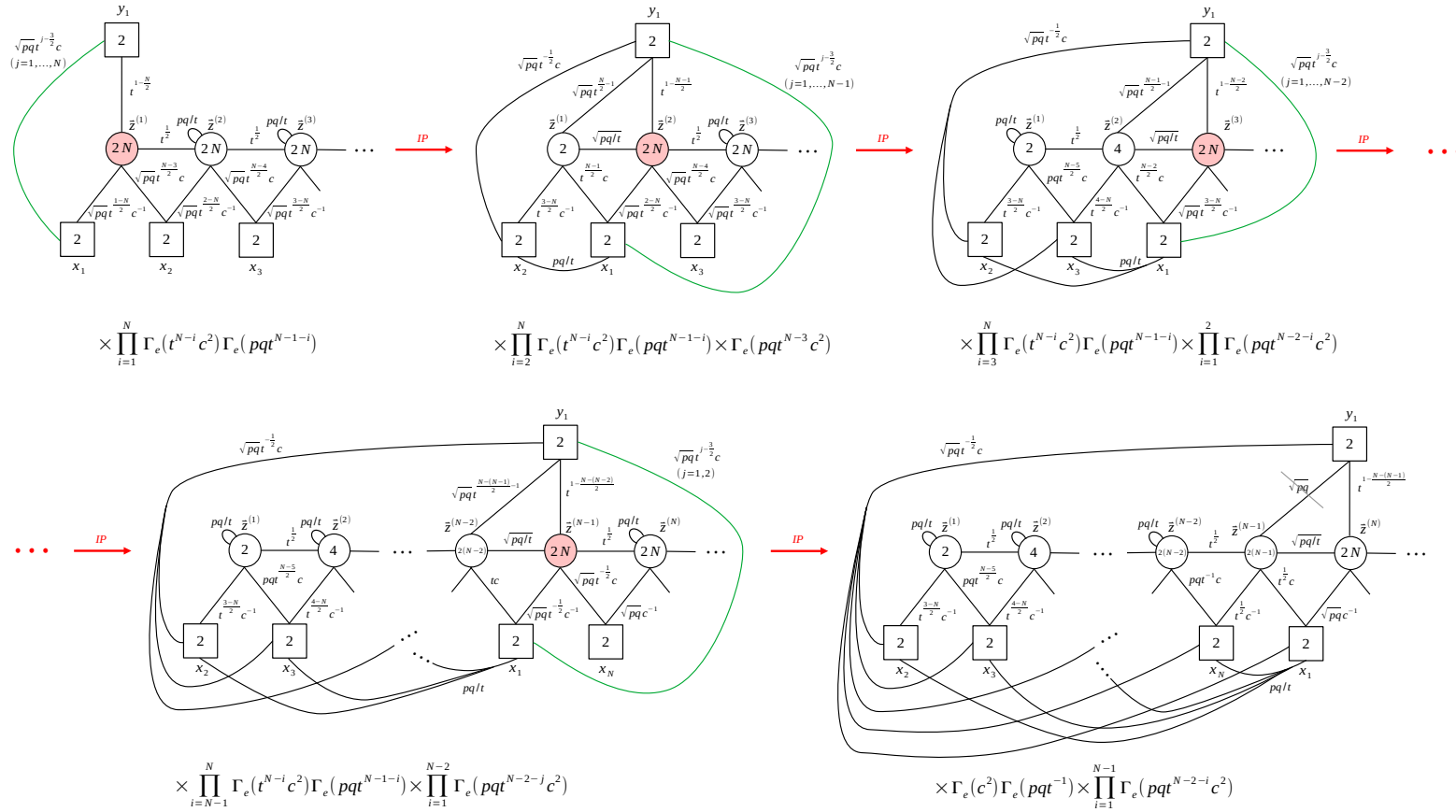


Figure 40. First round of applications of the IP duality.

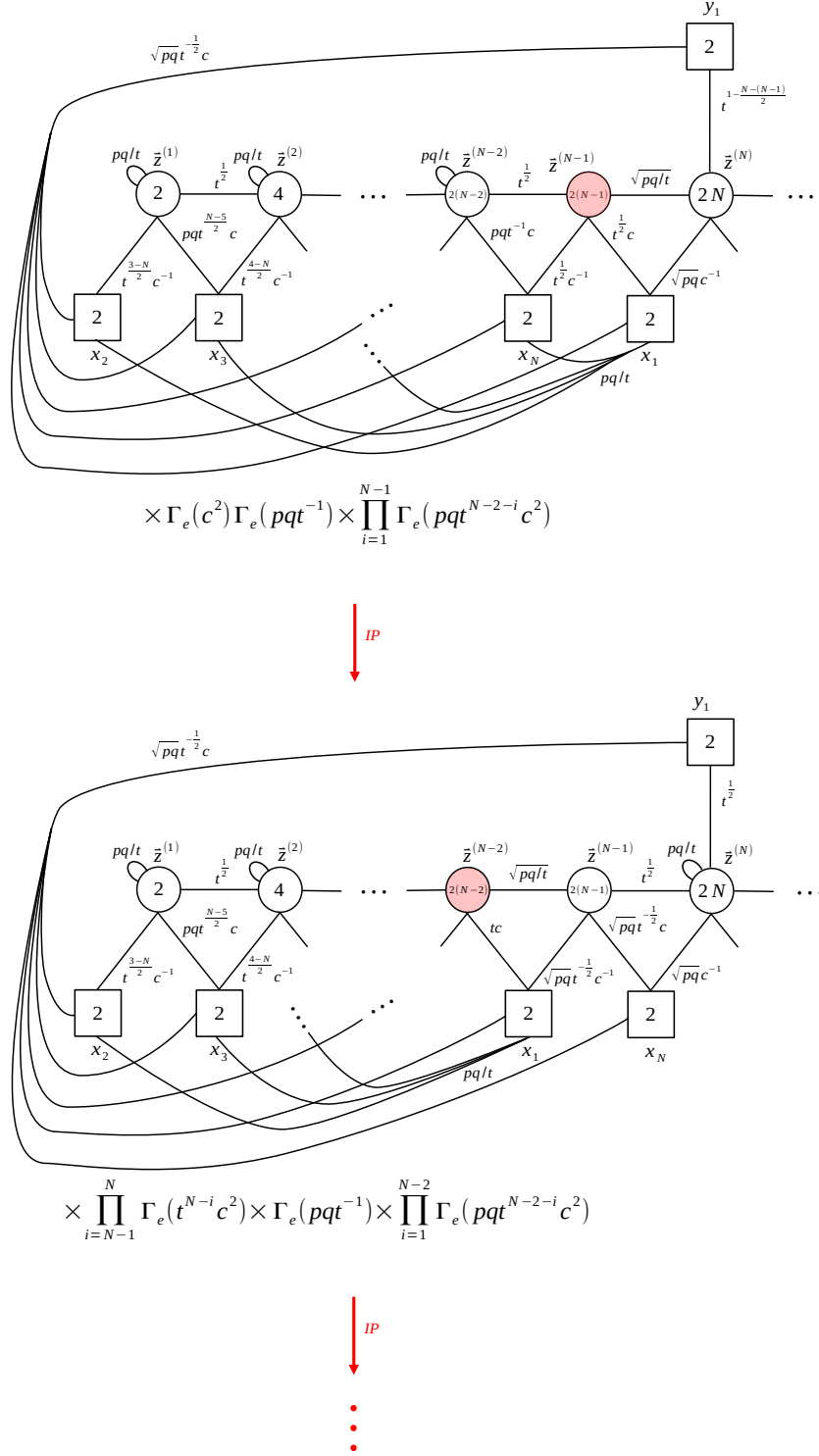


Figure 41. Second round of applications of the IP duality.

3.4 Method III: VEV propagation via the HW duality move

In this subsection we will illustrate the third and final strategy to implement the VEVs generated in the dualization algorithm, which uses the HW moves in Figure 32 to reach the final IR frame.

Consider the S-dualized SQCD in Figure 34, again focusing on the left part of the quiver to begin with. We apply the HW move to the sequence of \mathbf{B}_{01} - \mathbf{B}_{10} blocks highlighted in red in the first quiver in Figure 42 and reach the second quiver. Notice that the $USp(2N)_{z(1)}$ gauge node becomes a $USp(2)_{z(1)}$ node and two singlets have been produced: the $SU(2)_{y_1} \times SU(2)_{x_1}$ bifundamental and the one corresponding to $\Gamma_e(pqt^{-N})$, which actually cancels one of the singlets of Figure 34. We then apply again the HW move to the highlighted sequence of \mathbf{B}_{01} - \mathbf{B}_{10} blocks in the second quiver of Figure 42 to reach the third quiver and continue moving to the right.

After $N - 1$ dualizations we arrive at the first quiver in Figure 43. If we apply the HW duality move once again, we obtain the second theory in Figure 43 where the $USp(2N)_{z(N)}$ node remains $USp(2N)$ without any rank change and the vertical flavor has exactly charge $t^{1/2}$ and forms the standard cubic superpotential with the antisymmetric field. In particular, the VEV has been completely extinguished by this sequence of applications of the HW move. This implies that now the Identity-wall is actually symmetric and so it can be easily implemented by identifying the two adjacent nodes, which results in the third quiver in Figure 43. As expected, the result exactly coincides with the end point of the Higgsing in Figure 37.

Again we can perform an analogous sequence of the HW duality moves on the right part of the quiver in Figure 34 and obtain the mirror dual SQCD shown in Figure 38 after restoring the singlets of the original SQCD.

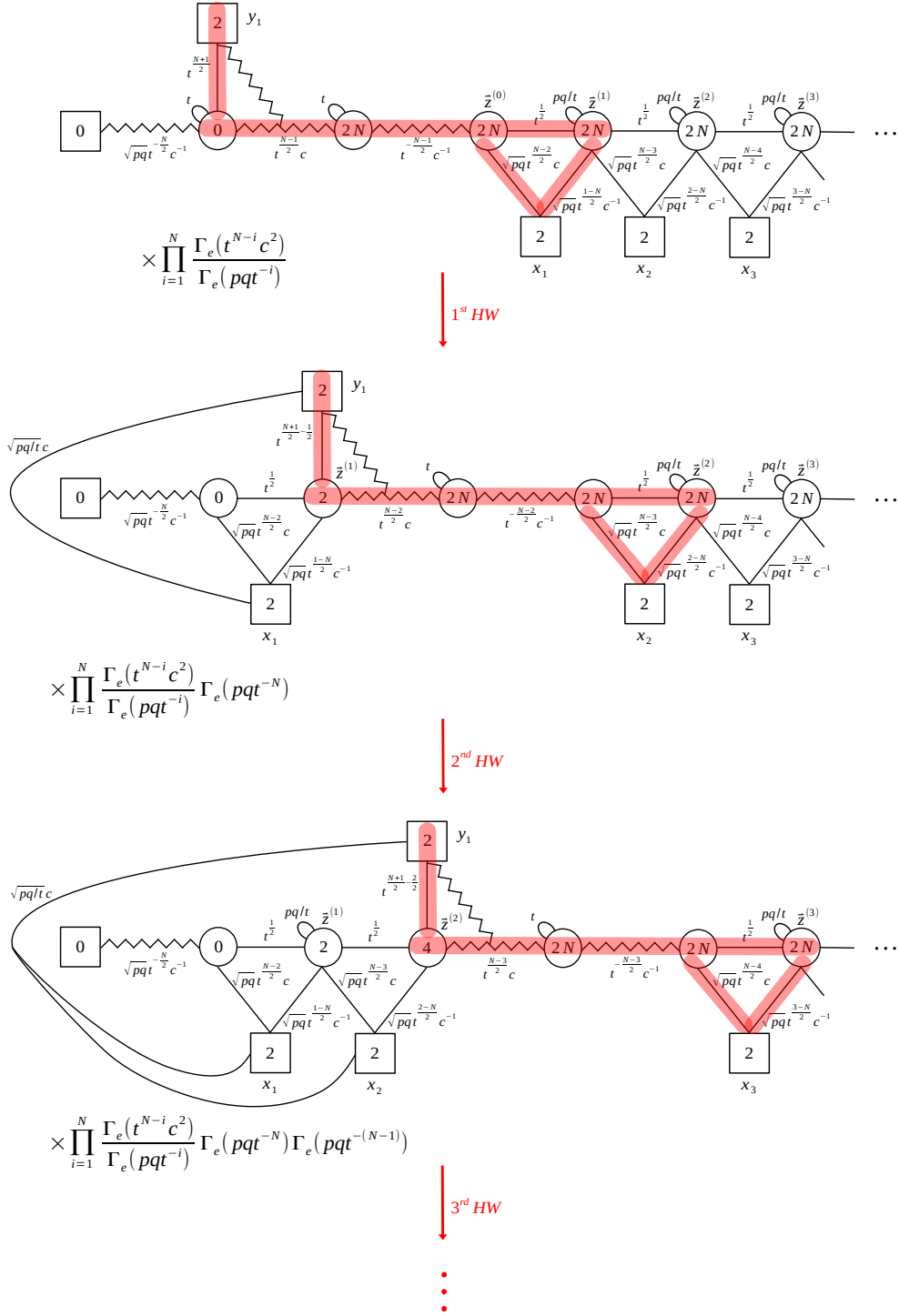


Figure 42. Initial applications of the HW duality move.

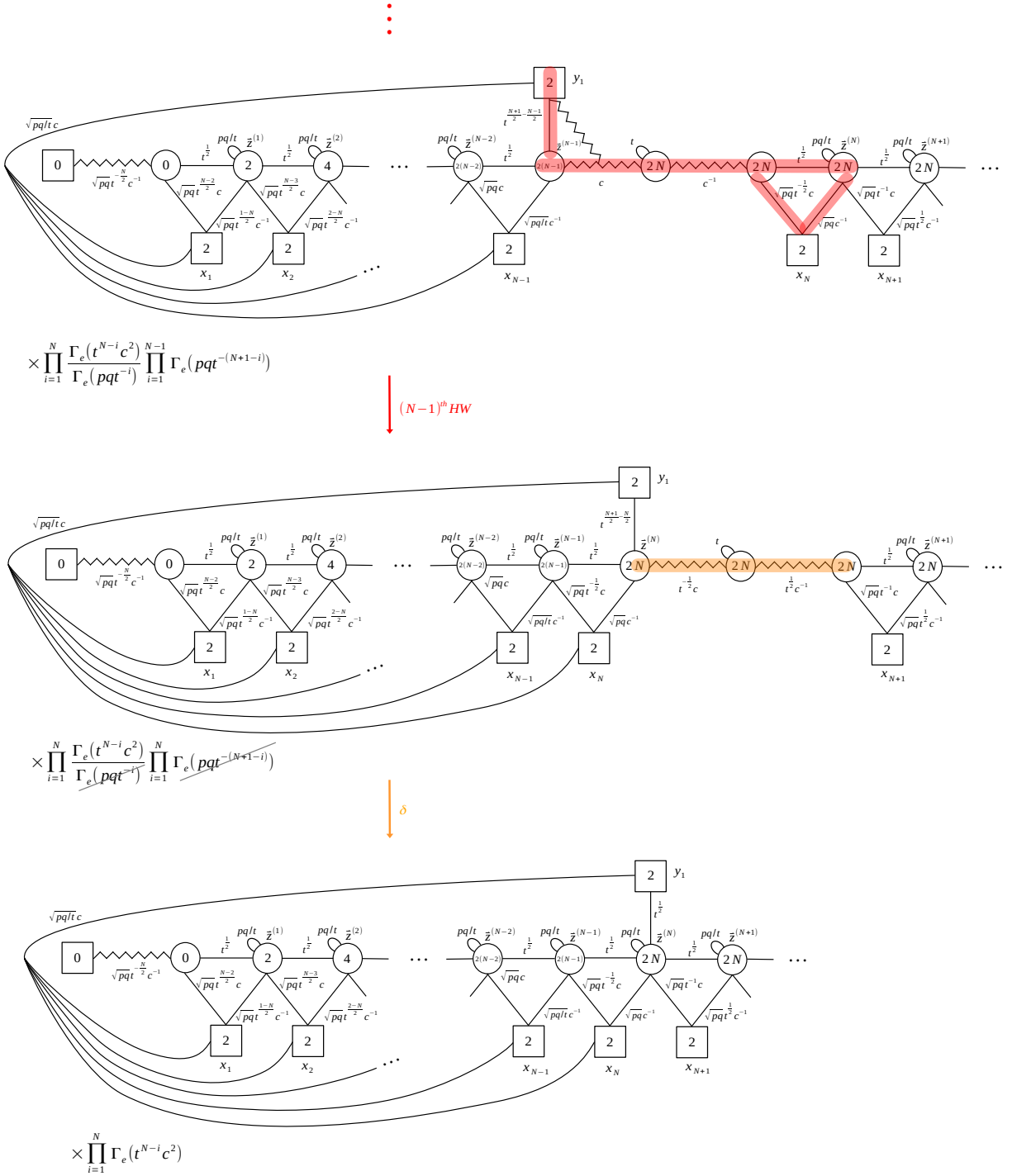


Figure 43. Last application of the HW duality move and the final manipulations leading to the IR frame.

4 Algorithm in 3d

In this section, we discuss the 3d version of the dualization algorithm. We will, in particular, present all of its basic ingredients, which are obtained as a limit of those in 4d that we saw in the previous two sections. We will not explicitly discuss any example of application of the algorithm in 3d, since this works exactly as in the 4d case.

4.1 $SL(2, \mathbb{Z})$ operators

We begin by introducing the $SL(2, \mathbb{Z})$ duality-walls.

\mathcal{S} -wall. As we already mentioned, in 3d we associate the \mathcal{S} generator of $SL(2, \mathbb{Z})$ with the $FT[U(N)]$ theory [96], which is the $T[U(N)]$ theory [62] modified by adding a set of singlet chiral fields in the adjoint representation of the manifest $U(N)_X$ flavor symmetry:⁹

$$\mathcal{Z}_{\mathcal{S}}^{(N)}(\vec{X}; \vec{Y}; m_A) \equiv \mathcal{Z}_{FT[U(N)]}(\vec{X}; -\vec{Y}; m_A) = \mathcal{Z}_{FT[U(N)]}(-\vec{X}; \vec{Y}; m_A) \quad (4.1)$$

and

$$\mathcal{Z}_{\mathcal{S}^{-1}}^{(N)}(\vec{X}; \vec{Y}; m_A) = \mathcal{Z}_{\mathcal{S}}^{(N)}(\vec{X}; -\vec{Y}; m_A) = \mathcal{Z}_{\mathcal{S}}^{(N)}(-\vec{X}; \vec{Y}; m_A). \quad (4.2)$$

We will schematically represent the 3d \mathcal{S} -wall as in Figure 44 to display both of its $U(N)$ global symmetries. We will distinguish between \mathcal{S} and \mathcal{S}^{-1} by a (+) and (−) label respectively.



Figure 44. The 3d \mathcal{S} -wall and \mathcal{S}^{-1} walls.

Similarly to its 4d counterpart, the $FE[USp(2N)]$ theory, the S_b^3 partition function [97–100] of $FT[U(N)]$ admits an integral form given by the following recursive definition:

$$\begin{aligned} \mathcal{Z}_{FT[U(N)]}(\vec{X}; \vec{Y}; m_A) &= e^{2\pi i Y_N \sum_{i=1}^N X_i} \prod_{i,j=1}^N s_b \left(i \frac{Q}{2} \pm (X_i - X_j) - 2m_A \right) \\ &\times \int d\vec{Z}_{N-1} \Delta_{N-1}^{(3d)}(\vec{Z}^{(N-1)}) e^{-2\pi i Y_N \sum_{a=1}^{N-1} Z_a^{(N-1)}} \prod_{a=1}^{N-1} \prod_{i=1}^N s_b \left(\pm (Z_a^{(N-1)} - X_i) + m_A \right) \\ &\times \mathcal{Z}_{FT[U(N-1)]} \left(Z_1^{(N-1)}, \dots, Z_{N-1}^{(N-1)}; Y_1, \dots, Y_{N-1}; m_A \right), \end{aligned} \quad (4.3)$$

where in the 3d partition function the integration measure is defined as

$$d\vec{Z}_n = \frac{\prod_{i=1}^n dZ_a}{n!}, \quad \Delta_N^{(3d)}(\vec{Z}) = \frac{1}{\prod_{a<b}^N s_b \left(i \frac{Q}{2} \pm (Z_a - Z_b) \right)}. \quad (4.4)$$

⁹Notice that w.r.t. to [22, 43] here we include an extra minus sign in front of either the \vec{X} or \vec{Y} mass parameters.

Here X_i , Y_j and m_A are the real mass parameters respectively for the $U(N)_X$, $U(N)_Y$, $U(1)_A$ global symmetries, where $U(1)_A$ is the axial symmetry which together with the trial R-symmetry $U(1)_R$ is obtained from a suitable linear combination of the Cartans of the $SO(4)_R \cong SU(2)_H \times SU(2)_C$ R-symmetry of $3d$ $\mathcal{N} = 4$ theories. The deformation by the real mass m_A then breaks supersymmetry to $\mathcal{N} = 2^*$ [101]. In particular our parametrization of $U(1)_A$ and $U(1)_R$ is such that the canonical R-symmetry under which all hypermultiplets have charge $\frac{1}{2}$ is obtained by setting the mixing coefficient R_A between $U(1)_A$ and $U(1)_R$ to $R_A = \frac{1}{2}$. Equivalently at the level of the sphere partition function to recover $\mathcal{N} = 4$ we should turn off m_A setting $m_A = i\frac{Q}{4}$.

The partition function (4.3) can be obtained as a limit of the $4d$ index of the $FE[USp(2N)]$ theory (2.1) as it was shown in [21, 31]. This consists of three main steps [21, 22, 31]. The first one is a circle reduction from $4d$ to $3d$, which in particular relates the $S^3 \times S^1$ index to the S_b^3 partition function. This is done by using the following property:

$$\lim_{\beta \rightarrow 0} \Gamma_e \left(e^{2\pi i \beta z}; p = e^{-2\pi \beta b}, q = e^{-2\pi \beta b^{-1}} \right) = e^{-\frac{i\pi}{6\beta} \left(i\frac{Q}{2} - z \right)} s_b \left(i\frac{Q}{2} - z \right), \quad (4.5)$$

where β is the S^1 radius that we send to zero. The $4d$ fugacities and the $3d$ real masses are related by

$$x_i = e^{2\pi i \beta X_i}, \quad y_j = e^{2\pi i \beta Y_j}, \quad t = e^{2\pi i \beta (iQ - 2m_A)}, \quad c = e^{2\pi i \beta \Delta}. \quad (4.6)$$

The second step is a real mass deformation that breaks the $USp(2N)$ symmetry to $U(N)$

$$X_i \rightarrow X_i + s, \quad Y_j \rightarrow Y_j + s \quad s \rightarrow +\infty, \quad (4.7)$$

which is done using the following property:

$$\lim_{z \rightarrow \pm\infty} s_b(z) = e^{\pm i\frac{\pi}{2} z^2}. \quad (4.8)$$

This leads to the $FM[U(N)](\vec{X}, \vec{Y}, \Delta)$ theory, introduced in [31], which contains a monopole superpotential.

Finally, we consider the real mass deformation

$$\Delta \rightarrow \pm\infty, \quad (4.9)$$

which leads to

$$\lim_{\Delta \rightarrow \pm\infty} FM[U(N)](\vec{X}, \vec{Y}, \Delta) = \mathcal{A} FT[U(N)](\vec{X}, \pm\vec{Y}), \quad (4.10)$$

where the prefactor \mathcal{A} can be determined by (4.5); see (5.21) in [22] for the result.

We also define an asymmetric \mathcal{S} -wall, where one of the $U(N)$ symmetries is broken to $U(M) \times U(1)$ with $M < N$. This is obtained by a deformation of the ordinary \mathcal{S} -wall that is completely analogous to the one considered in $4d$ in [22, 24], and it implies the following specialization of the real mass parameters for the broken symmetry:

$$Y_{M+j} = \frac{N - M + 1 - 2j}{2} (iQ - 2m_A) + V, \quad j = 1, \dots, N - M. \quad (4.11)$$

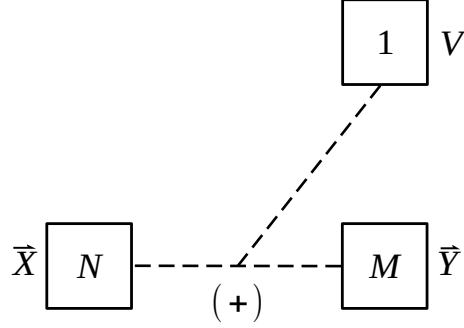


Figure 45. The asymmetric $3d$ \mathcal{S} -wall.

We will schematically represent the asymmetric \mathcal{S} -wall as in Figure 45.

Identity-wall. As we discussed extensively in $4d$, also in $3d$ we expect the $SL(2, \mathbb{Z})$ operators to obey the multiplication rules of the $SL(2, \mathbb{Z})$ group. In particular, we expect the \mathcal{S} -wall to satisfy the relations $\mathcal{S}\mathcal{S}^{-1} = 1$ and $\mathcal{S}^2 = -1$. Unlike in the $4d$ case, these two correspond to distinct identities satisfied by the partition function of the $3d$ \mathcal{S} -wall. Indeed, as it was shown in [22], from the $4d$ identity (2.4) one can obtain two identities, namely¹⁰

$$\int d\vec{Z}_N \Delta_N^{3d}(\vec{Z}; m_A) \mathcal{Z}_S^{(N)}(\vec{Z}; \vec{X}; m_A) \mathcal{Z}_S^{(N)}(\vec{Z}; -\vec{Y}; m_A) = \hat{\mathbb{I}}_{\vec{X} \leftarrow \vec{Y}}^{3d}(m_A) \quad (4.12)$$

and

$$\int d\vec{Z}_N \Delta_N^{3d}(\vec{Z}; m_A) \mathcal{Z}_S^{(N)}(\vec{Z}; \vec{X}; m_A) \mathcal{Z}_S^{(N)}(\vec{Z}; \vec{Y}; m_A) = \hat{\mathbb{I}}_{\vec{X} \rightarrow \vec{Y}}^{3d}(m_A), \quad (4.13)$$

depending on which limit we take between

$$X_i \rightarrow X_i + s, \quad Y_i \rightarrow Y_i + s \quad s \rightarrow +\infty, \quad (4.14)$$

and

$$X_i \rightarrow X_i + s, \quad Y_i \rightarrow Y_i - s \quad s \rightarrow +\infty. \quad (4.15)$$

In both cases, we also take $\Delta \rightarrow -\infty$. We defined the three-dimensional Identity operator

$$\hat{\mathbb{I}}_{\vec{X} \leftarrow \vec{Y}}^{3d}(m_A) = \frac{\sum_{\sigma \in S_N} \prod_{j=1}^N \delta(X_j - Y_{\sigma(j)})}{\Delta_N^{3d}(\vec{X}; m_A)} \quad (4.16)$$

with

$$\Delta_N^{3d}(\vec{X}; m_A) = \frac{\prod_{i,j=1}^N s_b \left(-i\frac{Q}{2} + (X_i - X_j) + 2m_A \right)}{\prod_{i < j}^N s_b \left(i\frac{Q}{2} \pm (X_i - X_j) \right)}. \quad (4.17)$$

¹⁰These identities were already known to follow from the closed-form expression of the round sphere partition function of the $T[SU(N)]$ found in [102, 103].

We also define the three-dimensional asymmetric Identity-wall $\hat{\mathbb{I}}_{\vec{X}, \vec{Y}, V}^{3d}(m_A)$ as

$$\hat{\mathbb{I}}_{\vec{X}, \vec{Y}, V}^{3d}(m_A) = \frac{1}{\Delta_N^{3d}(\vec{X}; m_A)} \sum_{\sigma \in S_N} \prod_{i=1}^N \delta(X_i - Y_{\sigma(i)}) \Big|_{Y_{M+j} = \frac{N-M+1-2j}{2}(iQ-2m_A)+V}. \quad (4.18)$$

Both the symmetric and the asymmetric Identity relations are represented in Figure 46.

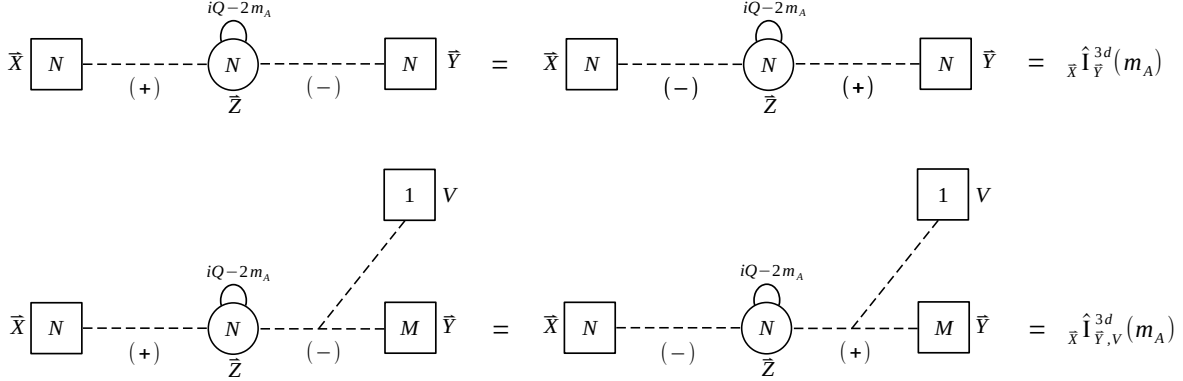


Figure 46. Gluing two \mathcal{S} -walls to gives an Identity-wall, in the symmetric case first line and in the asymmetric case second line.

\mathcal{T} -wall. The \mathcal{T} generator of $SL(2, \mathbb{Z})$ in $3d$ is simply associated with the addition of a CS level (see Figure 47).

$$\vec{X} \left[N_1 \right] \hat{\mathbb{I}}_{\vec{X}, \vec{Y}}^{3d}(m_A)$$

Figure 47. The $3d$ \mathcal{T} -wall.

We then define its contribution to the S_b^3 partition function as

$$\mathcal{Z}_{\mathcal{T}}^{(N)}(\vec{X}; \vec{Y}; m_A) = e^{\frac{i\pi N}{24}(8m_A^2(N-1)-4im_A Q(N-1)+Q^2)} e^{-i\pi \sum_{i=1}^N X_i^2} \hat{\mathbb{I}}_{\vec{X}, \vec{Y}}^{3d}(m_A), \quad (4.19)$$

which can be obtained as a limit of (2.9) by taking

$$X_i \rightarrow X_i + s, \quad Y_j \rightarrow Y_j + s, \quad V \rightarrow V + s, \quad s \rightarrow +\infty, \quad (4.20)$$

and then

$$\Delta \rightarrow \infty, \quad D \rightarrow \infty \quad (4.21)$$

with $v = e^{2\pi i \beta V}$ and $d = e^{2\pi i \beta D}$; the other variables are defined in (4.6). The first prefactor is included so to simplify the identities for the basic duality moves and to recover the relation $(\mathcal{S}\mathcal{T})^3 = 1$ as will see momentarily.

\mathcal{T}^T -wall. Finally, for completeness we also discuss the \mathcal{T}^T operator. This is not an independent operator, since it can be written in terms of the \mathcal{S} and \mathcal{T} generators as $\mathcal{T}^T = -\mathcal{T}\mathcal{S}\mathcal{T}$. Accordingly, we associate to it one copy of the $FT[U(N)]$ \mathcal{S} -wall theory with background CS level +1 for both of its $U(N)$ global symmetries (see Figure 48).

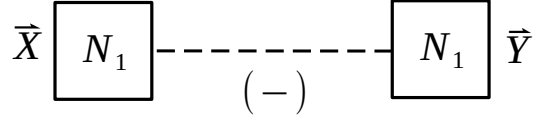


Figure 48. The 3d \mathcal{T}^T -wall.

The \mathcal{T}^T operator can also be obtained from the 4d \mathbb{T}^T operator like the \mathcal{S} and \mathcal{T} are obtained from \mathbb{S} and \mathbb{T} in 4d by taking some limits and discarding unwanted background CS couplings. Specifically, at the level of the sphere partition function, we can take the 3d limit of eq. (2.21) with $\Delta \rightarrow \infty$ and $D \rightarrow \infty$, which leads to

$$\begin{aligned} \mathcal{Z}_{\mathcal{T}^T}^{(N)}(\vec{X}; \vec{Y}; m_A) &= \int d\vec{Z}_N^{(1)} d\vec{Z}_N^{(2)} \Delta_N^{3d}(\vec{Z}^{(1)}; m_A) \Delta_N^{3d}(\vec{Z}^{(2)}; m_A) \mathcal{Z}_{\mathcal{T}}^{(N)}(\vec{X}; \vec{Z}^{(1)}; m_A) \\ &\quad \times \mathcal{Z}_{\mathcal{S}^{-1}}^{(N)}(\vec{Z}^{(1)}; \vec{Z}^{(2)}; m_A) \mathcal{Z}_{\mathcal{T}}^{(N)}(\vec{Z}^{(2)}; \vec{Y}; m_A) \\ &= e^{\frac{i\pi N}{12}(8m_A^2(N-1) - 4im_A Q(N-1) + Q^2)} e^{-i\pi(\sum_{i=1}^N X_i^2 + Y_i^2)} \mathcal{Z}_{\mathcal{S}^{-1}}^{(N)}(\vec{X}; \vec{Y}; m_A) \end{aligned} \quad (4.22)$$

after subtracting the flavor CS levels by +1 and -1 for $U(N)_X$ and $U(N)_Y$, respectively. If we replace $\mathcal{Z}_{\mathcal{S}^{-1}}^{(N)}(\vec{X}; \vec{Y}; m_A)$ by

$$\mathcal{Z}_{\mathcal{S}^{-1}}^{(N)}(\vec{X}; \vec{Y}; m_A) = \int d\vec{Z}_N \Delta_N^{3d}(\vec{Z}; m_A) \mathcal{Z}_{\mathcal{S}}^{(N)}(\vec{X}; \vec{Z}; m_A) \hat{\mathbb{I}}_{-\vec{Y}}^{3d}(m_A), \quad (4.23)$$

which corresponds to $\mathcal{S}^{-1} = -\mathcal{S}$, we can see this is exactly the relation $\mathcal{T}^T = -\mathcal{T}\mathcal{S}\mathcal{T}$.

$SL(2, \mathbb{Z})$ relations. We have already discussed the relation $\mathcal{S}^2 = -1$. The relation $(\mathcal{S}\mathcal{T})^3 = 1$ can be derived as shown in [22] as a limit of the braid relation (2.15).

Implementing the 3d limit following the steps above and turning on real masses for the $\Delta \rightarrow \infty$ and $D \rightarrow \infty$ we obtain the following relation

$$\mathcal{T}\mathcal{S}^{-1}\mathcal{T}\mathcal{S}^{-1}\mathcal{T} = \mathcal{S}^{-1}, \quad (4.24)$$

or equivalently, $(\mathcal{S}\mathcal{T})^3 = 1$ once we use (4.23) and implement the delta functions.

4.2 QFT building blocks

The fundamental QFT building blocks in 3d are those naturally associated with the possible types of 5-branes that we can have in the Hanany–Witten brane setup. We focus in particular on NS5, D5 and (1,1)-branes.

The \mathcal{B}_{10} block. To an NS5-brane with N D3-branes ending on its left and M on its right is associated a $U(N) \times U(M)$ bifundamental hypermultiplet, which we will also call \mathcal{B}_{10} block (see Figure 49).

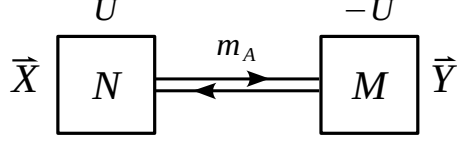


Figure 49. The \mathcal{B}_{10} block.

Its contribution to the S_b^3 partition function is given by:

$$\mathcal{Z}_{(1,0)}^{(N,M)}(\vec{X}; \vec{Y}; U; m_A) = e^{2\pi i U (\sum_{i=1}^N X_i - \sum_{j=1}^M Y_j)} \prod_{i=1}^N \prod_{j=1}^M s_b \left(\frac{iQ}{2} - m_A \pm (X_i - Y_j) \right). \quad (4.25)$$

Here U appears as an FI parameter.¹¹ This expression can be obtained from the $4d$ \mathcal{B}_{10} block in (2.22) by taking the $3d$ limit with the usual three steps. The first involves the $3d$ reduction where the $4d$ fugacities and the $3d$ real masses are related by

$$x_i = e^{2\pi i \beta X_i}, \quad y_j = e^{2\pi i \beta Y_j}, \quad t = e^{2\pi i \beta (iQ - 2m_A)}, \quad c = e^{2\pi i \beta \Delta}, \quad u = e^{2\pi i \beta U}. \quad (4.26)$$

The second step is a real mass deformation that breaks the $USp(2N) \times USp(2M)$ symmetry to $U(N) \times U(M)$

$$X_i \rightarrow X_i + s, \quad Y_j \rightarrow Y_j + s, \quad U \rightarrow U - s, \quad s \rightarrow +\infty, \quad (4.27)$$

Finally, we consider the real mass deformation $\Delta \rightarrow -\infty$, which in particular has the effect of removing the lower part of the triangle in Figure 17. This also makes the parameter $\pm U$ appear as an FI parameter and produces a background CS level ∓ 1 for the $U(N)$ and $U(M)$ nodes respectively. Removing all the exponential prefactors that are produced in the limit except for those encoding the FI's, from the index (2.22) of the \mathcal{B}_{10} block we recover the S_b^3 partition function (4.25) of the \mathcal{B}_{10} block.

Note that we can also obtain the block \mathcal{B}_{-10} by acting with $-I$ on each side of \mathcal{B}_{10} , which can be expressed by the following identity:

$$\begin{aligned} \mathcal{Z}_{(-1,0)}^{(N,M)}(\vec{X}; \vec{Y}; U; m_A) &= \oint d\vec{Z}_N d\vec{W}_M \Delta_N^{3d}(\vec{Z}; m_A) \Delta_M^{3d}(\vec{W}; m_A) \hat{\mathbb{Z}}_{-\vec{X}}^{\hat{3}d}(m_A) \hat{\mathbb{W}}_{-\vec{Y}}^{\hat{3}d}(m_A) \\ &\times e^{2\pi i U (\sum_{i=1}^N Z_i - \sum_{j=1}^M W_j)} \prod_{i=1}^N \prod_{j=1}^M s_b \left(\frac{iQ}{2} - m_A \pm (Z_i - W_j) \right) \\ &= e^{-2\pi i U (\sum_{i=1}^N X_i - \sum_{j=1}^M Y_j)} \prod_{i=1}^N \prod_{j=1}^M s_b \left(\frac{iQ}{2} - m_A \pm (X_i - Y_j) \right), \end{aligned} \quad (4.28)$$

which is simply $\mathcal{Z}_{(1,0)}^{(N,M)}(\vec{X}; \vec{Y}; -U; m_A)$ where the sign of U is flipped.

¹¹More precisely, at this level since the $U(N)$ and $U(M)$ symmetries are not gauged it is actually a background BF coupling. Inside quivers in which the $U(N)$ and $U(M)$ symmetries are gauged it really becomes an FI.

The \mathcal{B}_{01} block. To a (0,1)-brane with N D3-branes ending both on its left and on its right we associated a single $U(N)$ fundamental hypermultiplet, the \mathcal{B}_{01} block depicted in Figure 50. Similarly to the $4d$ \mathcal{B}_{01} block, we equip this with one copy of the Identity-wall to give it a structure with two sets of $U(N)$ indices.

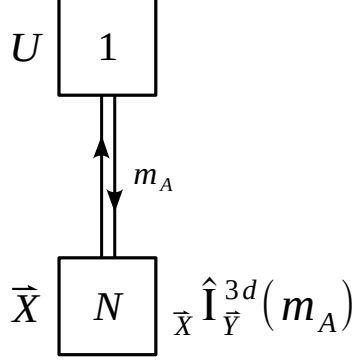


Figure 50. The symmetric \mathcal{B}_{01} block. Here and in the following figures, a parameter F close to a chiral corresponds to part of the argument of its contribution to the S_b^3 partition function $s_b\left(i\frac{Q}{2} - F + (\text{non-Abelian})\right)$.

Its contribution to the S_b^3 partition function is given by

$$\mathcal{Z}_{(0,1)}^{(N,N)}(\vec{X}; \vec{Y}; U; m_A) = \prod_{j=1}^N s_b\left(\frac{iQ}{2} - m_A \pm (X_j - U)\right) \hat{\mathbb{I}}_{\vec{X}\vec{Y}}^{3d}(m_A). \quad (4.29)$$

In analogy with what we did in $4d$, it is useful to generalize this to a D5 suspended between different numbers of D3-branes, say N D3's on the left and M D3's on the right. The associated partition function is given by

$$\mathcal{Z}_{(0,1)}^{(N,M)}(\vec{X}; \vec{Y}; U; m_A) = \prod_{j=1}^M s_b\left(\frac{iQ}{2} - m_A(N - M + 1) \pm (Y_j - U)\right) \hat{\mathbb{I}}_{\vec{X}\vec{Y},U}^{3d}(m_A). \quad (4.30)$$

Similarly to our previous discussion for the NS5 basic block, one can obtain the expression (4.30) for the S_b^3 partition function of the \mathcal{B}_{01} block as a limit of that (2.24) for the $4d$ index of the \mathcal{B}_{01} block with the identifications

$$x_i = e^{2\pi i\beta X_i}, \quad y_j = e^{2\pi i\beta Y_j}, \quad t = e^{2\pi i\beta(iQ - 2m_A)}, \quad u = e^{2\pi i\beta U}, \quad (4.31)$$

followed by the real mass $X_i \rightarrow X_i + s$, $Y_j \rightarrow Y_j + s$, $U \rightarrow U + s$, $s \rightarrow +\infty$. We can also introduce the block \mathcal{B}_{0-1} by acting with $-I$ on each side of \mathcal{B}_{01} which results into $\mathcal{Z}_{(0,-1)}^{(N,M)}(\vec{X}; \vec{Y}; U; m_A) = \mathcal{Z}_{(0,1)}^{(N,M)}(\vec{X}; \vec{Y}; -U; m_A)$.

The \mathcal{B}_{11} block. Finally, the QFT building block associated to a (1,1)-brane with N D3 branes ending on its left and M on its right is a $U(N) \times U(M)$ bifundamental hypermultiplet

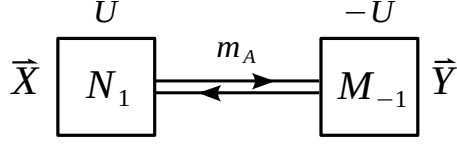


Figure 51. The \mathcal{B}_{11} block.

with the addition of background CS levels $+1$ and -1 respectively for the $U(N)$ and the $U(M)$ global symmetries, which we will also call \mathcal{B}_{11} block (see Figure 51).

At the level of the sphere partition function we have

$$\begin{aligned} \mathcal{Z}_{(1,1)}^{(N,M)}(\vec{X}; \vec{Y}; U; m_A) &= e^{-i\pi(\sum_{i=1}^N X_i^2 - \sum_{j=1}^M Y_j^2)} e^{2\pi i U(\sum_{i=1}^N X_i - \sum_{j=1}^M Y_j)} \\ &\times \prod_{i=1}^N \prod_{j=1}^M s_b\left(\frac{iQ}{2} - m_A \pm (X_i - Y_j)\right), \end{aligned} \quad (4.32)$$

which again can be obtained as the $3d$ limit of the $4d$ index (2.25) (with $D \rightarrow +\infty$ in addition to (4.27)) of the \mathcal{B}_{11} block after removing some of the exponential prefactors.

4.3 Basic duality moves

Having defined the $3d$ QFT blocks and the $SL(2, \mathbb{Z})$ operators, we are ready to present the $3d$ version of the basic duality moves that play a central role in the dualization algorithm. We will get them as a limit of the $4d$ ones, but we stress that they can be independently derived by iterative application of the Aharony duality [44].

4.3.1 \mathcal{S} -dualization

$\mathcal{B}_{-10} = \mathcal{S}\mathcal{B}_{01}\mathcal{S}^{-1}$. The first duality move is the \mathcal{S} -dualization of a $(0, 1)$ -brane into a $(-1, 0)$ -brane, a $\overline{\text{NS5}}$, which we interpret as the field theory duality in Figure 52.

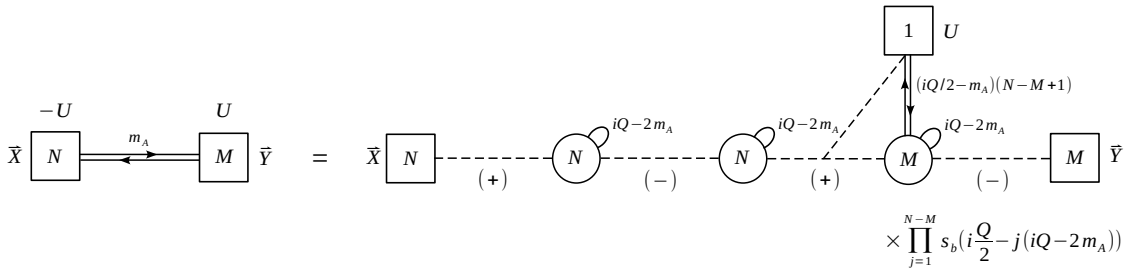


Figure 52. The $\mathcal{B}_{-10} = \mathcal{S}\mathcal{B}_{01}\mathcal{S}^{-1}$ duality move.

This corresponds to the following identity of S_b^3 partition functions:

$$\begin{aligned} \mathcal{Z}_{(-1,0)}^{(N,M)}(\vec{X}; \vec{Y}; U; m_A) &= \prod_{j=1}^{N-M} s_b \left(i\frac{Q}{2} - j(iQ - 2m_A) \right) \int \left(\prod_{k=1}^2 d\vec{Z}_M^{(k)} \Delta_M^{3d}(\vec{Z}^{(k)}; m_A) \right) \\ &\times \mathcal{Z}_S^{(N)}(\vec{X}; \vec{Z}^{(1)}) \mathcal{Z}_{(0,1)}^{(N,M)}(\vec{Z}^{(1)}; \vec{Z}^{(2)}; U; i\frac{Q}{2} - m_A) \mathcal{Z}_{S^{-1}}^{(M)}(\vec{Z}^{(2)}; \vec{Y}; m_A), \end{aligned} \quad (4.33)$$

where the partition function for the \mathcal{B}_{-10} block on the left hand side is given by that of \mathcal{B}_{10} with the FI parameter $-U$ as shown in (4.28). This identity can be obtained as a limit of the $4d$ one in (2.26) following the usual three steps. In the process we define the $3d$ parameters as

$$\begin{aligned} x_i &= e^{2\pi i\beta X_i}, & y_j &= e^{2\pi i\beta Y_j}, & Z_a^{(k)} &= e^{2\pi i\beta z_a^{(k)}}, \\ t &= e^{2\pi i\beta(iQ-2m_A)}, & c &= e^{2\pi i\beta\Delta}, & u &= e^{2\pi i\beta U}. \end{aligned} \quad (4.34)$$

Then we consider the real mass deformation breaking all the symplectic groups down to unitary:

$$X_i \rightarrow X_i + s, \quad Y_j \rightarrow Y_j + s, \quad Z_a^{(k)} \rightarrow Z_a^{(k)} + s, \quad U \rightarrow U + s, \quad s \rightarrow +\infty. \quad (4.35)$$

Finally, the last step is the real mass deformation

$$\Delta \rightarrow -\infty. \quad (4.36)$$

It turns out that all the exponential prefactors produced in the first two steps perfectly cancel between the two sides of the identity, while the only prefactor surviving in the last step is the FI containing U that we included in our definition (4.28) of the \mathcal{B}_{-10} block, thus providing a justification for it. In particular, it is crucial that all the factors involving the parameters that we sent to infinity cancel, so to give a well-defined identity also in $3d$.

$\mathcal{B}_{01} = \mathcal{S}\mathcal{B}_{10}\mathcal{S}^{-1}$. We next consider the QFT analogue of the \mathcal{S} -dualization of a $(1, 0)$ -brane into a $(0, 1)$ -brane shown in Figure 53.

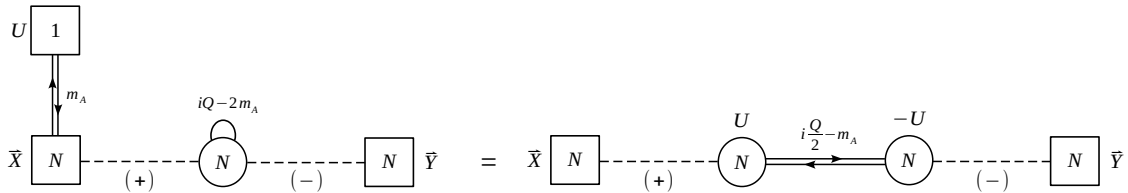


Figure 53. The $\mathcal{B}_{01} = \mathcal{S}\mathcal{B}_{10}\mathcal{S}^{-1}$ duality move.

In this case, the associated partition function identity is

$$\begin{aligned} \mathcal{Z}_{(0,1)}^{(N)}(\vec{X}; \vec{Y}; U; m_A) &= \int d\vec{Z}_N^{(1)} d\vec{Z}_N^{(2)} \Delta_N^{3d}(\vec{Z}^{(1)}) \Delta_N^{3d}(\vec{Z}^{(2)}) \mathcal{Z}_S^{(N)}(\vec{X}; \vec{Z}^{(1)}; m_A) \\ &\times \mathcal{Z}_{(1,0)}^{(N,N)}(\vec{Z}^{(1)}; \vec{Z}^{(2)}; U; i\frac{Q}{2} - m_A) \mathcal{Z}_{S^{-1}}^{(N)}(\vec{Z}^{(2)}; \vec{Y}; m_A). \end{aligned} \quad (4.37)$$

This can be obtained as a limit of the 4d identity (2.27) that is completely analogous to the previous duality move, now with $\Delta \rightarrow +\infty$.

$\mathcal{B}_{11} = \mathcal{S}\mathcal{B}_{1-1}\mathcal{S}^{-1}$. The last \mathcal{S} -dualization we consider is the one relating a (1, 1)-brane and a (1,-1)-brane shown in Figure 54.

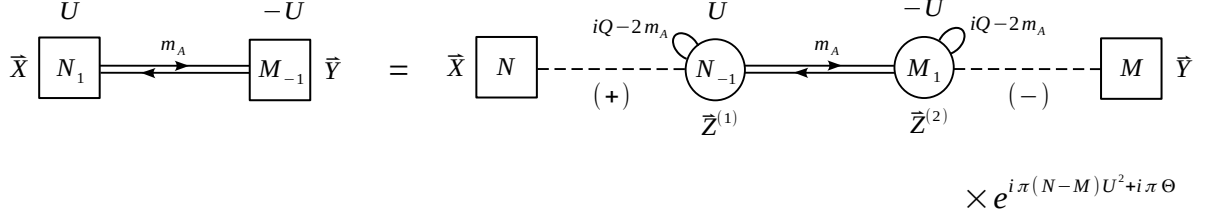


Figure 54. The $\mathcal{B}_{11} = \mathcal{S}\mathcal{B}_{1-1}\mathcal{S}^{-1}$ duality move.

At the level of the S_b^3 partition function, this duality move is encoded in the following identity:

$$\begin{aligned} \mathcal{Z}_{(1,1)}^{(N,M)}(\vec{X}; \vec{Y}; U; m_A) &= e^{i\pi(N-M)U^2 + i\pi\Theta} \int d\vec{Z}_N^{(1)} d\vec{Z}_M^{(2)} \Delta_N^{3d}(\vec{Z}^{(1)}; m_A) \Delta_M^{3d}(\vec{Z}^{(2)}; m_A) \\ &\quad \times \mathcal{Z}_{\mathcal{S}}^{(N)}(\vec{X}; \vec{Z}^{(1)}; m_A) \mathcal{Z}_{(1,-1)}^{(N,M)}(\vec{Z}^{(1)}; \vec{Z}^{(2)}; U; m_A) \mathcal{Z}_{\mathcal{S}^{-1}}^{(M)}(\vec{Z}^{(2)}; \vec{Y}; m_A), \end{aligned} \quad (4.38)$$

where

$$\begin{aligned} \Theta &= \frac{N-M}{24} [8m_a^2 ((N-M)^2 - 3(N+M) + 2) \\ &\quad - 4im_a Q (2(N-M)^2 - 3(N+M) + 1) - Q^2 (2(N-M)^2 + 1)]. \end{aligned} \quad (4.39)$$

We have defined the contribution of the (1, -1)-brane, that is the \mathcal{B}_{1-1} block, as

$$\begin{aligned} \mathcal{Z}_{(1,-1)}^{(N,M)}(\vec{X}; \vec{Y}; U; m_A) &= e^{i\pi(\sum_{i=1}^N X_i^2 - \sum_{j=1}^M Y_j^2)} e^{2\pi i U (\sum_{i=1}^N X_i - \sum_{j=1}^M Y_j)} \\ &\quad \times \prod_{i=1}^N \prod_{j=1}^M s_b \left(\frac{iQ}{2} - m_A \pm (X_i - Y_j) \right). \end{aligned} \quad (4.40)$$

Notice that this differs from the contribution of a (1, 1) for the fact that the CS levels are inverted. The identity (4.38) again can be obtained as a limit of (2.29) with

$$X_i \rightarrow X_i + s, \quad Y_j \rightarrow Y_j + s, \quad Z_a^{(k)} \rightarrow Z_a^{(k)} + s, \quad U \rightarrow U - s, \quad V \rightarrow V + s, \quad s \rightarrow +\infty \quad (4.41)$$

followed by $\Delta \rightarrow -\infty$ and $D \rightarrow +\infty$ satisfying $\Delta + D \rightarrow -\infty$, where V here and below is defined such that $v = e^{2\pi i \beta V}$. By looking at the result of the limit it is easy to check that one of the two parameters U and V is redundant, and we can take $V = 0$ to obtain (4.40). In other words, we can simply take $V \rightarrow s \rightarrow +\infty$ in (4.41) to obtain (4.40).

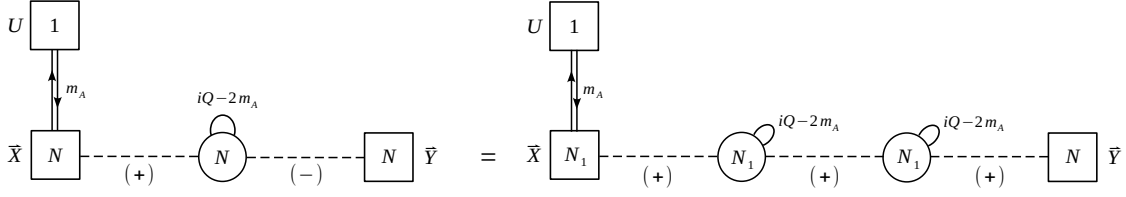


Figure 55. The $\mathcal{B}_{01} = \mathcal{T}\mathcal{B}_{01}\mathcal{T}^{-1}$ duality move.

4.3.2 \mathcal{T} -dualization

$\mathcal{B}_{01} = \mathcal{T}\mathcal{B}_{01}\mathcal{T}^{-1}$. A D5-brane is invariant under the \mathcal{T} -dualization as shown in Figure 55. Recalling that the inverse of \mathcal{T} is given by $\mathcal{T}^{-1} = \mathcal{S}\mathcal{T}\mathcal{S}\mathcal{T}\mathcal{S}$, we find that this dualization implies the following identity of S_b^3 partition functions:

$$\begin{aligned} \mathcal{Z}_{(0,1)}^{(N)}(\vec{X}; \vec{Y}; U; m_A) &= \int \left(\prod_{k=1}^6 d\vec{Z}_N^{(k)} \Delta_N^{3d}(\vec{Z}^{(k)}; m_A) \right) \mathcal{Z}_{\mathcal{T}}^{(N)}(\vec{X}; \vec{Z}^{(1)}; m_A) \\ &\times \mathcal{Z}_{(0,1)}^{(N)}(\vec{Z}^{(1)}; \vec{Z}^{(2)}; U; m_A) \mathcal{Z}_{\mathcal{S}}^{(N)}(\vec{Z}^{(2)}; \vec{Z}^{(3)}; m_A) \mathcal{Z}_{\mathcal{T}}^{(N)}(\vec{Z}^{(3)}; \vec{Z}^{(4)}; m_A) \\ &\times \mathcal{Z}_{\mathcal{S}}^{(N)}(\vec{Z}^{(4)}; \vec{Z}^{(5)}; m_A) \mathcal{Z}_{\mathcal{T}}^{(N)}(\vec{Z}^{(5)}; \vec{Z}^{(6)}; m_A) \mathcal{Z}_{\mathcal{S}}^{(N)}(\vec{Z}^{(6)}; \vec{Y}; m_A). \end{aligned} \quad (4.42)$$

We point out that this identity doesn't have any additional prefactor thanks to the fact that we defined the \mathcal{T} generator in (4.19) with an extra prefactor. Again this can be obtained as a limit of the corresponding 4d identity (2.32) with

$$\begin{aligned} X_i &\rightarrow X_i + s, & Y_j &\rightarrow Y_j + s, & Z_a^{(1,\dots,4)} &\rightarrow Z_a^{(1,\dots,4)} + s, \\ Z_a^{(5,6)} &\rightarrow Z_a^{(5,6)} - s, & U &\rightarrow U + s, & V &\rightarrow s, & s &\rightarrow +\infty \end{aligned} \quad (4.43)$$

followed by $\Delta \rightarrow -\infty$ and $D \rightarrow +\infty$ satisfying $\Delta + D \rightarrow -\infty$. Note that the sign of s for $Z^{(5,6)}$ is flipped to obtain \mathcal{S} rather than \mathcal{S}^{-1} directly. In addition, we simply take $V \rightarrow s \rightarrow +\infty$ because V becomes redundant after the limit, as mentioned before.

$\mathcal{B}_{11} = \mathcal{T}\mathcal{B}_{10}\mathcal{T}^{-1}$. We now consider the \mathcal{T} -dualization of a (1,0)-brane into a (1,1)-brane. Using again that $\mathcal{T}^{-1} = \mathcal{S}\mathcal{T}\mathcal{S}\mathcal{T}\mathcal{S}$ this corresponds to the duality in Figure 56.

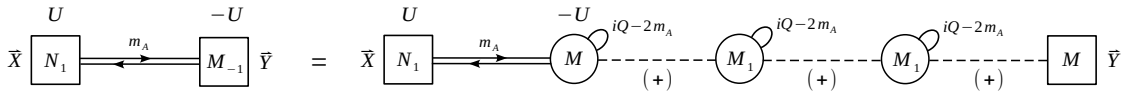


Figure 56. The $\mathcal{B}_{11} = \mathcal{T}\mathcal{B}_{10}\mathcal{T}^{-1} = \mathcal{T}\mathcal{B}_{10}\mathcal{S}\mathcal{T}\mathcal{S}\mathcal{T}\mathcal{S}$ duality move.

At the level of partition functions we have the following identity:

$$\begin{aligned}
\mathcal{Z}_{(1,1)}^{(N,M)}(\vec{X}; \vec{Y}; U; m_A) &= \int d\vec{Z}_N^{(1)} \Delta_N^{3d}(\vec{Z}^{(1)}; m_A) \left(\prod_{k=2}^6 d\vec{Z}_M^{(k)} \Delta_M^{3d}(\vec{Z}^{(k)}; m_A) \right) \mathcal{Z}_{\mathcal{T}}^{(N)}(\vec{X}; \vec{Z}^{(1)}; m_A) \\
&\times \mathcal{Z}_{(1,0)}^{(N,M)}(\vec{Z}^{(1)}; \vec{Z}^{(2)}; U; m_A) \mathcal{Z}_S^{(M)}(\vec{Z}^{(2)}; \vec{Z}^{(3)}; m_A) \mathcal{Z}_{\mathcal{T}}^{(M)}(\vec{Z}^{(3)}; \vec{Z}^{(4)}; m_A) \\
&\times \mathcal{Z}_S^{(M)}(\vec{Z}^{(4)}; \vec{Z}^{(5)}; m_A) \mathcal{Z}_{\mathcal{T}}^{(M)}(\vec{Z}^{(5)}; \vec{Z}^{(6)}; m_A) \mathcal{Z}_S^{(M)}(\vec{Z}^{(6)}; \vec{Y}; m_A),
\end{aligned} \tag{4.44}$$

which again can be obtained as a limit of the corresponding 4d identity (2.34) with

$$\begin{aligned}
X_i &\rightarrow X_i + s, & Y_j &\rightarrow Y_j + s, & Z_a^{(1,\dots,4)} &\rightarrow Z_a^{(1,\dots,4)} + s, \\
Z_a^{(5,6)} &\rightarrow Z_a^{(5,6)} - s, & U &\rightarrow U - s, & V &\rightarrow s, & s &\rightarrow +\infty
\end{aligned} \tag{4.45}$$

followed by $\Delta \rightarrow -\infty$ and $D \rightarrow +\infty$ satisfying $\Delta + D \rightarrow -\infty$. Again, we simply send $V \rightarrow s \rightarrow +\infty$ to obtain the identity independent of V .

$\mathcal{B}_{10} = \mathcal{T}\mathcal{B}_{-1}\mathcal{T}^{-1}$. Lastly, we consider the \mathcal{T} -dualization of a $(1, -1)$ -brane into a $(1, 0)$ -brane, which corresponds to the duality in Figure 57.

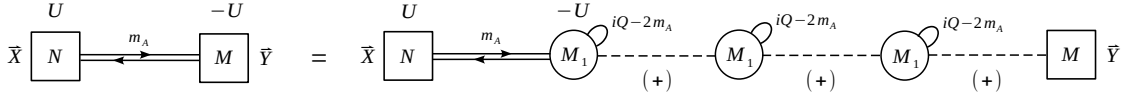


Figure 57. The $\mathcal{B}_{10} = \mathcal{T}\mathcal{B}_{-1}\mathcal{T}^{-1} = \mathcal{T}\mathcal{B}_{-1}STSTS$ duality move.

This translates into the identity

$$\begin{aligned}
\mathcal{Z}_{(1,0)}^{(N,M)}(\vec{X}; \vec{Y}; U; m_A) &= \int d\vec{Z}_N^{(1)} \Delta_N^{3d}(\vec{Z}^{(1)}; m_A) \left(\prod_{k=2}^6 d\vec{Z}_M^{(k)} \Delta_M^{3d}(\vec{Z}^{(k)}; m_A) \right) \mathcal{Z}_{\mathcal{T}}^{(N)}(\vec{X}; \vec{Z}^{(1)}; m_A) \\
&\times \mathcal{Z}_{(1,-1)}^{(N,M)}(\vec{Z}^{(1)}; \vec{Z}^{(2)}; U; m_A) \mathcal{Z}_S^{(M)}(\vec{Z}^{(2)}; \vec{Z}^{(3)}; m_A) \mathcal{Z}_{\mathcal{T}}^{(M)}(\vec{Z}^{(3)}; \vec{Z}^{(4)}; m_A) \\
&\times \mathcal{Z}_S^{(M)}(\vec{Z}^{(4)}; \vec{Z}^{(5)}; m_A) \mathcal{Z}_{\mathcal{T}}^{(M)}(\vec{Z}^{(5)}; \vec{Z}^{(6)}; m_A) \mathcal{Z}_S^{(M)}(\vec{Z}^{(6)}; \vec{Y}; m_A),
\end{aligned} \tag{4.46}$$

where we recall that the contribution of a $(1, -1)$ -brane was defined in (4.40). Once again, this identity can be obtained from the corresponding 4d identity (2.34) with the limit (4.45).

4.3.3 \mathcal{T}^T -dualization

We also discuss below the basic moves involving the $SL(2, \mathbb{Z})$ element $\mathcal{T}^T = -\mathcal{T}ST$ with inverse $(\mathcal{T}^T)^{-1} = -STS$.

$\mathcal{B}_{11} = \mathcal{T}^T\mathcal{B}_{01}(\mathcal{T}^T)^{-1}$. The \mathcal{T}^T -dualization of a $(0, 1)$ -brane into a $(1, 1)$ -brane corresponds to the duality in Figure 58.

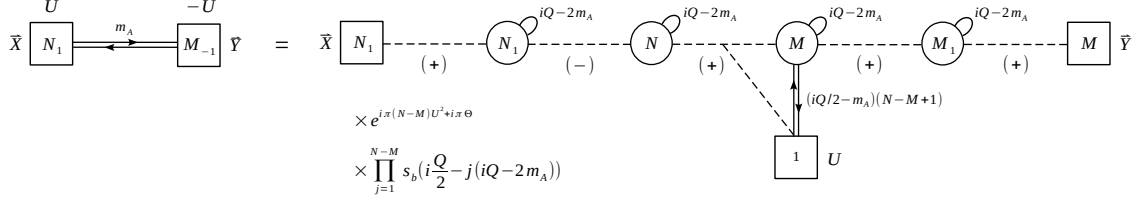


Figure 58. The $\mathcal{B}_{11} = \mathcal{T}^T \mathcal{B}_{01} (\mathcal{T}^T)^{-1} = \mathcal{T} \mathcal{S} \mathcal{T} \mathcal{B}_{01} \mathcal{S} \mathcal{T} \mathcal{S}$ duality move.

We then have the following identity of S_b^3 partition functions:

$$\begin{aligned}
\mathcal{Z}_{(1,1)}^{(N,M)}(\vec{X}; \vec{Y}; U; m_A) &= e^{i\pi(N-M)U^2 - i\pi\Theta} \prod_{j=1}^{N-M} s_b\left(i\frac{Q}{2} - j(iQ - 2m_A)\right) \\
&\times \int \left(\prod_{k=1}^3 d\vec{Z}_N^{(k)} \Delta_N^{3d}(\vec{Z}^{(k)}; m_A) \right) \left(\prod_{k=4}^6 d\vec{Z}_M^{(k)} \Delta_M^{3d}(\vec{Z}^{(k)}; m_A) \right) \\
&\times \mathcal{Z}_{\mathcal{T}}^{(N)}(-\vec{X}; \vec{Z}^{(1)}; m_A) \mathcal{Z}_{\mathcal{S}}^{(N)}(\vec{Z}^{(1)}; \vec{Z}^{(2)}; m_A) \mathcal{Z}_{\mathcal{T}}^{(N)}(\vec{Z}^{(2)}; \vec{Z}^{(3)}; m_A) \\
&\times \mathcal{Z}_{(0,1)}^{(N,M)}(\vec{Z}^{(3)}; \vec{Z}^{(4)}; U; i\frac{Q}{2} - m_A) \mathcal{Z}_{\mathcal{S}}^{(M)}(\vec{Z}^{(4)}; \vec{Z}^{(5)}; m_A) \mathcal{Z}_{\mathcal{T}}^{(M)}(\vec{Z}^{(5)}; \vec{Z}^{(6)}; m_A) \\
&\times \mathcal{Z}_{\mathcal{S}}^{(M)}(\vec{Z}^{(6)}; -\vec{Y}; m_A), \tag{4.47}
\end{aligned}$$

where we recall that Θ was defined in (4.39). Note that we have inserted the extra signs of $-\vec{X}$ and $-\vec{Y}$ on the right hand side, which reflect the minus sign of $\mathcal{T}^T = -\mathcal{T} \mathcal{S} \mathcal{T}$ and its inverse. This identity can be obtained, as usual, as a limit of (2.35) with

$$\begin{aligned}
X_i &\rightarrow X_i - s, & Y_j &\rightarrow Y_j - s, & Z_a^{(1,\dots,4)} &\rightarrow Z_a^{(1,\dots,4)} + s, \\
Z_a^{(5,6)} &\rightarrow Z_a^{(5,6)} - s, & U &\rightarrow U + s, & V &\rightarrow s, & s &\rightarrow +\infty
\end{aligned} \tag{4.48}$$

followed by $\Delta \rightarrow -\infty$ and $D \rightarrow +\infty$ satisfying $\Delta + D \rightarrow -\infty$.

$\mathcal{B}_{10} = \mathcal{T}^T \mathcal{B}_{10} (\mathcal{T}^T)^{-1}$. A (1,0)-brane is transparent under the T^T -dualization, which is translated into the non-trivial duality in Figure 59.

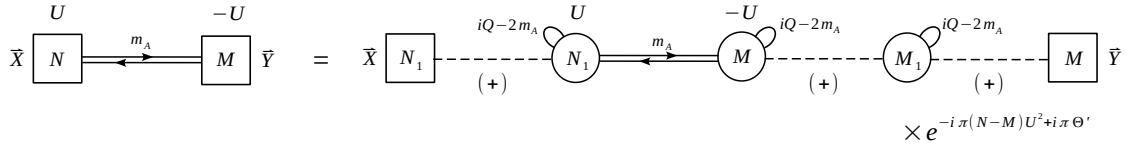


Figure 59. The $\mathcal{B}_{10} = \mathcal{T}^T \mathcal{B}_{10} (\mathcal{T}^T)^{-1} = \mathcal{T} \mathcal{S} \mathcal{T} \mathcal{B}_{10} \mathcal{S} \mathcal{T} \mathcal{S}$ duality move.

The associated S_b^3 partition function identity is

$$\begin{aligned}
\mathcal{Z}_{(1,0)}^{(N,M)}(\vec{X}; \vec{Y}; U; m_A) &= e^{-i\pi(N-M)U^2 - i\pi\Theta'} \\
&\times \int \left(\prod_{k=1}^3 d\vec{Z}_N^{(k)} \Delta_N^{3d}(\vec{Z}^{(k)}; m_A) \right) \left(\prod_{k=4}^6 d\vec{Z}_M^{(k)} \Delta_N^{3d}(\vec{Z}^{(k)}; m_A) \right) \\
&\times \mathcal{Z}_{\mathcal{T}}^{(N)}(-\vec{X}; \vec{Z}^{(1)}; m_A) \mathcal{Z}_{\mathcal{S}}^{(N)}(\vec{Z}^{(1)}; \vec{Z}^{(2)}; m_A) \mathcal{Z}_{\mathcal{T}}^{(N)}(\vec{Z}^{(2)}; \vec{Z}^{(3)}; m_A) \\
&\times \mathcal{Z}_{(1,0)}^{(N,M)}(\vec{Z}^{(3)}; \vec{Z}^{(4)}; U; m_A) \mathcal{Z}_{\mathcal{S}}^{(M)}(\vec{Z}^{(4)}; \vec{Z}^{(5)}; m_A) \mathcal{Z}_{\mathcal{T}}^{(M)}(\vec{Z}^{(5)}; \vec{Z}^{(6)}; m_A) \\
&\times \mathcal{Z}_{\mathcal{S}}^{(M)}(\vec{Z}^{(6)}; -\vec{Y}; m_A), \tag{4.49}
\end{aligned}$$

where we defined

$$\Theta' = \frac{N-M}{12} (iQ - 2m_A)^2 [(N-M)^2 - 1]. \tag{4.50}$$

This identity can be obtained as a limit of (2.36) with

$$\begin{aligned}
X_i &\rightarrow X_i + s, & Y_j &\rightarrow Y_j + s, & Z_a^{(1)} &\rightarrow Z_a^{(1)} - s, \\
Z_a^{(k>1)} &\rightarrow Z_a^{(k>1)} + s, & U &\rightarrow U - s, & V &\rightarrow s, & s &\rightarrow +\infty
\end{aligned} \tag{4.51}$$

followed by $\Delta \rightarrow -\infty$ and $D \rightarrow +\infty$ satisfying $\Delta + D \rightarrow -\infty$.

$\mathcal{B}_{0,-1} = \mathcal{T}^T \mathcal{B}_{1,-1} (\mathcal{T}^T)^{-1}$. Lastly, we consider the \mathcal{T}^T -dualization of a $(1, -1)$ -brane into a $(0, -1)$ -brane, or $\overline{D5}$, which corresponds to the duality in Figure 60

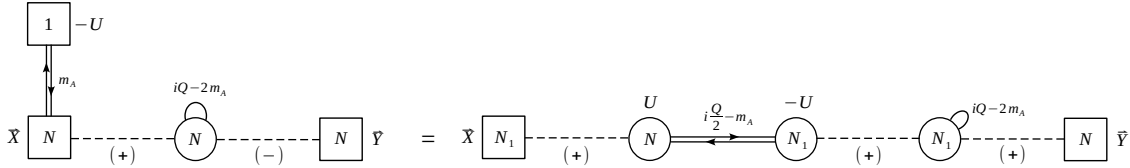


Figure 60. The $\mathcal{B}_{0,-1} = \mathcal{T}^T \mathcal{B}_{1,-1} (\mathcal{T}^T)^{-1}$ duality move.

At the level of S_b^3 partition function we have the following identity:

$$\begin{aligned}
\mathcal{Z}_{(0,-1)}^{(N)}(\vec{X}; \vec{Y}; U; m_A) &= \int \left(\prod_{k=1}^6 d\vec{Z}_N^{(k)} \Delta_N^{3d}(\vec{Z}^{(k)}; m_A) \right) \mathcal{Z}_{\mathcal{T}}^{(N)}(-\vec{X}; \vec{Z}^{(1)}; m_A) \\
&\times \mathcal{Z}_{\mathcal{S}}^{(N)}(\vec{Z}^{(1)}; \vec{Z}^{(2)}; m_A) \mathcal{Z}_{\mathcal{T}}^{(N)}(\vec{Z}^{(2)}; \vec{Z}^{(3)}; m_A) \\
&\times \mathcal{Z}_{(1,-1)}^{(N,N)} \left(\vec{Z}^{(3)}; \vec{Z}^{(4)}; U; i\frac{Q}{2} - m_A \right) \mathcal{Z}_{\mathcal{S}}^{(N)}(\vec{Z}^{(4)}; \vec{Z}^{(5)}; m_A) \\
&\times \mathcal{Z}_{\mathcal{T}}^{(N)}(\vec{Z}^{(5)}; \vec{Z}^{(6)}; m_A) \mathcal{Z}_{\mathcal{S}}^{(N)}(\vec{Z}^{(6)}; -\vec{Y}; m_A), \tag{4.52}
\end{aligned}$$

where $\mathcal{Z}_{(0,-1)}^{(N,M)}(\vec{X}; \vec{Y}; U; m_A) = \mathcal{Z}_{(0,1)}^{(N,M)}(\vec{X}; \vec{Y}; -U; m_A)$, which we obtain from the corresponding $4d$ identity (2.37) with the limit (4.51).

4.4 The Hanany–Witten duality move

As we stressed many times, the algorithm to dualize a quiver into its mirror dual works exactly in the same way in $4d$ and in $3d$. In particular, also in $3d$ we might end up with a theory in which some operator has a non-trivial VEV after we dualize the blocks of the chopped quiver via the basic duality moves. This will happen every time we start from a quiver with gauge nodes of unequal ranks, and it is the manifestation of the fact that in the brane setup after applying \mathcal{S} -duality we have D5-branes with different numbers of D3's on the left and on the right. One then has to reorder the branes using Hanany–Witten (HW) moves until we reach the situation in which all D5-branes have an equal number of D3's on the left and on the right. In such a situation we are able to read off the mirror dual quiver gauge theory. In field theory this operation amounts to studying the aforementioned VEVs. In Section 3, we have seen three equivalent ways of studying these VEVs. One of these was a duality that realizes the HW move in the field theory language. In order to complete the algorithm we then need an analogous duality in $3d$. The $3d$ HW duality move is given in Figure 61.

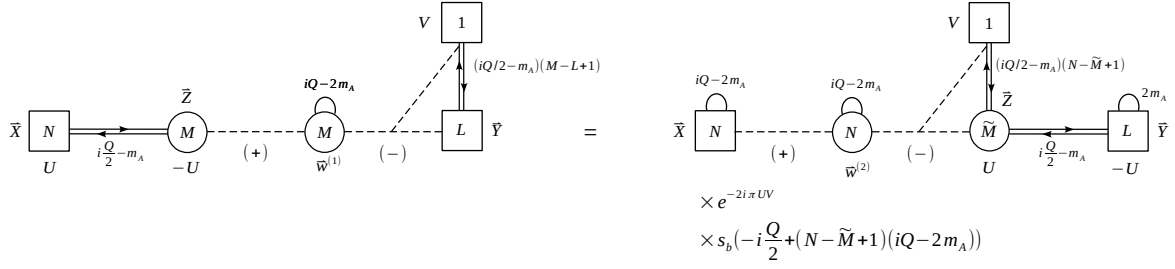


Figure 61. The HW duality move in $3d$.

We can obtain the corresponding partition function identity by studying a limit of the index identity (3.1) associated to the $4d$ HW move duality, which is realized by

$$X_i \rightarrow X_i + s, \quad Y_j \rightarrow Y_j + s, \quad Z_a \rightarrow Z_a + s, \quad U \rightarrow U - s, \quad V \rightarrow V + s, \quad s \rightarrow +\infty \quad (4.53)$$

followed by $\Delta \rightarrow -\infty$. Then this limit results in the following $3d$ partition function identity for $N \geq \tilde{M} \geq 0$ as consistent with the S-rule:

$$\begin{aligned} & \int d\vec{Z}_M \Delta_M^{3d}(\vec{Z}) \mathcal{Z}_{(1,0)}^{(N,M)} \left(\vec{X}; \vec{Z}; U; i\frac{Q}{2} - m_A \right) \hat{\mathcal{Z}}_{\vec{Y},V}^{3d}(m_A) \\ & \times \prod_{j=1}^L s_b \left(\frac{iQ}{2} - \left(\frac{iQ}{2} - m_A \right) (M - L + 1) \pm (Y_j - V) \right) \\ & = e^{-2i\pi UV} s_b \left(-i\frac{Q}{2} + (N - \tilde{M} + 1)(iQ - 2m_A) \right) \end{aligned}$$

$$\begin{aligned}
& \times \prod_{i,j=1}^N s_b \left(-i\frac{Q}{2} + 2m_A \pm (X_i - X_j) \right) \prod_{i,j=1}^L s_b \left(i\frac{Q}{2} - 2m_A \pm (Y_i - Y_j) \right) \\
& \times \int d\vec{Z}_{\widetilde{M}} \Delta_{\widetilde{M}}^{3d}(\vec{Z}) \prod_{j=1}^{\widetilde{M}} s_b \left(\frac{iQ}{2} - \left(\frac{iQ}{2} - m_A \right) (N - \widetilde{M} + 1) \pm (Z_j - V) \right) \\
& \times \widehat{\mathbb{X}}_{\vec{Z},V}^{3d}(m_A) \mathcal{Z}_{(1,0)}^{(\widetilde{M},L)} \left(\vec{Z}; \vec{Y}; U; i\frac{Q}{2} - m_A \right). \tag{4.54}
\end{aligned}$$

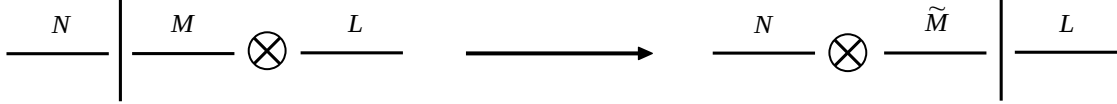


Figure 62. The HW brane move swapping NS5 (a solid vertical line) and D5 (a crossed circle), where $\widetilde{M} = N + L - M + 1$.

This encodes in field theory the Hanany–Witten move that swaps a $(1, 0)$ with a $(0, 1)$ -brane as shown in Figure 62, where before the transition we have N -D3 branes on the left of the $(1, 0)$, M D3-branes between the $(1, 0)$ and the $(0, 1)$ -brane, and L D3-branes on the right of the $(0, 1)$, while after the transition we have N D3-branes on the left of the $(0, 1)$, \widetilde{M} D3-branes between the $(0, 1)$ and the $(1, 0)$, and L D3-branes on the right of the $(1, 0)$. One can also consider HW moves swapping a $(1, 0)$ and a $(1, 1)$ -brane as shown in Figure 63. These moves are not strictly necessary, since we can read off a gauge theory from the brane setup even if we have $(1, 1)$ -branes with a different number of D3’s on each side. Nevertheless, this is still interesting since the two equivalent brane configurations before and after the HW move are usually associated with distinct gauge theories, leading to a non-trivial IR duality. In field theory, this amounts to using the Giveon–Kutasov duality [104] to dualize the gauge node associated with the D3-branes suspended between the $(1, 0)$ and the $(1, 1)$ -brane involved in the HW move.

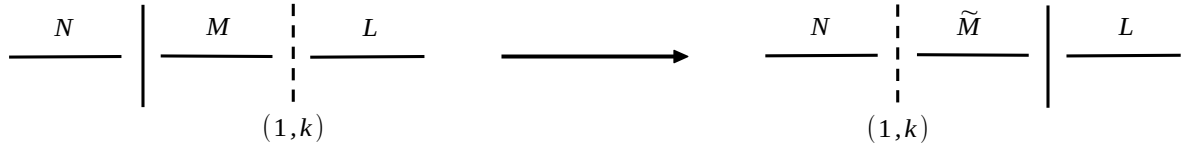


Figure 63. The HW brane move swapping NS5 (a solid vertical line) and $(1, k)$ (a dashed vertical line), where $\widetilde{M} = N + L - M + |k|$, which in field theory is realized by a local application of the Giveon–Kutasov duality

The Giveon–Kutasov duality relates a $3d \mathcal{N} = 2 U(N_c)_k$ theory with N_f fundamental flavors $Q^i, \widetilde{Q}_i, i = 1, \dots, N_f$ and no superpotential, $\mathcal{W} = 0$, to a $U(N_f + |k| - N_c)_{-k}$ theory with N_f fundamental flavors $q_i, \widetilde{q}^i, N_f^2$ gauge singlets M_j^i and superpotential $\widehat{\mathcal{W}} = M_j^i q_i \widetilde{q}^j$. The reason why we can apply this duality is because the node of the quiver that we want

to dualize has a non-zero CS level due to the presence of the (1, 1)-brane, which makes the $\mathcal{N} = 2$ adjoint chiral in the $\mathcal{N} = 4$ vector multiplet massive so that at low energies we have an effective $\mathcal{N} = 2$ theory with only fundamental flavors and a quartic superpotential. The identity of the S_b^3 partition functions associated with the Giveon–Kutasov duality is [105, 106]

$$\begin{aligned}
& \int d\vec{Z}_{N_c} \Delta_{N_c}^{3d}(\vec{Z}) e^{-ik\pi \sum_{i=1}^{N_c} Z_i^2 - \pi i \eta \sum_{i=1}^N Z_i} \prod_{i=1}^{N_c} \prod_{a=1}^{N_f} s_b \left(i \frac{Q}{2} \mp Z_i - \mu_a^\pm \right) \\
&= e^{\frac{i\pi}{24}(k^2+2) - \frac{i\pi}{2}\phi} \prod_{a,b=1}^{N_f} s_b \left(i \frac{Q}{2} - \mu_a^+ - \mu_b^- \right) \\
&\quad \times \int d\vec{Z}'_{N'_c} \Delta_{N'_c}^{3d}(\vec{Z}') e^{ik\pi \sum_{i=1}^{N'_c} Z_i'^2 + \pi i \eta \sum_{i=1}^{N'_c} Z_i'} \prod_{i=1}^{N'_c} \prod_{a=1}^{N_f} s_b \left(\mp Z_i' + \mu_a^\pm \right). \tag{4.55}
\end{aligned}$$

where $k > 0$ and

$$\begin{aligned}
\phi = k & \left(\sum_{a=1}^{N_f} \left((\mu_a^+)^2 + (\mu_a^-)^2 \right) - \frac{Q^2}{4} k (k - 2N'_c) + \frac{1}{2} \eta^2 - iQk \sum_{a=1}^{N_f} (\mu_a^+ + \mu_a^-) \right. \\
& \left. + \eta \sum_{a=1}^{N_f} (\mu_a^+ - \mu_a^-) + \frac{1}{2} \left(iQN'_c - \sum_{a=1}^{N_f} (\mu_a^+ + \mu_a^-) \right)^2 \right) \tag{4.56}
\end{aligned}$$

where μ_a^\pm are the real masses for the $U(N_f) \times U(N_f)/U(1)$ flavor symmetry.

Notice the exponential prefactors that can be interpreted as contact terms for the global symmetries [107, 108]. These are crucial since inside a quiver such symmetries are actually gauged, and the contact terms induce CS couplings for the gauge nodes that are adjacent to the quiver we dualized. This is expected from the brane perspective, since moving a (1, 1) through a (1, 0) not only affects the CS level of the gauge node associated to the D3's suspended between them by changing its sign, but also those of the nodes associated to the adjacent intervals. Moreover, the gauge singlets produced with the duality might give mass to/produce adjoint chiral fields for the adjacent nodes, again compatibly with the fact that their CS levels change after the dualization.

In the next section, we will encounter the 4d analogue of the Hanany–Witten move between a (1, 0) and a (1, 1)-brane. Also in that case the theories before and after the transition can be related by a simple dualization of the relevant gauge node in the quiver, but in 4d the basic duality will be once again the Intriligator–Pouliot duality. This is compatible with the fact that the Giveon–Kutasov duality in 3d can also be obtained from the Intriligator–Pouliot duality in 4d.

5 Duality webs

In this section we apply the algorithm to construct a web of dualities for an SQCD example both in 4d and in 3d.

5.1 $4d$ $PSL(2, \mathbb{Z})$ duality web

Using the $PSL(2, \mathbb{Z})$ duality moves we introduced in Section 2 we construct the web of dualities in Figure 64. We start from the SQCD with $N_c = 2$ and $N_f = 4$, which we call Theory A and depict in the upper left corner of the figure, and sequentially apply different duality moves corresponding to S , $(T^T)^{-1}$, S , and T^{-1} to reach the other corners of the diagram. Theory B is the mirror dual of Theory A , i.e. its S -dual. Theory C_1 is obtained by acting with $(T^T)^{-1}$ on Theory B . In addition to C_1 we have two extra frames, C_2 and C_3 shown in Figure 65, which are obtained by IP dualizations. Theory D is obtained by acting with S on C_1 (or C_2 , or C_3) and the web closes by acting with T^{-1} on Theory D to go back to Theory A , since $S(T^T)^{-1}ST^{-1} = S(STS)ST^{-1} = 1$.

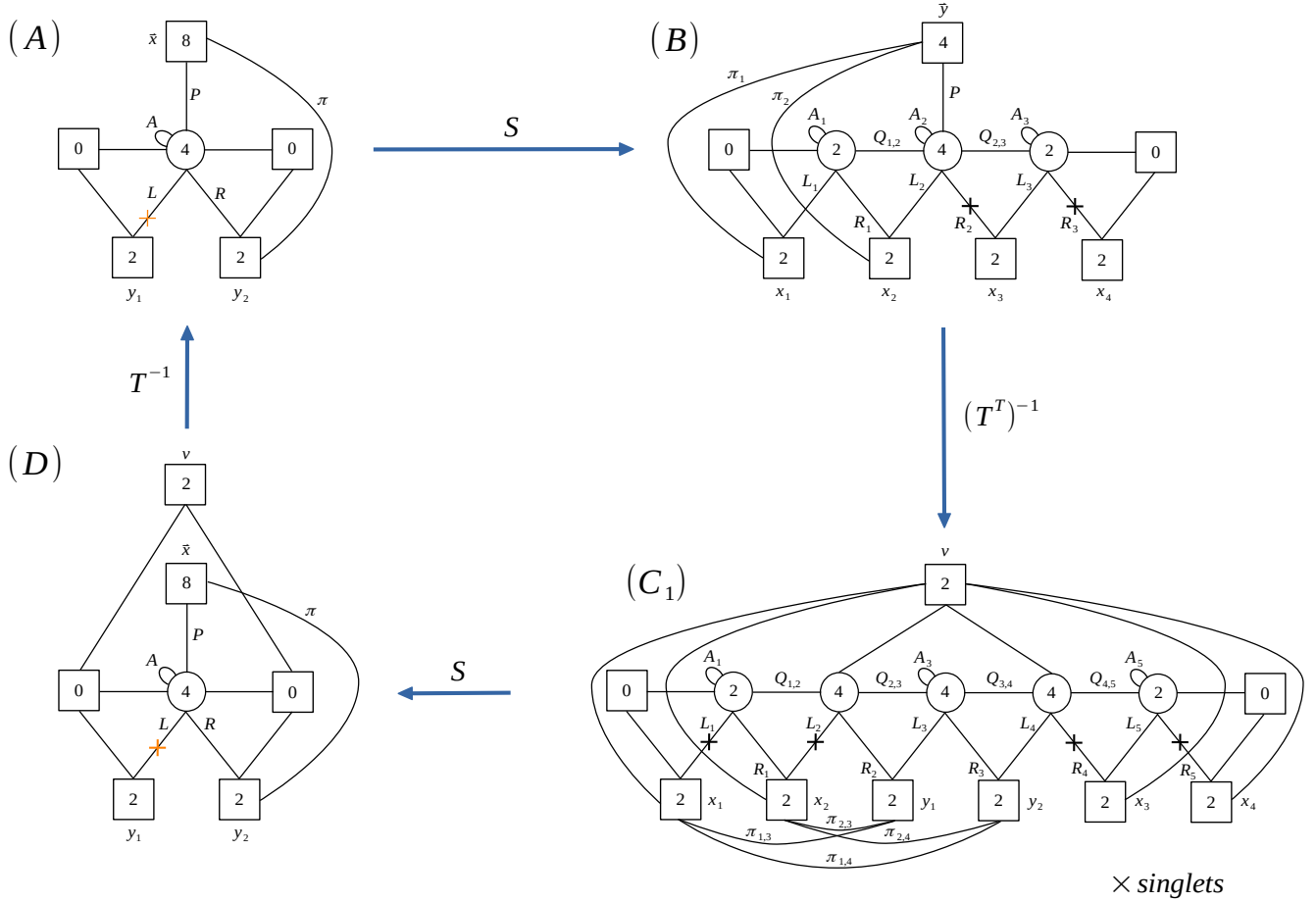


Figure 64. A $PSL(2, \mathbb{Z})$ duality web for the $4d$ SQCD with $N_c = 2$ and $N_f = 4$. The theory C_1 has extra singlets that we specify in Figures 67 and 68.

We have already discussed in details the S -dualization of the SQCD for generic N_c and N_f in Subsection 3.1, so in Figure 66 we just briefly summarize the resulting mirror duality for the particular case $N_c = 2$ and $N_f = 4$.

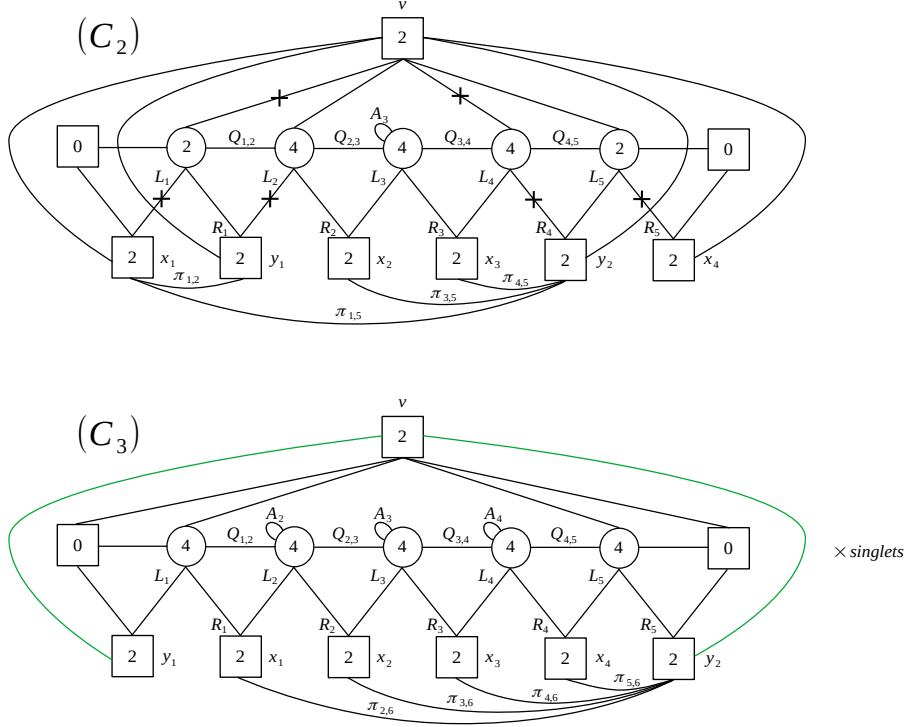


Figure 65. The IP dual frames C_2 and C_3 . Theory C_3 has extra singlets that we specify in Figure 68.

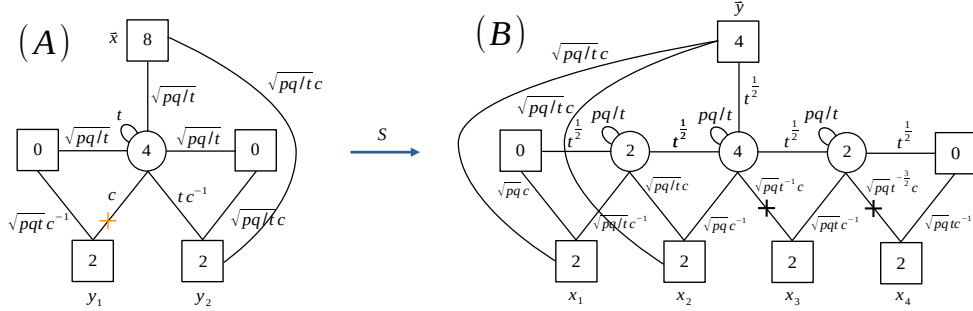


Figure 66. Theory A S-dualized to Theory B.

Let us now focus on how to get the other dual frames by sequential duality moves. In Figure 67 we show how Theory C_1 is obtained by taking the $(T^T)^{-1}$ -dualization of Theory B. We first chop Theory B into the QFT blocks. Notice that, as shown in the figure, the nodes that we are un-gauging have an antisymmetric field with charges corresponding to pq/t . Similarly the QFT blocks B_{10} and B_{01} appearing have $t \rightarrow pq/t$ w.r.t. their definition in Section 2. We then dualize each block using the basic $(T^T)^{-1} = (STS)$ -moves (the inverse of the T^T -moves in Section 2.3) and we glue them together. Since we dualize QFT blocks where t is replaced by pq/t , the S-walls appearing in Figure 67 are defined with $t \rightarrow pq/t$,

and we color them in orange to emphasize this replacement. Lastly, we recognize the several identity walls corresponding to $\mathbb{T}^T(\mathbb{T}^T)^{-1} = 1$ as in Figure 10 and finally reach Theory C_1 , which is the desired $(\mathbb{T}^T)^{-1}$ -dual theory.

The C_2 and C_3 theories can be obtained, as depicted in Figure 68, by applying the IP duality to the gauge nodes colored in red, which do not have antisymmetric fields.

This operation can be regarded as the $4d$ field theory analogue of swapping an NS5 and a (1,1)-brane. In this case, as opposed to the swapping of NS5 and D5-branes, it is possible to read off a gauge theory from the brane system both before and after the move, which results in equivalent, i.e. IR dual, theories.

We then can S-dualize each one of these theories to reach Theory D . Let's start with theory C_1 , which we chop into QFT blocks as shown in the upper part of Figure 69. We dualize each block using the basic S-moves in Figures (2.26) and (2.29). Then we glue them together to get Theory D after the Identity-walls are implemented. One can similarly show that the S-dualization of C_2 and C_3 yields again Theory D .

One should note that Theory D is actually the same field theory as Theory A but realized in terms of B_{11} blocks rather than with B_{10} blocks (if we keep track of the trivial rank-zero nodes and the $SU(2)_v$ node attached to them) Although Theory A and Theory D already coincide as field theories, we still implement the \mathbb{T}^{-1} -dualization of Theory D . As we saw in Section 2, under \mathbb{T}^{-1} the B_{01} block is transparent while the B_{11} block is turned into a B_{10} so that we indeed expect to obtain Theory A from Theory D . As shown in Figure 70 we chop Theory D into QFT blocks, dualize each block using the basic \mathbb{T}^{-1} -moves and glue them together. We now recognize the Identity-walls corresponding to $\mathbb{T}^{-1}\mathbb{T} = 1$ and after implementing them we obtain Theory A , closing the duality web.

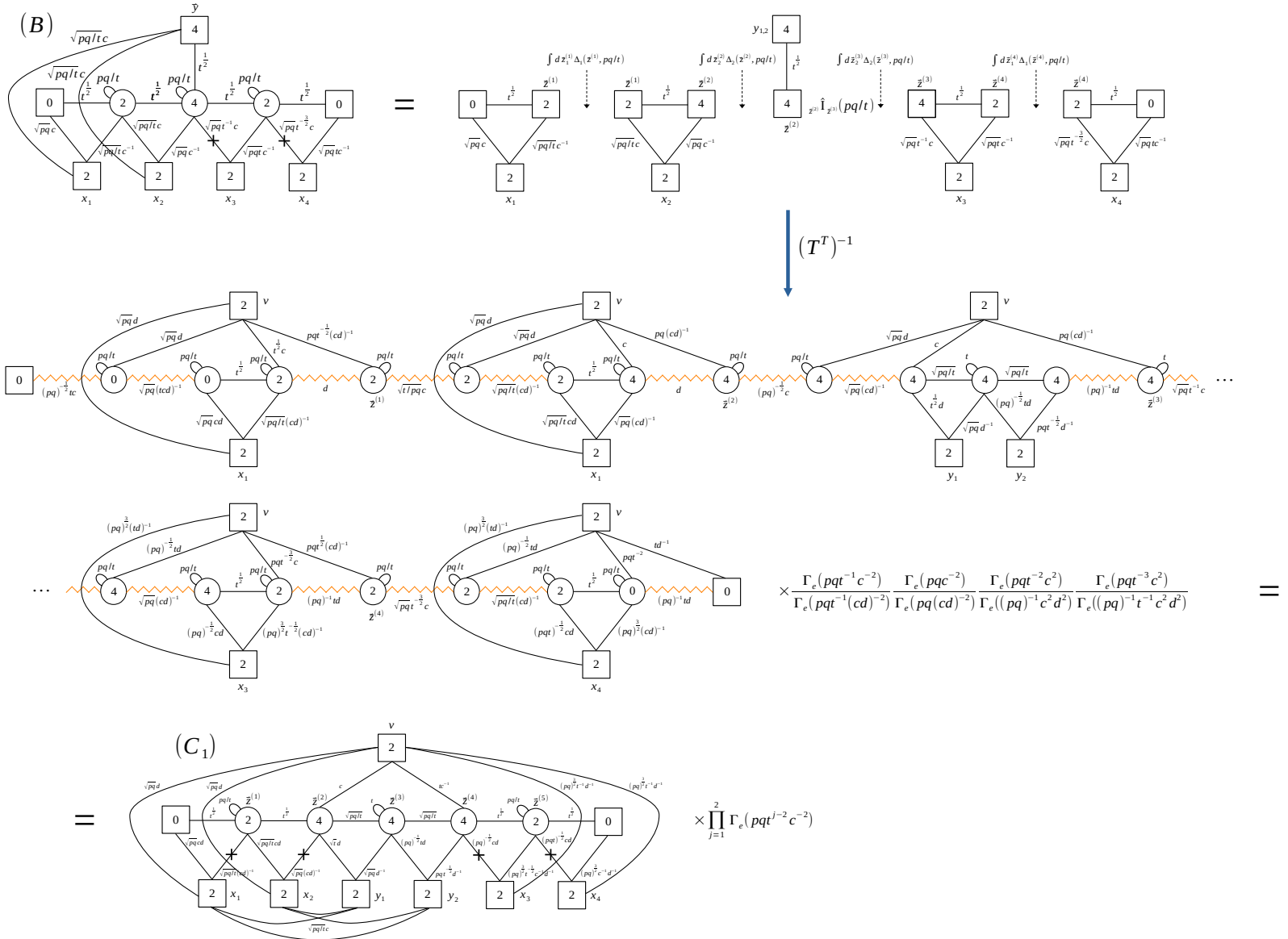


Figure 67. Theory B $(T^T)^{-1}$ -dualized to Theory C₁.

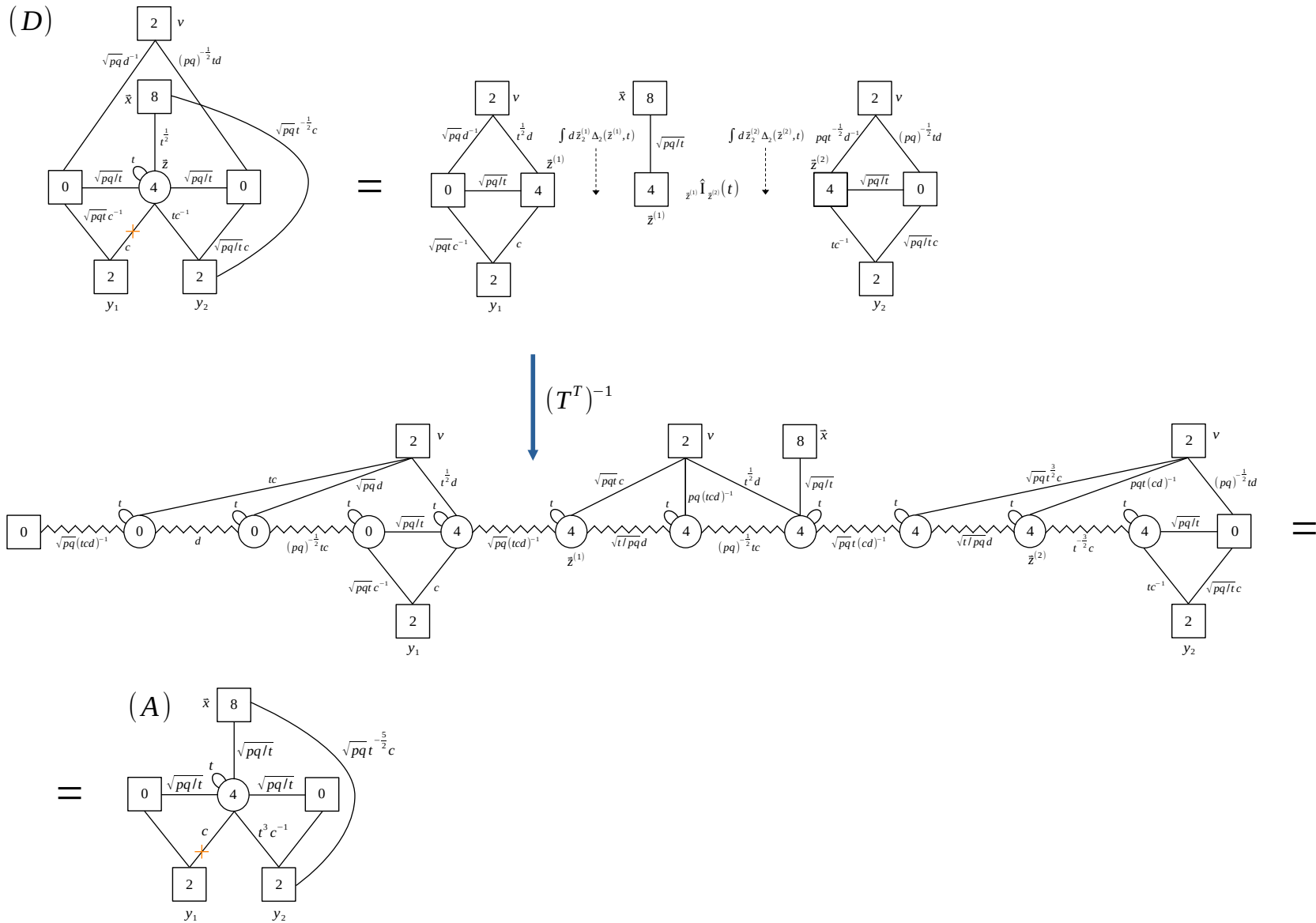


Figure 70. Theory D T^{-1} -dualized to Theory A .

5.2 4d operators map

It is worth studying the symmetry and the operator map of the theories to better understand how the duality web works. The global symmetry in the IR is given by

$$USp(8)_x \times USp(4)_y \times U(1)_t \times U(1)_c. \quad (5.1)$$

However, this symmetry is not fully manifest in all the frames. The manifest UV symmetry in each dual frame is given as follows:

$$A: \quad USp(8)_x \times SU(2)_{y_1} \times SU(2)_{y_2} \times U(1)_t \times U(1)_c, \quad (5.2)$$

$$B: \quad \prod_{i=1}^4 SU(2)_{x_i} \times USp(4)_y \times U(1)_t \times U(1)_c, \quad (5.3)$$

$$C_i: \quad \prod_{i=1}^4 SU(2)_{x_i} \times SU(2)_{y_1} \times SU(2)_{y_2} \times SU(2)_v \times U(1)_d \times U(1)_t \times U(1)_c, \quad (5.4)$$

$$D: \quad USp(8)_x \times SU(2)_{y_1} \times SU(2)_{y_2} \times U(1)_t \times U(1)_c. \quad (5.5)$$

Notice that C_1 , C_2 , and C_3 have an extra $U(1)_d \times SU(2)_v$ symmetry, which doesn't appear in the other frames. By the duality we then expect this not to be a faithful symmetry in the IR, i.e. it acts trivially on the spectrum of the theory. In consistency with this claim, we checked that all the anomalies involving these symmetries vanish. Namely, we have checked that

$$\text{Tr } SU(2)_v^2 U(1)_a = 0 \quad (5.6)$$

for any abelian symmetry $U(1)_a$, and the other anomalies involving $SU(2)_v$ trivially vanish. Moreover, we have checked that the linear and cubic $U(1)_R$ anomalies, calculated assuming mixing with all the abelian symmetries, are independent from the mixing with $U(1)_d$, which implies that all the anomalies involving $U(1)_d$ vanish.

We next construct some gauge invariant operators and explain their symmetry group representations and how they are mapped under the duality web. Firstly let us construct operators in Theory A , which is the same as Theory D . Specifically, we list five types of operators in Table 1, which combine to form representations of the enhanced $USp(8)_x \times USp(4)_y$ symmetry in the IR.

	$USp(8)_x \times SU(2)_{y_1} \times SU(2)_{y_2}$	$U(1)_R$	$U(1)_t$	$U(1)_c$
$\text{Tr } P^2$	$(\mathbf{27}, \mathbf{1}, \mathbf{1})$	2	-1	0
$\text{Tr } PL$	$(\mathbf{8}, \mathbf{2}, \mathbf{1})$	1	-1/2	1
π	$(\mathbf{8}, \mathbf{1}, \mathbf{2})$	1	-1/2	1
$\text{Tr } LR$	$(\mathbf{1}, \mathbf{2}, \mathbf{2})$	0	1	0
$\text{Tr } A$	$(\mathbf{1}, \mathbf{1}, \mathbf{1})$	0	1	0

Table 1. Gauge invariant chiral operators in Theory $A =$ Theory D .

The operators rearrange into representations of the full enhanced symmetry according to the following branching rules for $USp(4)_y \rightarrow SU(2)_{y_1} \times SU(2)_{y_2}$:

$$\text{Tr } LR, \quad \text{Tr } A \quad \longrightarrow \quad (\mathbf{1}, \mathbf{2}, \mathbf{2}) \oplus (\mathbf{1}, \mathbf{1}, \mathbf{1}) = (\mathbf{1}, \mathbf{5}), \quad (5.7)$$

$$\text{Tr } PL, \quad \pi \quad \longrightarrow \quad (\mathbf{8}, \mathbf{2}, \mathbf{1}) \oplus (\mathbf{8}, \mathbf{1}, \mathbf{2}) = (\mathbf{8}, \mathbf{4}), \quad (5.8)$$

$$\text{Tr } P^2 \quad \longrightarrow \quad (\mathbf{27}, \mathbf{1}, \mathbf{1}) = (\mathbf{27}, \mathbf{1}). \quad (5.9)$$

For Theory B we consider the operators that are listed in Table 2.

	$\prod_{i=1}^4 SU(2)_{x_i} \times USp(4)_y$	$U(1)_R$	$U(1)_t$	$U(1)_c$
$\text{Tr } P^2$	$(\mathbf{1}, \mathbf{1}, \mathbf{1}, \mathbf{1}, \mathbf{5})$	0	1	0
π_1	$(\mathbf{2}, \mathbf{1}, \mathbf{1}, \mathbf{1}, \mathbf{4})$	1	-1/2	1
π_2	$(\mathbf{1}, \mathbf{2}, \mathbf{1}, \mathbf{1}, \mathbf{4})$	1	-1/2	1
$\text{Tr } PR_2$	$(\mathbf{1}, \mathbf{1}, \mathbf{2}, \mathbf{1}, \mathbf{4})$	1	-1/2	1
$\text{Tr } PQ_{2,3}R_3$	$(\mathbf{1}, \mathbf{1}, \mathbf{1}, \mathbf{2}, \mathbf{4})$	1	-1/2	1
$\text{Tr } L_1R_1$	$(\mathbf{2}, \mathbf{2}, \mathbf{1}, \mathbf{1}, \mathbf{1})$	2	-1	0
$\text{Tr } L_1Q_{1,2}R_2$	$(\mathbf{2}, \mathbf{1}, \mathbf{2}, \mathbf{1}, \mathbf{1})$	2	-1	0
$\text{Tr } L_1Q_{1,2}Q_{2,3}R_3$	$(\mathbf{2}, \mathbf{1}, \mathbf{1}, \mathbf{2}, \mathbf{1})$	2	-1	0
$\text{Tr } L_2R_2$	$(\mathbf{1}, \mathbf{2}, \mathbf{2}, \mathbf{1}, \mathbf{1})$	2	-1	0
$\text{Tr } L_2Q_{2,3}R_2$	$(\mathbf{1}, \mathbf{2}, \mathbf{1}, \mathbf{2}, \mathbf{1})$	2	-1	0
$\text{Tr } L_3R_3$	$(\mathbf{1}, \mathbf{1}, \mathbf{2}, \mathbf{2}, \mathbf{1})$	2	-1	0
$\text{Tr } A_1$	$(\mathbf{1}, \mathbf{1}, \mathbf{1}, \mathbf{1}, \mathbf{1})$	2	-1	0
$\text{Tr } A_2$	$(\mathbf{1}, \mathbf{1}, \mathbf{1}, \mathbf{1}, \mathbf{1})$	2	-1	0
$\text{Tr } A_3$	$(\mathbf{1}, \mathbf{1}, \mathbf{1}, \mathbf{1}, \mathbf{1})$	2	-1	0

Table 2. Gauge invariant chiral operators in Theory B .

Again they combine into representations of $USp(8)_x \times USp(4)_y$ according to the following branching rules of $USp(8)_x \rightarrow \prod_{i=1}^4 SU(2)_{x_i}$:

$$\text{Tr } P^2 \quad \longrightarrow \quad (\mathbf{1}, \mathbf{1}, \mathbf{1}, \mathbf{1}, \mathbf{5}) = (\mathbf{1}, \mathbf{5}), \quad (5.10)$$

$$\begin{aligned} \pi_1, \pi_2 \\ \text{Tr } PR_2, \text{Tr } PQ_{2,3}R_3 \end{aligned} \quad \longrightarrow \quad \begin{aligned} &(\mathbf{2}, \mathbf{1}, \mathbf{1}, \mathbf{1}, \mathbf{4}) \oplus (\mathbf{1}, \mathbf{2}, \mathbf{1}, \mathbf{1}, \mathbf{4}) \\ &\oplus (\mathbf{1}, \mathbf{1}, \mathbf{2}, \mathbf{1}, \mathbf{4}) \oplus (\mathbf{1}, \mathbf{1}, \mathbf{1}, \mathbf{2}, \mathbf{4}) \\ &= (\mathbf{8}, \mathbf{4}), \end{aligned} \quad (5.11)$$

$$\begin{aligned} \text{Tr } L_1R_1, \text{Tr } L_1Q_{1,2}R_2, \text{Tr } L_1Q_{1,2}Q_{2,3}R_3, \\ \text{Tr } L_2R_2, \text{Tr } L_2Q_{2,3}R_2, \text{Tr } L_3R_3, \\ \text{Tr } A_1, \text{Tr } A_2, \text{Tr } A_3 \end{aligned} \quad \longrightarrow \quad \begin{aligned} &(\mathbf{2}, \mathbf{2}, \mathbf{1}, \mathbf{1}, \mathbf{1}) \oplus (\mathbf{2}, \mathbf{1}, \mathbf{2}, \mathbf{1}, \mathbf{1}) \\ &\oplus (\mathbf{2}, \mathbf{1}, \mathbf{1}, \mathbf{2}, \mathbf{1}) \oplus (\mathbf{1}, \mathbf{2}, \mathbf{2}, \mathbf{1}, \mathbf{1}) \\ &\oplus (\mathbf{1}, \mathbf{2}, \mathbf{1}, \mathbf{2}, \mathbf{1}) \oplus (\mathbf{1}, \mathbf{1}, \mathbf{2}, \mathbf{2}, \mathbf{1}) \\ &\oplus (\mathbf{1}, \mathbf{1}, \mathbf{1}, \mathbf{1}, \mathbf{1}) \oplus (\mathbf{1}, \mathbf{1}, \mathbf{1}, \mathbf{1}, \mathbf{1}) \\ &\oplus (\mathbf{1}, \mathbf{1}, \mathbf{1}, \mathbf{1}, \mathbf{1}) \\ &= (\mathbf{27}, \mathbf{1}). \end{aligned} \quad (5.12)$$

We then consider the operators of theory C_1 that are listed in Table 3.

	$\prod_{i=1}^4 SU(2)_{x_i} \times SU(2)_{y_1} \times SU(2)_{y_2}$	$U(1)_R$	$U(1)_t$	$U(1)_c$
$\text{Tr } L_1 R_1$	$(\mathbf{2}, \mathbf{2}, \mathbf{1}, \mathbf{1}, \mathbf{1}, \mathbf{1})$	2	-1	0
$\text{Tr } L_1 Q_{1,2} Q_{2,3} Q_{3,4} R_4$	$(\mathbf{2}, \mathbf{1}, \mathbf{2}, \mathbf{1}, \mathbf{1}, \mathbf{1})$	2	-1	0
$\text{Tr } L_1 Q_{1,2} Q_{2,3} Q_{3,4} Q_{4,5} R_5$	$(\mathbf{2}, \mathbf{1}, \mathbf{1}, \mathbf{2}, \mathbf{1}, \mathbf{1})$	2	-1	0
$\text{Tr } L_2 Q_{2,3} Q_{3,4} R_4$	$(\mathbf{1}, \mathbf{2}, \mathbf{2}, \mathbf{1}, \mathbf{1}, \mathbf{1})$	2	-1	0
$\text{Tr } L_2 Q_{2,3} Q_{3,4} Q_{4,5} R_5$	$(\mathbf{1}, \mathbf{2}, \mathbf{1}, \mathbf{2}, \mathbf{1}, \mathbf{1})$	2	-1	0
$\text{Tr } L_5 R_5$	$(\mathbf{1}, \mathbf{1}, \mathbf{2}, \mathbf{2}, \mathbf{1}, \mathbf{1})$	2	-1	0
$\pi_{1,3}$	$(\mathbf{2}, \mathbf{1}, \mathbf{1}, \mathbf{1}, \mathbf{2}, \mathbf{1})$	1	-1/2	1
$\pi_{2,3}$	$(\mathbf{1}, \mathbf{2}, \mathbf{1}, \mathbf{1}, \mathbf{2}, \mathbf{1})$	1	-1/2	1
$\pi_{1,4}$	$(\mathbf{2}, \mathbf{1}, \mathbf{1}, \mathbf{1}, \mathbf{1}, \mathbf{2})$	1	-1/2	1
$\pi_{2,4}$	$(\mathbf{1}, \mathbf{2}, \mathbf{1}, \mathbf{1}, \mathbf{1}, \mathbf{2})$	1	-1/2	1
$\text{Tr } L_3 Q_{3,4} R_4$	$(\mathbf{1}, \mathbf{1}, \mathbf{2}, \mathbf{1}, \mathbf{2}, \mathbf{1})$	1	-1/2	1
$\text{Tr } L_3 Q_{3,4} Q_{4,5} R_5$	$(\mathbf{1}, \mathbf{1}, \mathbf{1}, \mathbf{2}, \mathbf{2}, \mathbf{1})$	1	-1/2	1
$\text{Tr } L_4 R_4$	$(\mathbf{1}, \mathbf{1}, \mathbf{2}, \mathbf{1}, \mathbf{1}, \mathbf{2})$	1	-1/2	1
$\text{Tr } L_4 Q_{4,5} R_5$	$(\mathbf{1}, \mathbf{1}, \mathbf{1}, \mathbf{2}, \mathbf{1}, \mathbf{2})$	1	-1/2	1
$\text{Tr } L_3 R_3$	$(\mathbf{1}, \mathbf{1}, \mathbf{1}, \mathbf{1}, \mathbf{2}, \mathbf{2})$	0	1	0
$\text{Tr } A_1$	$(\mathbf{1}, \mathbf{1}, \mathbf{1}, \mathbf{1}, \mathbf{1}, \mathbf{1})$	2	-1	0
$\text{Tr } A_3$	$(\mathbf{1}, \mathbf{1}, \mathbf{1}, \mathbf{1}, \mathbf{1}, \mathbf{1})$	0	1	0
$\text{Tr } A_5$	$(\mathbf{1}, \mathbf{1}, \mathbf{1}, \mathbf{1}, \mathbf{1}, \mathbf{1})$	2	-1	0
$\text{Tr } Q_{2,3}^2 = \text{Tr } Q_{3,4}^2$	$(\mathbf{1}, \mathbf{1}, \mathbf{1}, \mathbf{1}, \mathbf{1}, \mathbf{1})$	2	-1	0

Table 3. Gauge invariant chiral operators in Theory C_1 and their charges under the faithful symmetries.

Notice that these operators transform trivially under $U(1)_d \times SU(2)_v$, in accordance with the expectation that this symmetry is not faithful in the IR.¹² Again they can be arranged into representations of the full enhanced symmetry according to the following branching rules of $USp(8)_x \times USp(4)_y \rightarrow \prod_{i=1}^4 SU(2)_{x_i} \times SU(2)_{y_1} \times SU(2)_{y_2}$:

$$\begin{aligned}
\text{Tr } L_3 R_3, \quad \text{Tr } A_3 &\longrightarrow (\mathbf{1}, \mathbf{1}, \mathbf{1}, \mathbf{1}, \mathbf{2}, \mathbf{2}) \oplus (\mathbf{1}, \mathbf{1}, \mathbf{1}, \mathbf{1}, \mathbf{1}, \mathbf{1}) \\
&= (\mathbf{1}, \mathbf{5}), \tag{5.13} \\
\pi_{1,3}, \pi_{2,3}, \pi_{1,4}, \pi_{2,4}, \text{Tr } L_3 Q_{3,4} R_4, \\
\text{Tr } L_3 Q_{3,4} Q_{4,5} R_5, \text{Tr } L_4 R_4, \text{Tr } L_4 Q_{4,5} R_5 &\longrightarrow \begin{aligned} &(\mathbf{2}, \mathbf{1}, \mathbf{1}, \mathbf{1}, \mathbf{2}, \mathbf{1}) \oplus (\mathbf{1}, \mathbf{2}, \mathbf{1}, \mathbf{1}, \mathbf{2}, \mathbf{1}) \\ &\oplus (\mathbf{2}, \mathbf{1}, \mathbf{1}, \mathbf{1}, \mathbf{1}, \mathbf{2}) \oplus (\mathbf{1}, \mathbf{2}, \mathbf{1}, \mathbf{1}, \mathbf{1}, \mathbf{2}) \\ &\oplus (\mathbf{1}, \mathbf{1}, \mathbf{2}, \mathbf{1}, \mathbf{2}, \mathbf{1}) \oplus (\mathbf{1}, \mathbf{1}, \mathbf{1}, \mathbf{2}, \mathbf{2}, \mathbf{1}) \\ &\oplus (\mathbf{1}, \mathbf{1}, \mathbf{2}, \mathbf{1}, \mathbf{1}, \mathbf{2}) \oplus (\mathbf{1}, \mathbf{1}, \mathbf{1}, \mathbf{2}, \mathbf{1}, \mathbf{2}) \\ &= (\mathbf{8}, \mathbf{4}), \end{aligned} \tag{5.14}
\end{aligned}$$

¹²There are still gauge invariant chiral operators that we can in principle construct which are charged under $U(1)_d \times SU(2)_v$, but they are expected to vanish in the chiral ring by consistency with the operator map implied by the duality.

$$\begin{aligned}
& \text{Tr } L_1 R_1, \text{Tr } L_1 Q_{1,2} Q_{2,3} Q_{3,4} R_4, & (\mathbf{2}, \mathbf{2}, \mathbf{1}, \mathbf{1}, \mathbf{1}, \mathbf{1}) \oplus (\mathbf{2}, \mathbf{1}, \mathbf{2}, \mathbf{1}, \mathbf{1}, \mathbf{1}) \\
& \text{Tr } L_1 Q_{1,2} Q_{2,3} Q_{3,4} Q_{4,5} R_5, \text{Tr } L_2 Q_{2,3} Q_{3,4} R_4, & \oplus (\mathbf{2}, \mathbf{1}, \mathbf{1}, \mathbf{2}, \mathbf{1}, \mathbf{1}) \oplus (\mathbf{1}, \mathbf{2}, \mathbf{2}, \mathbf{1}, \mathbf{1}, \mathbf{1}) \\
& \text{Tr } L_2 Q_{2,3} Q_{3,4} Q_{4,5} R_5, \text{Tr } L_5 R_5, & \oplus (\mathbf{1}, \mathbf{2}, \mathbf{1}, \mathbf{2}, \mathbf{1}, \mathbf{1}) \oplus (\mathbf{1}, \mathbf{1}, \mathbf{2}, \mathbf{2}, \mathbf{1}, \mathbf{1}) \\
& \text{Tr } A_1, \text{Tr } A_5, \text{Tr } Q_{2,3}^2 = \text{Tr } Q_{3,4}^2 & \oplus (\mathbf{1}, \mathbf{1}, \mathbf{1}, \mathbf{1}, \mathbf{1}, \mathbf{1}) \oplus (\mathbf{1}, \mathbf{1}, \mathbf{1}, \mathbf{1}, \mathbf{1}, \mathbf{1}) \\
& & \oplus (\mathbf{1}, \mathbf{1}, \mathbf{1}, \mathbf{1}, \mathbf{1}, \mathbf{1}) \\
& & = (\mathbf{27}, \mathbf{1}), \tag{5.15}
\end{aligned}$$

From the above identification of the $USp(8)_x \times USp(4)_y$ representations, we can easily find the map of operators under the duality web as follows:

$$\{\text{Tr } LR, \text{Tr } A\}_{A,D} \leftrightarrow \{\text{Tr } P^2\}_B \leftrightarrow \{\text{Tr } L_3 R_3, \text{Tr } A_3\}_{C_1}, \tag{5.16}$$

$$\{\text{Tr } PL, \pi\}_{A,D} \leftrightarrow \{\pi_1, \pi_2, \text{Tr } PR_2, \text{Tr } PQ_{2,3} R_3\}_B \leftrightarrow \left\{ \begin{array}{l} \pi_{1,3}, \pi_{2,3}, \pi_{1,4}, \pi_{2,4}, \text{Tr } L_3 Q_{3,4} R_4, \\ \text{Tr } L_3 Q_{3,4} Q_{4,5} R_5, \text{Tr } L_4 R_4, \text{Tr } L_4 Q_{4,5} R_5 \end{array} \right\}_{C_1}, \tag{5.17}$$

$$\begin{aligned}
\{\text{Tr } P^2\}_{A,D} & \leftrightarrow \left\{ \begin{array}{l} \text{Tr } L_1 R_1, \text{Tr } L_1 Q_{1,2} R_2, \text{Tr } L_1 Q_{1,2} Q_{2,3} R_3, \\ \text{Tr } L_2 R_2, \text{Tr } L_2 Q_{2,3} R_2, \text{Tr } L_3 R_3, \\ \text{Tr } A_1, \text{Tr } A_2, \text{Tr } A_3 \end{array} \right\}_B \\
& \leftrightarrow \left\{ \begin{array}{l} \text{Tr } L_1 R_1, \text{Tr } L_1 Q_{1,2} Q_{2,3} Q_{3,4} R_4, \\ \text{Tr } L_1 Q_{1,2} Q_{2,3} Q_{3,4} Q_{4,5} R_5, \text{Tr } L_2 Q_{2,3} Q_{3,4} R_4, \\ \text{Tr } L_2 Q_{2,3} Q_{3,4} Q_{4,5} R_5, \text{Tr } L_5 R_5, \\ \text{Tr } A_1, \text{Tr } A_5, \text{Tr } Q_{2,3}^2 = \text{Tr } Q_{3,4}^2 \end{array} \right\}_{C_1}. \tag{5.18}
\end{aligned}$$

The existence of these operators can also be confirmed by computing the supersymmetric index in a power series. For example, we have evaluated the indices of Theory $A = D$ and Theory B as follows:

$$\begin{aligned}
\mathcal{I}_A = \mathcal{I}_B = \mathcal{I}_D &= 1 + (pq)^{\frac{5}{21}} t^{-1} c^{-2} + \mathbf{5}_y (pq)^{\frac{3}{7}} t + \mathbf{8}_x \mathbf{4}_y (pq)^{\frac{19}{42}} t^{-\frac{1}{2}} c + (pq)^{\frac{10}{21}} t^{-2} c^{-4} \\
&+ (pq)^{\frac{11}{21}} t^2 c^{-2} + \mathbf{27}_x (pq)^{\frac{4}{7}} t^{-1} + \dots \tag{5.19}
\end{aligned}$$

and found a perfect match as expected. In the index expansion, \mathbf{m}_x and \mathbf{n}_y denote the characters of the representations of dimensions \mathbf{m} and \mathbf{n} of $USp(8)_x$ and $USp(4)_y$, respectively, and we have used a trial R -charge defined as follows:

$$R_{\text{trial}} = R + \frac{6}{7} Q_t + \frac{1}{3} Q_c \tag{5.20}$$

where R is the R -charge shown in the tables, and Q_t and Q_c are the $U(1)_t$ and $U(1)_c$ charges, respectively. The mixing coefficients are chosen for convenience of the computation.

The three sets of the operators we explained correspond to the third, fourth, and seventh terms of the expanded index. In addition, there are other terms only charged under the Abelian symmetries. For example, the second term corresponds to a singlet flipping the dressed meson $\text{Tr } AL^2$ in Theory A , which turns out to decouple in the IR by the a -maximization. If we call this operator β_1 , the fifth term is β_1^2 , whereas the sixth term corresponds to $\text{Tr } R^2$. Their counterparts in Theory B can easily be identified. The second,

fifth, and sixth terms correspond to $\text{Tr}L_1^2$, $(\text{Tr}L_1^2)^2$, and the singlet flipping $\text{Tr}R_2^2$ in Theory B, respectively.

For Theory C_i , on the other hand, the computation of the index is more complicated. We have evaluated the index of C_1 up to $(pq)^{\frac{10}{21}}$ with the simplification $x_i = y_j = 1$, which agrees with the index from the other dual frames (5.19). Moreover, we have found that this partially unrefined index of Theory C_1 there is no dependence on the fugacities v and d for the $SU(2)_v \times U(1)_d$, which again confirms our expectation that this symmetry acts trivially in the IR.

The operators of Theory C_2 and Theory C_3 , some of which are listed in Table 4, combine similarly to form representations of the IR $USp(8)_x \times USp(4)_y$ symmetry.

	$\prod_{i=1}^4 SU(2)_{x_i} \times SU(2)_{y_1} \times SU(2)_{y_2}$	$U(1)_R$	$U(1)_t$	$U(1)_c$
$\text{Tr } L_1 Q_{1,2} R_2$	(2, 2, 1, 1, 1, 1)	2	-1	0
$\text{Tr } L_1 Q_{1,2} Q_{2,3} R_3$	(2, 1, 2, 1, 1, 1)	2	-1	0
$\text{Tr } L_1 Q_{1,2} Q_{2,3} Q_{3,4} Q_{4,5} R_5$	(2, 1, 1, 2, 1, 1)	2	-1	0
$\text{Tr } L_3 R_3$	(1, 2, 2, 1, 1, 1)	2	-1	0
$\text{Tr } L_3 Q_{3,4} Q_{4,5} R_5$	(1, 2, 1, 2, 1, 1)	2	-1	0
$\text{Tr } L_4 Q_{4,5} R_5$	(1, 1, 2, 2, 1, 1)	2	-1	0
$\pi_{1,2}$	(2, 1, 1, 1, 2, 1)	1	-1/2	1
$\pi_{1,5}$	(2, 1, 1, 1, 1, 2)	1	-1/2	1
$\pi_{3,5}$	(1, 2, 1, 1, 1, 2)	1	-1/2	1
$\pi_{4,5}$	(1, 1, 2, 1, 1, 2)	1	-1/2	1
$\text{Tr } L_2 R_2$	(1, 2, 1, 1, 2, 1)	1	-1/2	1
$\text{Tr } L_2 Q_{2,3} R_3$	(1, 1, 2, 1, 2, 1)	1	-1/2	1
$\text{Tr } L_2 Q_{2,3} Q_{3,4} Q_{4,5} R_5$	(1, 1, 1, 2, 2, 1)	1	-1/2	1
$\text{Tr } L_5 R_5$	(1, 1, 1, 2, 1, 2)	1	-1/2	1
$\text{Tr } L_2 Q_{2,3} Q_{3,4} R_4$	(1, 1, 1, 1, 2, 2)	0	1	0
$\text{Tr } A_3$	(1, 1, 1, 1, 1, 1)	2	-1	0
$\text{Tr } Q_{1,2}^2$	(1, 1, 1, 1, 1, 1)	2	-1	0
$\text{Tr } Q_{4,5}^2$	(1, 1, 1, 1, 1, 1)	2	-1	0
$\text{Tr } Q_{2,3}^2 = \text{Tr } Q_{3,4}^2$	(1, 1, 1, 1, 1, 1)	0	1	0
$\text{Tr } L_2 R_2$	(2, 2, 1, 1, 1, 1)	2	-1	0
$\text{Tr } L_2 Q_{2,3} R_3$	(2, 1, 2, 1, 1, 1)	2	-1	0
$\text{Tr } L_2 Q_{2,3} Q_{3,4} R_4$	(2, 1, 1, 2, 1, 1)	2	-1	0
$\text{Tr } L_3 R_3$	(1, 2, 2, 1, 1, 1)	2	-1	0
$\text{Tr } L_3 Q_{3,4} R_4$	(1, 2, 1, 2, 1, 1)	2	-1	0
$\text{Tr } L_4 R_4$	(1, 1, 2, 2, 1, 1)	2	-1	0
$\pi_{2,6}$	(2, 1, 1, 1, 1, 2)	1	-1/2	1
$\pi_{3,6}$	(1, 2, 1, 1, 1, 2)	1	-1/2	1
$\pi_{4,6}$	(1, 1, 2, 1, 1, 2)	1	-1/2	1
$\pi_{5,6}$	(1, 1, 1, 2, 1, 2)	1	-1/2	1
$\text{Tr } L_1 R_1$	(2, 1, 1, 1, 2, 1)	1	-1/2	1
$\text{Tr } L_1 Q_{1,2} R_2$	(1, 2, 1, 1, 2, 1)	1	-1/2	1
$\text{Tr } L_1 Q_{1,2} Q_{2,3} R_3$	(1, 1, 2, 1, 2, 1)	1	-1/2	1
$\text{Tr } L_1 Q_{1,2} Q_{2,3} Q_{3,4} R_4$	(1, 1, 1, 2, 2, 1)	1	-1/2	1
$\text{Tr } L_1 Q_{1,2} Q_{2,3} Q_{3,4} Q_{4,5} R_5$	(1, 1, 1, 1, 2, 2)	0	1	0
$\text{Tr } A_2$	(1, 1, 1, 1, 1, 1)	2	-1	0
$\text{Tr } A_3$	(1, 1, 1, 1, 1, 1)	2	-1	0
$\text{Tr } A_4$	(1, 1, 1, 1, 1, 1)	2	-1	0
$\text{Tr } Q_{i,i+1}^2$	(1, 1, 1, 1, 1, 1)	0	1	0

Table 4. Gauge invariant chiral operators in Theories C_2 (the upper box) and C_3 (the lower box).

5.3 3d $SL(2, \mathbb{Z})$ duality web

In 3d, starting from the $\mathcal{N} = 4$ SQCD, we can build an analogous duality web by acting with the $SL(2, \mathbb{Z})$ basic moves. The 3d version of the web is shown in Figure 71 together with the brane systems (see Figure 72 for the charge assignments of the fields). Notice that we move from frame C_1 to C_2 and C_3 by applying the Giveon–Kutasov duality which implements the HW moves exchanging NS5 and (1,1)-branes in the brane setup, similarly to what we did in 4d using the IP duality instead.

The frames $C_{1,2,3}$ correspond to theories with CS couplings. Notice in particular that in the first two frames when we integrate out the massive adjoint at the nodes where the CS coupling is turned on, a quartic superpotential for the bifundamentals is generated. These quartic superpotentials preserve the $U(1)_A$ symmetry which becomes part of the larger R-symmetry group since all these frames have enhanced $\mathcal{N} = 4$ supersymmetry as expected by the duality.

We can reach the 3d web in Figure 71 from the 4d web in Figure 64 taking the limit:

$$X_i \rightarrow X_i + s, \quad Y_j \rightarrow Y_j + s, \quad Z_a \rightarrow Z_a + s, \quad V \rightarrow V + s, \quad s \rightarrow +\infty \quad (5.21)$$

followed by $\Delta \rightarrow -\infty$. Alternatively we can apply the 3d dualization algorithm. We illustrate below the dualization from of theory A into B . In the first row of Figure 73 theory A is chopped into QFT blocks. Applying the basic moves in Figure 52 and 53 we get the dualized theory in the second row of figure 73. Notice that, for the leftmost block, we apply the duality move in Figure 52 with a Cartan’s reparametrization such that $\mathcal{S} \rightarrow \mathcal{S}^{-1}$ and viceversa (if one does not implement such a reparametrization, the first and second blocks would glue with $\mathcal{S}\mathcal{S}$ rather than as $\mathcal{S}\mathcal{S}^{-1}$). Now, as shown in the third and fourth row of figure 73, we can propagate the VEVs on the two sides of the quiver using the Hanany–Witten move in Figure 61. After these two iterations, we land on the theory B shown in the last row of figure 73.

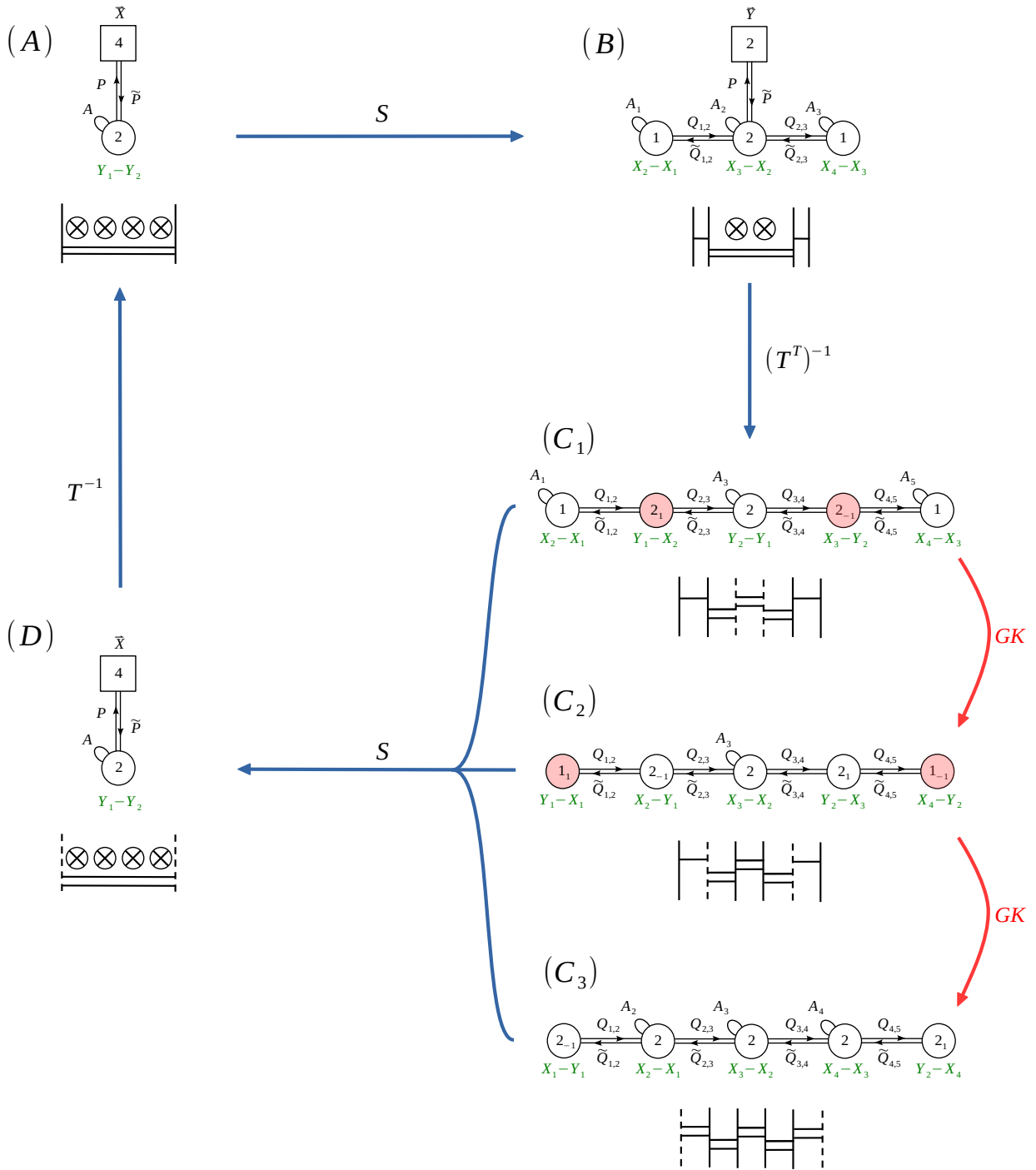


Figure 71. A $3d$ $SL(2, \mathbb{Z})$ web with the corresponding brane setups, where NS5, D5, and $(1, 1)$ -branes are denoted by a solid vertical line, a crossed circle, and a dashed vertical line, respectively. The FI parameters at each gauge node are denoted in green.

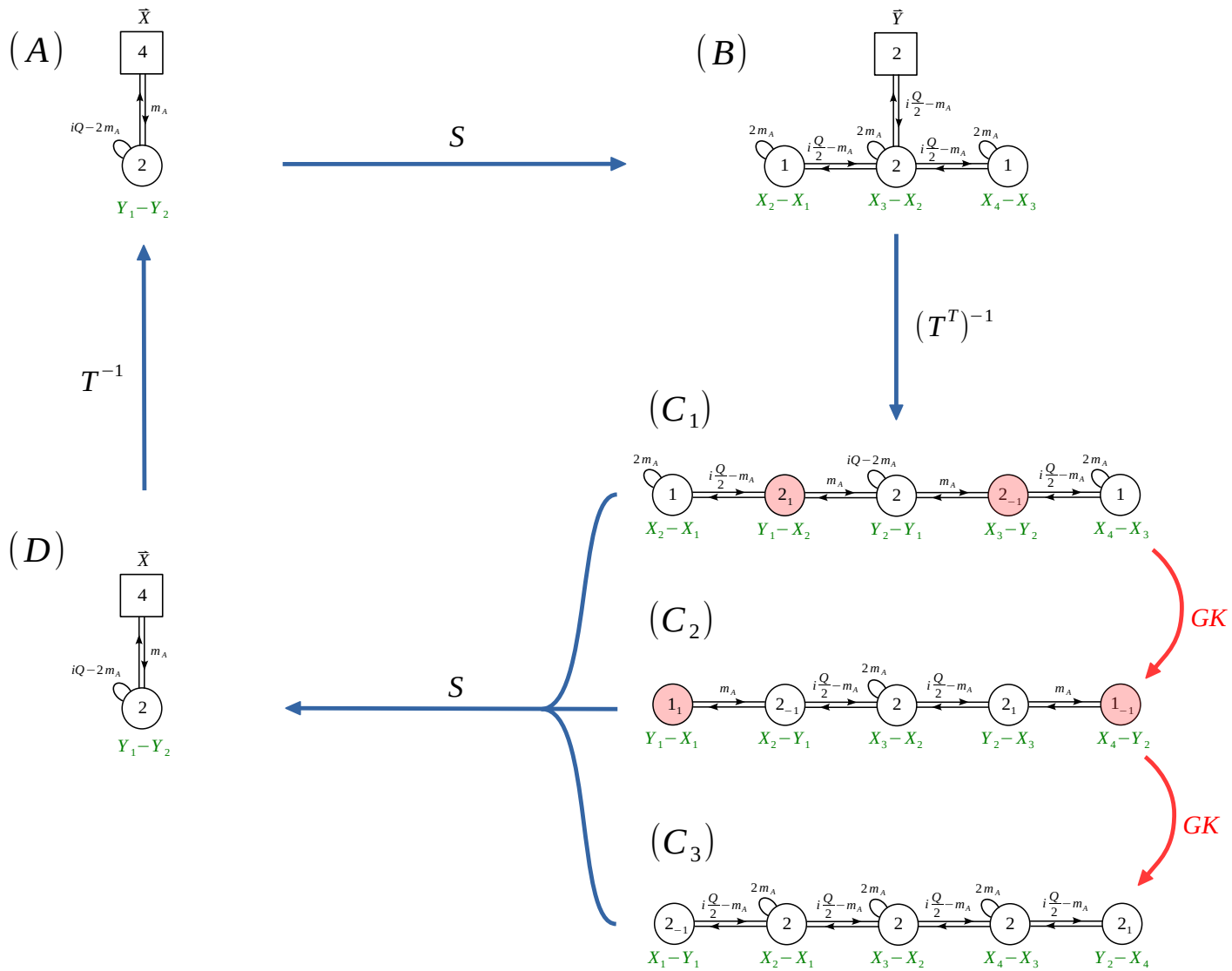


Figure 72. The charge assignment for the 3d $SL(2, \mathbb{Z})$ web.

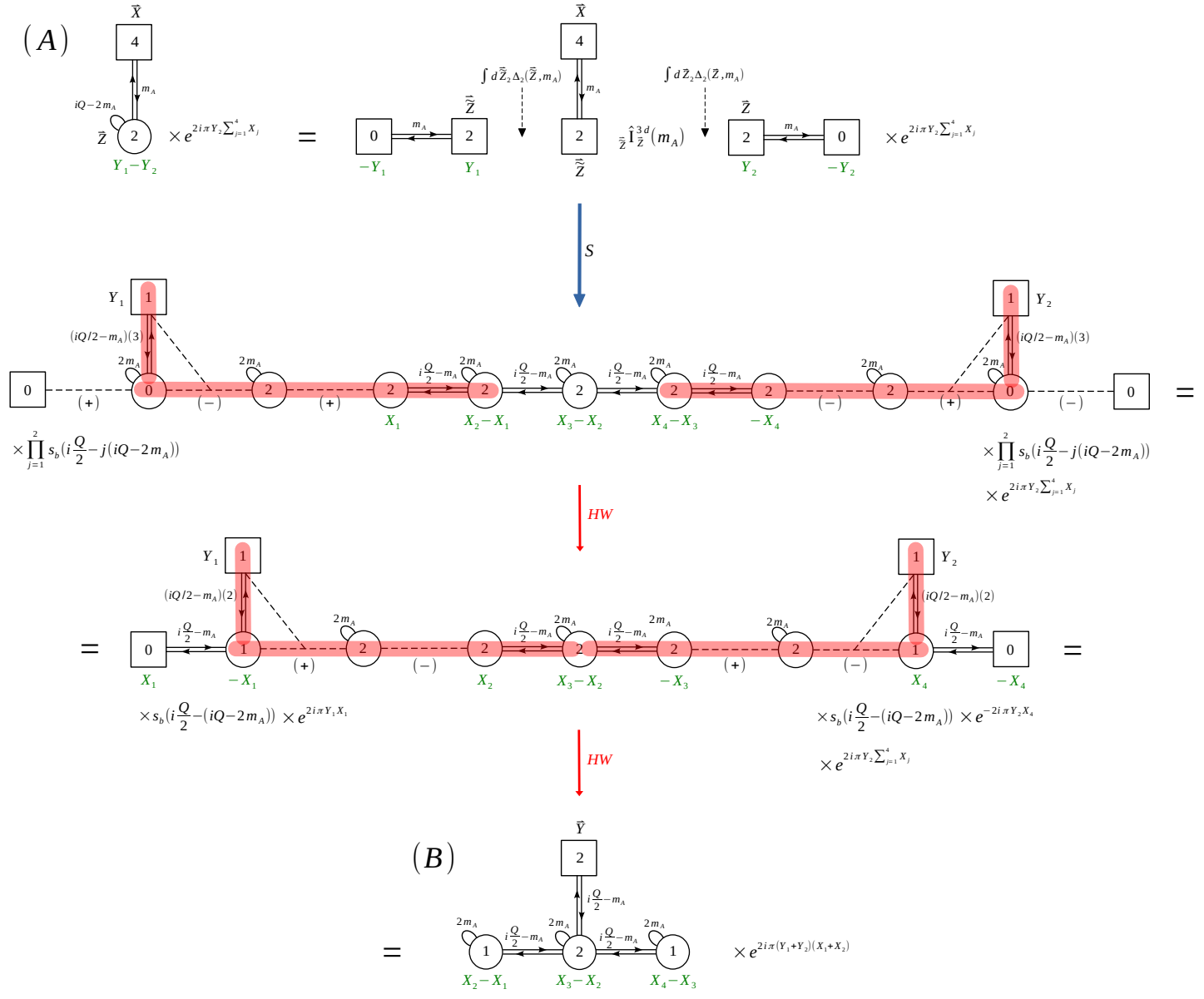


Figure 73. The S-dualization of theory A.

5.4 3d operators map

It is interesting to see how the operator map works in the 3d case to better understand the web of dualities. The global symmetry group of the three theories in the IR is

$$SU(4)_X \times SU(2)_Y \times U(1)_A, \quad (5.22)$$

but the UV manifest symmetries in the theories of the web are the following:

$$\begin{aligned} A = D : & \quad \underbrace{\frac{U(4)_X}{U(1)}}_{SU(4)_X} \times \frac{\prod_{j=1}^2 U(1)_{Y_j}}{U(1)} \times U(1)_A, \\ B : & \quad \underbrace{\frac{U(2)_Y}{U(1)}}_{SU(2)_Y} \times \frac{\prod_{i=1}^4 U(1)_{X_i}}{U(1)} \times U(1)_A, \\ C_i : & \quad \frac{\prod_{i=1}^4 U(1)_{X_i}}{U(1)} \times \frac{\prod_{j=1}^2 U(1)_{Y_j}}{U(1)} \times U(1)_A, \end{aligned} \quad (5.23)$$

where we are using the parametrization of the various symmetries that we obtained from the algorithm and that is specified in Figure 72, but we should remember that is an off-shell parametrization in 3d and that we should decoupled a diagonal $U(1)$ both from the X and from the Y symmetries. In the following we will keep the off-shell parametrization since it makes it easier to identify how the operators rearrange into representations of the enhanced symmetry and to map them across the various frames.

We now analyze each theory discussing its symmetries and the gauge invariant operators with the lowest dimension. Notice that operators with charges $(iQ - 2m_A)$ or $2m_A$ have R -charge 1 when we set the canonical parameterization $m_A = \frac{iQ}{4}$, which is the lowest R -charge possible in an interacting 3d $\mathcal{N} = 4$ theory.

Let us start from Theory A , which is equivalent to Theory D . The manifest global symmetry group is given by

$$\frac{U(4)_X}{U(1)} \times \frac{\prod_{j=1}^2 U(1)_{Y_j}}{U(1)} \times U(1)_A, \quad (5.24)$$

where $\frac{U(4)_X}{U(1)} = SU(4)_X$ is the flavor symmetry, while $\frac{\prod_{j=1}^2 U(1)_{Y_j}}{U(1)}$ is the topological symmetry associated to the $U(2)$ gauge node. The lowest dimension gauge invariant operators are listed in Table 5.

Notice that the $U(2)$ gauge node is balanced so according to [62] the topological symmetry is enhanced to $\frac{\prod_{j=1}^2 U(1)_{Y_j}}{U(1)} \rightarrow SU(2)_Y$. In fact some of the operators in Table 5 combine to form representations of the IR global symmetry $SU(4)_X \times SU(2)_Y$ and provide the moment maps for it:

$$\text{Tr } P\tilde{P} \longrightarrow (\mathbf{15}, 0) = (\mathbf{15}, \mathbf{1}), \quad (5.25)$$

$$\text{Tr } A, M^{(\pm)} \longrightarrow (\mathbf{1}, 0, 0) \oplus (\mathbf{1}, 1, -1) \oplus (\mathbf{1}, -1, 1) = (\mathbf{1}, \mathbf{3}). \quad (5.26)$$

	$SU(4)_X \times \prod_{j=1}^2 U(1)_{Y_j}$	$U(1)_A$	$U(1)_R$
$\text{Tr } P\tilde{P}$	$(\mathbf{15}, 0, 0)$	2	0
$\text{Tr } A$	$(\mathbf{1}, 0, 0)$	-2	2
$M^{(+)}$	$(\mathbf{1}, 1, -1)$	-2	2
$M^{(-)}$	$(\mathbf{1}, -1, +1)$	-2	2

Table 5. Gauge invariant operators in Theory $A =$ Theory D . We denote by $M^{(\pm)} = M^{\{\pm 1, 0\}}$ the fundamental monopoles of the $U(2)$ gauge group.

Notice that only the off-diagonal combination $U(1)_{Y_2} - U(1)_{Y_1}$ acts non-trivially and is the one that is enhanced to $SU(2)_Y$, while the diagonal combination $U(1)_{Y_1} + U(1)_{Y_2}$ acts trivially and should be decoupled as we previously mentioned.

In Theory B the manifest symmetry is

$$\frac{U(2)_Y}{U(1)} \times \frac{\prod_{i=1}^4 U(1)_{X_i}}{U(1)} \times U(1)_A, \quad (5.27)$$

where $\frac{U(2)_Y}{U(1)} = SU(2)_Y$ is the flavor symmetry, while $\frac{\prod_{i=1}^4 U(1)_{X_i}}{U(1)}$ after decoupling a diagonal $U(1)$ is a combination of the topological symmetries of the three gauge nodes which we parametrize as specified in Figure 72. We consider the operators in Table 6, which have the lowest scaling dimensions and will provide the moment maps for the enhanced symmetry.

	$SU(2)_Y \times \prod_{i=1}^4 U(1)_{X_i}$	$U(1)_A$	$U(1)_R$
$\text{Tr } P\tilde{P}$	$(\mathbf{3}, 0, 0, 0, 0)$	-2	2
$\text{Tr } A_1$	$(\mathbf{1}, 0, 0, 0, 0)$	2	0
$\text{Tr } A_2$	$(\mathbf{1}, 0, 0, 0, 0)$	2	0
$\text{Tr } A_3$	$(\mathbf{1}, 0, 0, 0, 0)$	2	0
$M^{(\pm, 0, 0)}$	$(\mathbf{1}, \pm 1, \mp 1, 0, 0)$	2	0
$M^{(0, \pm, 0)}$	$(\mathbf{1}, 0, \pm 1, \mp 1, 0)$	2	0
$M^{(0, 0, \pm)}$	$(\mathbf{1}, 0, 0, \pm 1, \mp 1)$	2	0
$M^{(\pm, \pm, 0)}$	$(\mathbf{1}, \pm 1, 0, \mp 1, 0)$	2	0
$M^{(0, \pm, \pm)}$	$(\mathbf{1}, 0, \pm 1, 0, \mp 1)$	2	0
$M^{(\pm, \pm, \pm)}$	$(\mathbf{1}, \pm 1, 0, 0, \mp 1)$	2	0

Table 6. Gauge invariant operators in Theory B . We used the convention $M^{(\pm, \pm, \pm)} = M^{(\pm 1, \{\pm 1, 0\}, \pm 1)}$ for the fundamental monopoles of the $U(1) \times U(2) \times U(1)$ gauge groups.

All the gauge nodes are balanced, so the three topological symmetries get enhanced to $\frac{\prod_{i=1}^4 U(1)_{X_i}}{U(1)} \rightarrow SU(4)_X$. The operators combine to form representation of the IR global

symmetry $SU(4)_X \times SU(2)_Y$ as

$$\begin{aligned}
& M^{(\pm,0,0)}, M^{(0,\pm,0)}, M^{(0,0,\pm)} \\
& M^{(\pm,\pm,0)}, M^{(0,\pm,\pm)}, M^{(\pm,\pm,\pm)} \longrightarrow \\
& \quad \text{Tr } A_1, \text{Tr } A_2, \text{Tr } A_3 \\
& \quad (\mathbf{1}, \pm 1, \mp 1, 0, 0) \oplus (\mathbf{1}, 0, \pm 1, \mp 1, 0) \oplus (\mathbf{1}, 0, 0, \pm 1, \mp 1) \\
& \quad \oplus (\mathbf{1}, \pm 1, 0, \mp 1, 0) \oplus (\mathbf{1}, 0, \pm 1, 0, \mp 1) \oplus (\mathbf{1}, \pm 1, 0, 0, \mp 1) \\
& \quad \oplus (\mathbf{1}, 0, 0, 0) \oplus (\mathbf{1}, 0, 0, 0) \oplus (\mathbf{1}, 0, 0, 0) \oplus \\
& \quad = (\mathbf{15}, \mathbf{1}),
\end{aligned} \tag{5.28}$$

$$\text{Tr } P\tilde{P} \longrightarrow (\mathbf{3}, 0, 0, 0) = (\mathbf{1}, \mathbf{3}). \tag{5.29}$$

In the three C_i theories the manifest symmetry is

$$\frac{\prod_{i=1}^4 U(1)_{X_i}}{U(1)} \times \frac{\prod_{j=1}^2 U(1)_{Y_j}}{U(1)} \times U(1)_A, \tag{5.30}$$

where all the symmetries, except for the axial symmetry, are topological. The central node is balanced, so we expect the enhancement $\frac{\prod_{j=1}^2 U(1)_{Y_j}}{U(1)} \rightarrow SU(2)_Y$. On the other hand, if we look at the other gauge nodes, since they have non-zero CS level, their monopoles are not gauge invariant and have to be dressed with bifundamental fields. The lowest dimension gauge invariant operators of Theory C_1 are listed in Table 7.

	$\prod_{i=1}^4 U(1)_{X_i} \times \prod_{j=1}^2 U(1)_{Y_j}$	$U(1)_A$	$U(1)_R$
Tr A_1	(0, 0, 0, 0, 0, 0)	2	0
Tr A_3	(0, 0, 0, 0, 0, 0)	-2	2
Tr A_5	(0, 0, 0, 0, 0, 0)	2	0
Tr $(Q_{2,3}\tilde{Q}_{2,3})$	(0, 0, 0, 0, 0, 0)	2	0
$M^{(\pm,0,0,0,0)}$	($\pm 1, \mp 1, 0, 0, 0, 0$)	2	0
$M^{(0,0,\pm,0,0)}$	(0, 0, 0, 0, $\pm 1, \mp 1$)	-2	2
$M^{(0,0,0,0,\pm)}$	(0, 0, $\pm 1, \mp 1, 0, 0$)	2	0
$M^{(+,+,+,+,0)}\tilde{Q}_{2,3}\tilde{Q}_{3,4}$	(1, 0, -1, 0, 0, 0)	2	0
$M^{(-,-,-,-,0)}Q_{2,3}Q_{3,4}$	(-1, 0, 1, 0, 0, 0)	2	0
$M^{(+,+,+,+,+)}\tilde{Q}_{2,3}\tilde{Q}_{3,4}$	(1, 0, 0, -1, 0, 0)	2	0
$M^{(-,-,-,-,-)}Q_{2,3}Q_{3,4}$	(-1, 0, 0, 1, 0, 0)	2	0
$M^{(0,+,+,+,0)}\tilde{Q}_{2,3}\tilde{Q}_{3,4}$	(0, 1, -1, 0, 0, 0)	2	0
$M^{(0,-,-,-,0)}Q_{2,3}Q_{3,4}$	(0, -1, 1, 0, 0, 0)	2	0
$M^{(0,+,+,+,+)}\tilde{Q}_{2,3}\tilde{Q}_{3,4}$	(0, 1, 0, -1, 0, 0)	2	0
$M^{(0,-,-,-,-)}Q_{2,3}Q_{3,4}$	(0, -1, 0, 1, 0, 0)	2	0

Table 7. Gauge invariant operators in Theory C_1 . We used the convention $M^{(\pm,\pm,\pm,\pm,\pm)} = M^{(\pm 1, \{\pm 1, 0\}, \{\pm 1, 0\}, \{\pm 1, 0\}, \pm 1)}$ for the fundamental monopoles of the $U(1) \times U(2)^3 \times U(1)$ gauge groups.

These operators rearrange into the representation of the IR global symmetry $SU(4)_X \times$

$SU(2)_Y$ as follows:

$$\begin{aligned}
& \begin{array}{l} \text{Tr } A_1, \text{ Tr } A_5 \\ \text{Tr } (Q_{2,3}\tilde{Q}_{2,3}) \\ M^{(\pm,0,0,0,0)}, M^{(0,0,0,0,\pm)} \\ M^{(+,+,+,+,0)}\tilde{Q}_{2,3}\tilde{Q}_{3,4}, M^{(-,-,-,0)}Q_{2,3}Q_{3,4} \\ M^{(+,+,+,+,+)}\tilde{Q}_{2,3}\tilde{Q}_{3,4}, M^{(-,-,-,-)}Q_{2,3}Q_{3,4} \\ M^{(0,+,+,+,0)}\tilde{Q}_{2,3}\tilde{Q}_{3,4}, M^{(0-,-,-,0)}Q_{2,3}Q_{3,4} \\ M^{(0,+,+,+,+)}\tilde{Q}_{2,3}\tilde{Q}_{3,4}, M^{(0-,-,-,-)}Q_{2,3}Q_{3,4} \end{array} \longrightarrow \begin{array}{l} (0,0,0,0,0) \oplus (0,0,0,0,0) \\ \oplus (0,0,0,0,0) \\ \oplus (\pm 1, \mp 1, 0, 0, 0) \oplus (0, 0, 0, 0, \pm 1, \mp 1) \\ \oplus (\pm 1, 0, \mp 1, 0, 0, 0) \oplus (\pm 1, 0, 0, \mp 1, 0, 0) \\ \oplus (0, \pm 1, \mp 1, 0, 0, 0) \oplus (0, \pm 1, 0, \mp 1, 0, 0) \\ = \quad (\mathbf{15}, \mathbf{1}), \end{array}
\end{aligned} \tag{5.31}$$

$$\begin{aligned}
\text{Tr } A_3, M^{(0,0,\pm,0,0)} \longrightarrow & (0,0,0,0,0) \oplus (0,0,0,0,\pm 1, \mp 1) \\
= & (\mathbf{1}, \mathbf{3}).
\end{aligned} \tag{5.32}$$

After we have grouped operators in representations of the IR symmetry group it is easy to see that they are mapped as follows:

$$\left\{ \text{Tr } P\tilde{P} \right\}_{A,D} \leftrightarrow \left\{ \begin{array}{l} M^{(\pm,0,0)}, M^{(0,\pm,0)}, M^{(0,0,\pm)} \\ M^{(\pm,\pm,0)}, M^{(0,\pm,\pm)}, M^{(\pm,\pm,\pm)} \\ \text{Tr } A_1, \text{ Tr } A_2, \text{ Tr } A_3 \end{array} \right\}_B \leftrightarrow \left\{ \begin{array}{l} \text{Tr } A_1, \text{ Tr } A_3 \\ \text{Tr } (Q_{2,3}\tilde{Q}_{2,3}) \\ M^{(\pm,0,0,0,0)}, M^{(0,0,0,0,\pm)} \\ M^{(+,+,+,+,0)}\tilde{Q}_{2,3}\tilde{Q}_{3,4}, M^{(-,-,-,0)}Q_{2,3}Q_{3,4} \\ M^{(+,+,+,+,+)}\tilde{Q}_{2,3}\tilde{Q}_{3,4}, M^{(-,-,-,-)}Q_{2,3}Q_{3,4} \\ M^{(0,+,+,+,0)}\tilde{Q}_{2,3}\tilde{Q}_{3,4}, M^{(0-,-,-,0)}Q_{2,3}Q_{3,4} \\ M^{(0,+,+,+,+)}\tilde{Q}_{2,3}\tilde{Q}_{3,4}, M^{(0-,-,-,-)}Q_{2,3}Q_{3,4} \end{array} \right\}_{C_1}. \tag{5.33}$$

$$\left\{ \text{Tr } A, M^{(\pm)} \right\}_{A,D} \leftrightarrow \left\{ \text{Tr } P\tilde{P} \right\}_B \leftrightarrow \left\{ \text{Tr } A_3, M^{(0,0,\pm,0,0)} \right\}_{C_1}. \tag{5.34}$$

This operator map provides further evidence that the map of symmetries that results from the algorithm is the correct one.

In a similar way one can construct operators in the theories C_2 and C_3 and verify both that they rearrange into representations of the enhanced IR symmetry and that they are mapped correctly across the duality.

Acknowledgments

CH is partially supported by the National Natural Science Foundation of China under Grant No. 12247103, the Institute for Basic Science (IBS-R018-D1, IBS-R018-Y2) and the STFC consolidated grant ST/T000694/1. MS is partially supported by the ERC Consolidator Grant #864828 ‘‘Algebraic Foundations of Supersymmetric Quantum Field Theory (SCFTAlg)’’ and by the Simons Collaboration for the Nonperturbative Bootstrap under grant #494786 from the Simons Foundation.

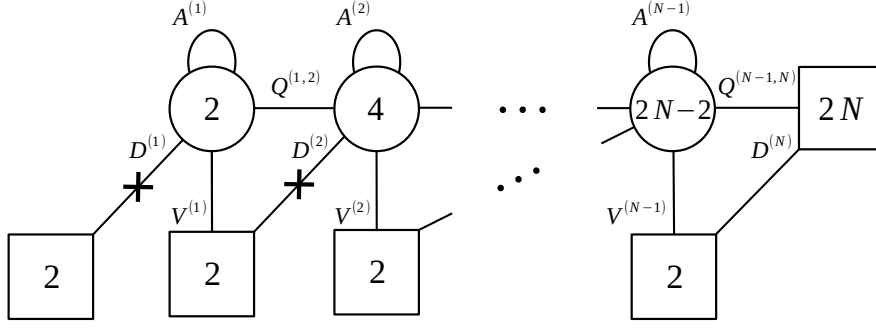


Figure 74. The $E[USp(2N)]$ theory. Each $2n$ node, square or round, represents an $USp(2n)$ group. The crosses denote the β_n singlets.

A The $FE[USp(2N)]$ theory, the S-wall

We collect here a few definitions following the notation of [22]. The $E[USp(2N)]$ theory is described by the quiver in Figure 74. In the superpotential the bifundamentals $Q^{(n,n+1)}$ couple to the antisymmetrics $A^{(n)}$, we then have a cubic coupling between the chirals in each triangle of the quiver and the flipping terms with the singlets β_n coupled to the diagonal mesons

$$\begin{aligned}
\mathcal{W}_{E[USp(2N)]} = & \sum_{n=1}^{N-1} \text{Tr}_n \left[A^{(n)} \left(\text{Tr}_{n+1} Q^{(n,n+1)} Q^{(n,n+1)} - \text{Tr}_{n-1} Q^{(n-1,n)} Q^{(n-1,n)} \right) \right] \\
& + \sum_{n=1}^{N-1} \text{Tr}_{y_{n+1}} \text{Tr}_n \text{Tr}_{n+1} \left(V^{(n)} Q^{(n,n+1)} D^{(n+1)} \right) + \\
& + \sum_{n=1}^{N-1} \beta_n \text{Tr}_{y_n} \text{Tr}_n \left(D^{(n)} D^{(n)} \right). \tag{A.1}
\end{aligned}$$

Above Tr_n is over the color indices of the n -th $USp(2n)$ gauge node, while Tr_{y_n} denotes the trace over the the n -th $SU(2)$ flavor symmetry and $\text{Tr}_N = \text{Tr}_x$ is the trace over $USp(2N)_x$ flavor indices. All the traces include the J antisymmetric tensor of $USp(2n)$. The global symmetry in the IR is enhanced as

$$USp(2N)_x \times \prod_{n=1}^N SU(2)_{y_n} \times U(1)_t \times U(1)_c \quad \rightarrow \quad USp(2N)_x \times USp(2N)_y \times U(1)_t \times U(1)_c.$$

In Figure 75 we indicate the charges of all the fields. Some of the gauge invariant operators of $E[USp(2N)]$ and their transformations properties are given in Table 8, where we defined B_{nm} as a matrix of operators charged only under $U(1)_c$ and $U(1)_t$, which include the singlets β_n .

The $FE[USp(2N)]$ theory, which we identified in the main text as the $4d$ S-wall, is defined as $E[USp(2N)]$ with one extra set of singlets O_H , as well as a singlet β_N , interacting via the

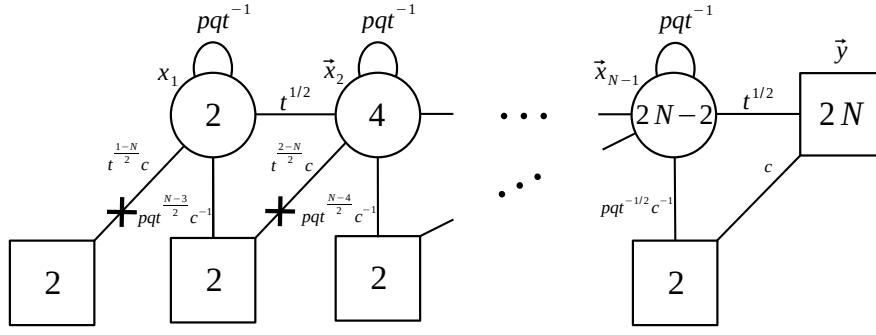


Figure 75. The trial R-charges and the charges under the other abelian symmetries represented in the form of $(pq)^{R/2}c^{Q_c}t^{Q_t}$, where R is the trial R-charge, Q_c is the charge under $U(1)_c$, and Q_t is the charge under $U(1)_t$.

	$USp(2N)_x$	$USp(2N)_y$	$U(1)_t$	$U(1)_c$	$U(1)_{R_0}$
H	$\mathbf{N}(2\mathbf{N} - \mathbf{1}) - \mathbf{1}$	$\mathbf{1}$	1	0	0
C	$\mathbf{1}$	$\mathbf{N}(2\mathbf{N} - \mathbf{1}) - \mathbf{1}$	-1	0	2
II	\mathbf{N}	\mathbf{N}	0	+1	0
B_{nm}	$\mathbf{1}$	$\mathbf{1}$	$m - n$	-2	$2n$

Table 8. $E[USp(2N)]$ operators and their transformations properties.

superpotential

$$\mathcal{W}_{FE[USp(2N)]} = \mathcal{W}_{E[USp(2N)]} + \text{Tr}_x(\mathbf{O}_H\mathbf{H}) + \beta_N \text{Tr}_x \text{Tr}_{y_N} D^{(N)} D^{(N)}. \quad (\text{A.2})$$

B Asymmetric S-walls

An asymmetric S-wall is defined as an S-wall deformed by a superpotential term breaking one of the flavour $USp(2N)$ symmetries down to $USp(2M) \times SU(2)_v$ (with $M < N$). Details about this deformation and its effect can be found in [22].

The deformation translates into the following specializations of $(N - M)$ components of the $USp(2N)_z$ fugacities \vec{z} :

$$\vec{z} = \{z_1, \dots, z_M, t^{\frac{N-M-1}{2}} v, \dots, t^{-\frac{N-M-1}{2}} v\}. \quad (\text{B.1})$$

The $\vec{z} = \{z_1, \dots, z_M\}$ fugacities parametrize $USp(2M)_z$, and v is the Cartan of $SU(2)_v$. The result of this procedure is what we depict schematically as the asymmetric S-wall shown in Figure 76.

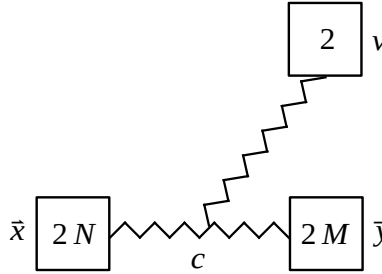


Figure 76. Schematic representation of the asymmetric S-wall.

It also useful to give a Lagrangian description of the result. In order to do that we have to choose whether the broken $USp(2N)$ is the manifest or emergent one. This choice gives rise to two different descriptions that are related by mirror symmetry. As it is shown below, in the case of breaking the manifest $USp(2N)_x$ symmetry the result is given in Figure 77. If instead we break the emergent $USp(2N)_y$ symmetry the result is given in Figure 78.

In fact, up to singlets, the theory in Figure 77 coincides with the $FE_\rho^\sigma[USp(2N)]$ theory of [24] with $\rho = [1^N]$ and $\sigma = [N - M, 1^M]$. This theory is related to the one in Figure 78 by mirror symmetry which swaps ρ and σ .

Specialization of the manifest symmetry

We first consider the case where we break the manifest $USp(2N)_x$ symmetry with the specialization (B.1) to obtain the first quiver depicted in Figure 79. The factor $\hat{A}_{N-M}(v; pq/t)$, defined in eq. (3.5) contains $(N - M - 1)$ vanishing $\Gamma_e(pq)$. This fact, together with the pattern of the t -charges of the green chirals attached to the $USp(2N - 2)$ gauge node, indicates that some of the green mesons acquire a VEV which Higgses the $USp(2N - 2)$ node down to $USp(2M)$. The first Higgsing then triggers the Higgsings of the nodes on its left and the VEV continues to propagate towards the left of the quiver.

Instead of studying this sequential Higgsing, we proceed using sequential IP dualizations. We begin by IP dualizing the first $USp(2)$ gauge node and continue applying the IP duality moving towards the right. These dualizations do not change the ranks of the gauge nodes

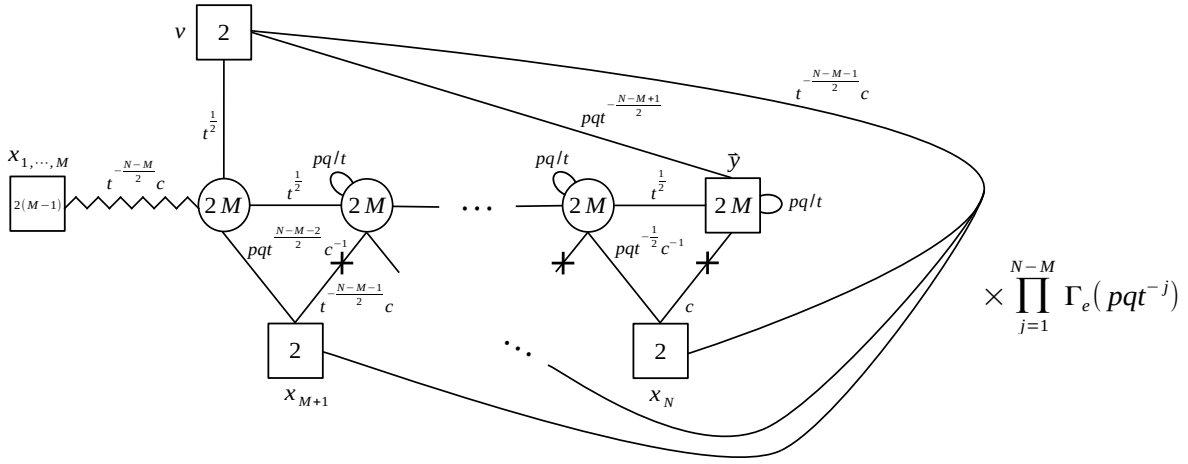


Figure 77. An S-wall with broken manifest $USp(2N)_x$.

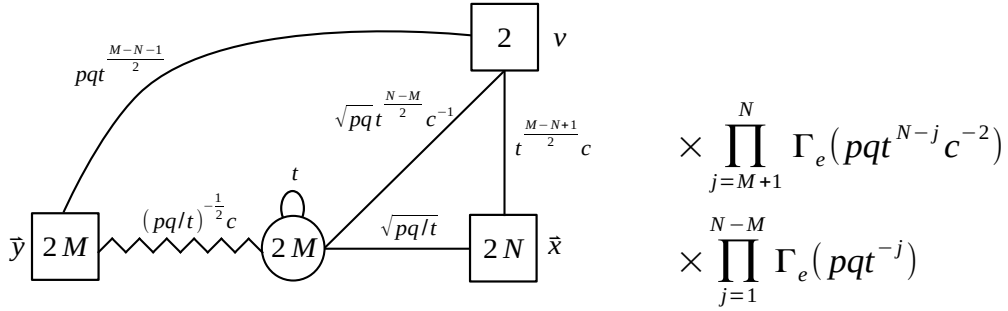


Figure 78. An S-wall with broken emergent $USp(2N)_y$.

but at each step the antisymmetric of the next node becomes massive such that we can then apply IP there, and so on. The result after the dualization of the $(N-2)$ -th gauge node is depicted as the second quiver in Figure 79.

Now we IP dualize the $(N-1)$ -th node. Here the duality has the effect of trading VEVs for mass deformations. More precisely, the duality leaves the rank unchanged and has two main effects on the fields:

- After the dualization, the $USp(2N-2) \times SU(2)_v$ chirals read

$$\prod_{j=1}^{N-M} \prod_{i=1}^{N-1} \Gamma_e \left(\sqrt{pqt}^{j-\frac{N-M+2}{2}} v^{\pm} z_i^{(N-1)\pm} \right),$$

where $\vec{z}^{(N-1)}$ are the fugacities for the gauge group $USp(2N-2)$. From the above expression we see that all of them become massive and only the $j=1$ chiral survives. The flipping fields produced by the IP duality cancel exactly with the $\hat{A}_{N-M}(v; pq/t)$ term.

- A set of $(N - M)$ legs connecting the $USp(2N - 4)$ gauge node to $SU(2)_v$ is produced

$$\prod_{j=1}^{N-M} \prod_{i=1}^{N-2} \Gamma_e \left(\sqrt{pqt}^{\frac{N-M+1}{2}-j} z_i^{(N-2)\pm} v^\pm \right) = 1,$$

where $\bar{z}^{(N-2)}$ are the fugacities for the gauge group $USp(2N - 4)$. All of them are massive.

After integrating out the massive fields and keeping track of all the singlets, we get the third quiver in Figure 79. Then we apply again the IP duality on the same node. Notice that, since we integrated out massive fields before the second dualization, we don't go back to the original theory and obtain the last theory in Figure 79.

As highlighted in the first quiver in Figure 80, now the $USp(2N - 4)$ node has no antisymmetric so we can apply the IP duality and reach the second quiver in Figure 80. The $USp(2N - 4)$ node becomes an $USp(2M)$ node and the $SU(2)_v$ flavor *moves* to its left. We can keep applying IP dualities towards the left of the quiver with the effect of creating a sequence of $USp(2M)$ nodes and moving the $SU(2)_v$ flavor to the left. After dualizing the M -th node we reach the third quiver in Figure 80. Notice that the $SU(2)_v$ leg attached to the red $(M - 1)$ -th gauge node has charge $\sqrt{p\bar{q}}$ and hence it becomes massive. Now if we keep applying IP dualities along the tail the $SU(2)_v$ flavor does not move anymore while the ranks of the gauge groups remain unchanged. After the IP dualization of the last $USp(2)$ node, we reach the last quiver in Figure 80, which coincides with the result anticipated in Figure 77.

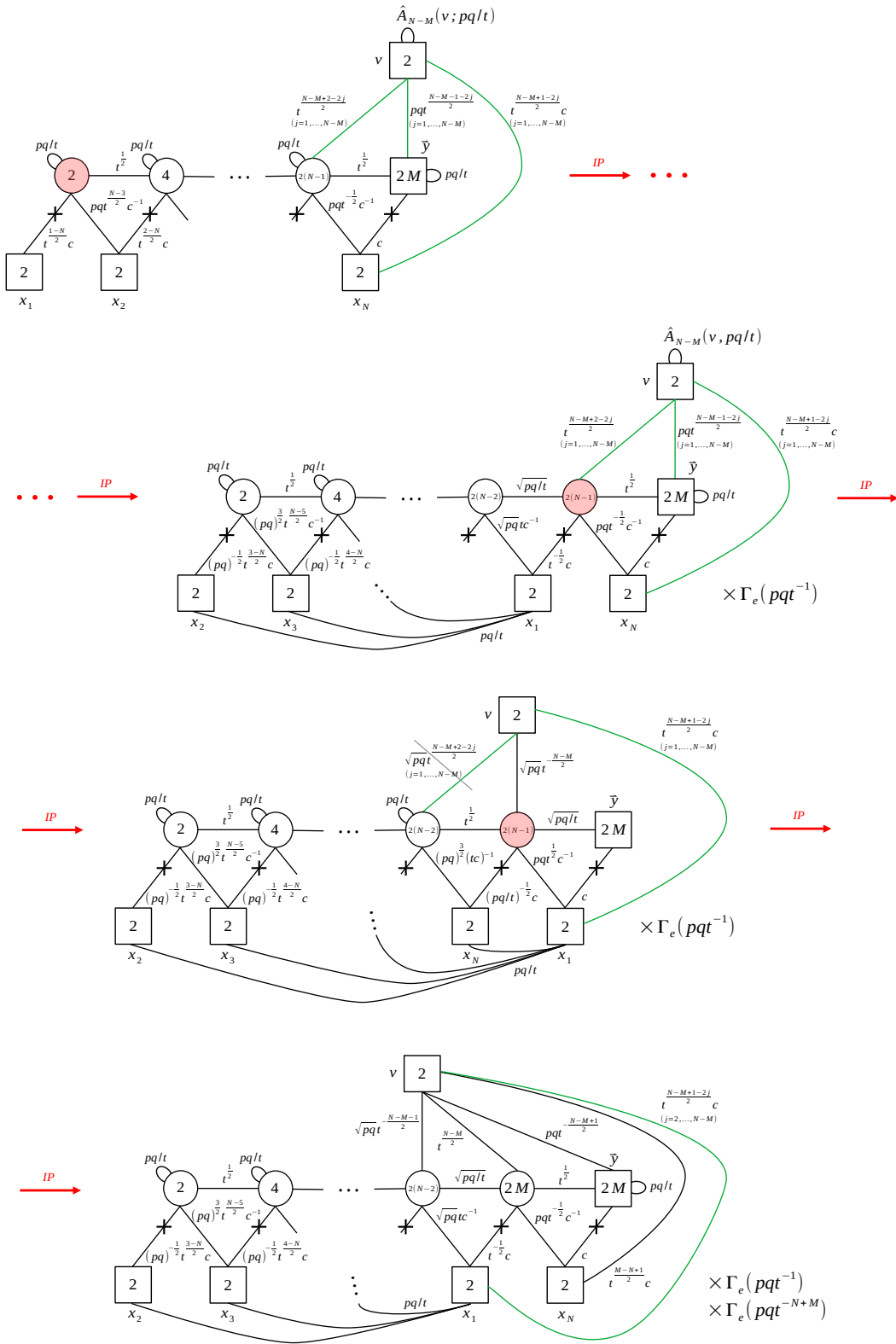


Figure 79. The first part of the derivation of the Lagrangian form of an asymmetric S-wall with the specialized manifest symmetry. The grey dash in the third quiver indicates a set of massive fields.

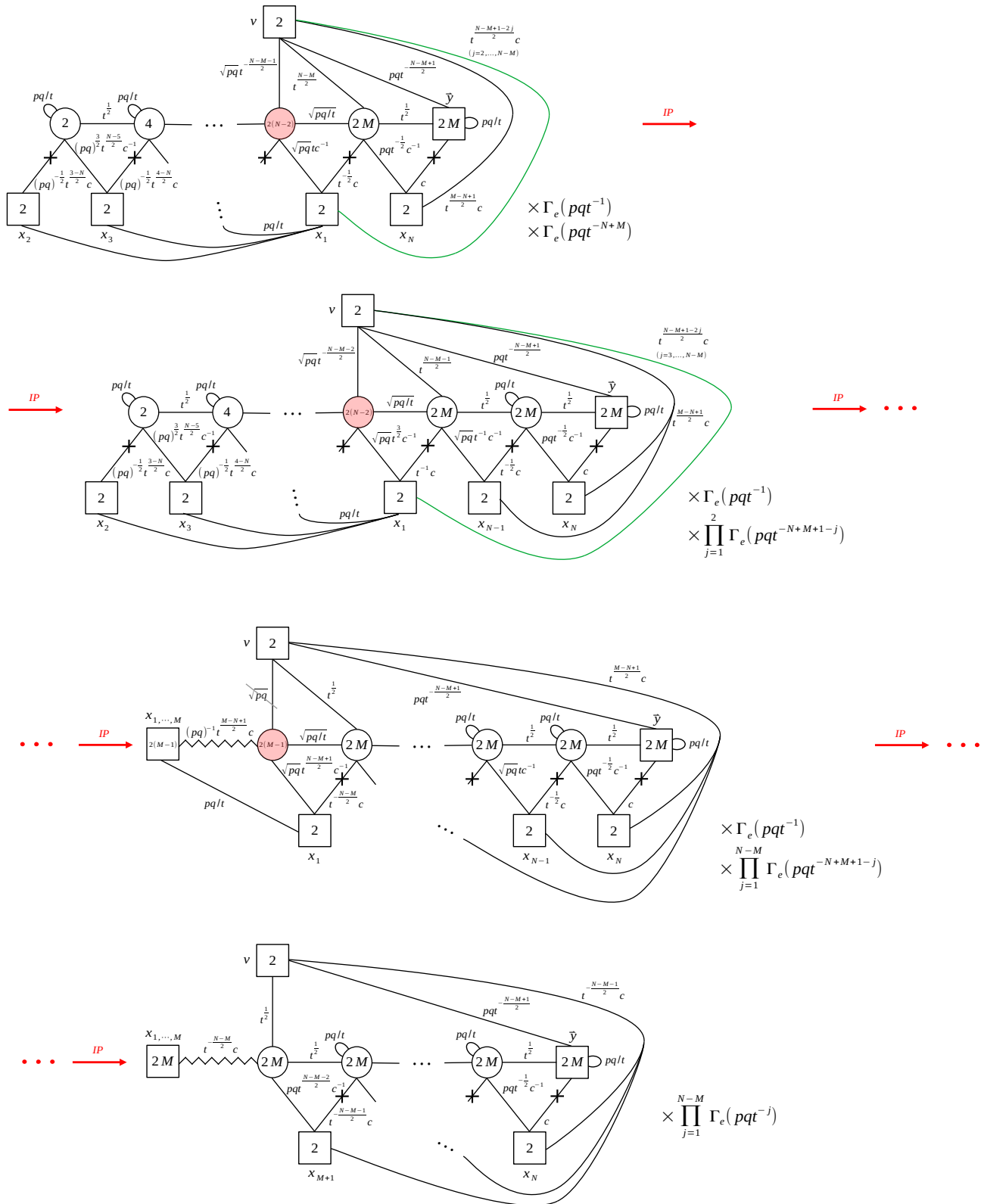


Figure 80. The second part of the derivation of the Lagrangian form of an asymmetric S-wall with the specialized manifest symmetry. The grey dash in the third quiver indicates a massive field.

Specialization of the emergent symmetry

Now we consider the case in which the broken symmetry is the emergent one. We choose to specialize in geometric progression the first $(N - M)$ fugacities of the $SU(2)_{y_j}$ symmetries from the left to get the first quiver in Figure 81. The specialization has the effect of breaking the $SU(2)_{y_j}$, for $j = 1, \dots, M - N$, down to $U(1)_v$. Indeed focusing on the contribution of chiral fields of the saw charged under k -th gauge node for $k = 1, \dots, N - M - 1$, we see that the specialization yields

$$\begin{aligned} & \prod_{i=1}^k \Gamma_e \left(t^{\frac{k-N}{2}} c \left(t^{\frac{N-M+1}{2} - k} v \right)^{\pm} z_i^{(k)\pm} \right) \Gamma_e \left(pqt^{\frac{N-k-2}{2}} c^{-1} \left(t^{\frac{N-M+1}{2} - (k+1)} v \right)^{\pm} z_i^{(k)\pm} \right) = \\ & = \prod_{i=1}^k \Gamma_e \left(t^{\frac{3k-2N+M-1}{2}} c v^{-1} z_i^{(k)\pm} \right) \Gamma_e \left(pqt^{\frac{2N-3k-M-3}{2}} c^{-1} v z_i^{(k)\pm} \right). \end{aligned}$$

For $k = N - M$, on the other hand, we get a slight different result, since no chiral of the saw connected to this gauge node becomes massive.

We then apply the IP duality on the first $USp(2)$ which confines, since it sees 6 chirals, to obtain the second quiver in Figure 81. Now the $USp(4)$ has no antisymmetric and sees 8 chirals, so it also confines. We continue sequentially confining the nodes until we reach the third quiver in Figure 81. At this point the legs can be rearranged in such a way that the $SU(2)_v$ symmetry is restored. If we now apply the IP duality on the $USp(2N - 2M)$ node, the effect is that it becomes $USp(2)$ instead of confining. After this dualization we get the fourth quiver in Figure 81. Notice that the legs in the saw have been rearranged by the IP duality such that now $SU(2)_v$ is exchanged with $SU(2)_{y_{N-M-1}}$ and also a bifundamental between the two is produced. If we keep applying the IP duality along the tail, we get increasing ranks starting from $USp(2)$. After we have dualized the $(N - 1)$ -th node we find the last theory in Figure 81, which corresponds to the anticipated form of an S-wall with the specialized emergent symmetry of Figure 78.

As a final comment we check that we recover the symmetric S-wall in the case $M = N$, in which there is no breaking. In the case of the breaking of the manifest $USp(2N)_y$ symmetry, as it can be seen from Figure 77, this is trivial. On the other hand starting from Figure 78 we need to perform a couple of steps to recover the symmetric S-wall as shown in Figure 82.

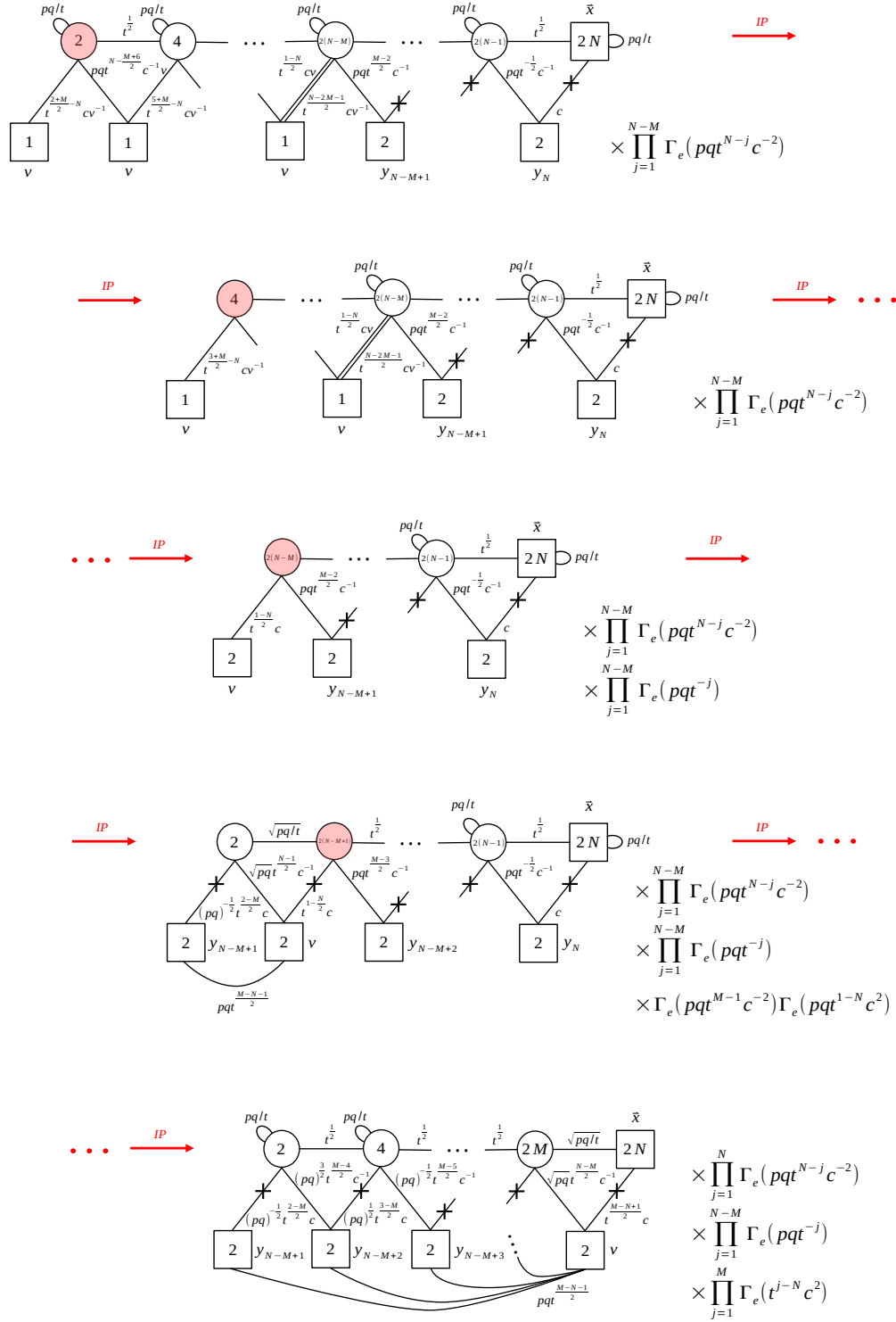


Figure 81. Derivation of the Lagrangian form of an asymmetric S-wall with the specialized emergent symmetry.

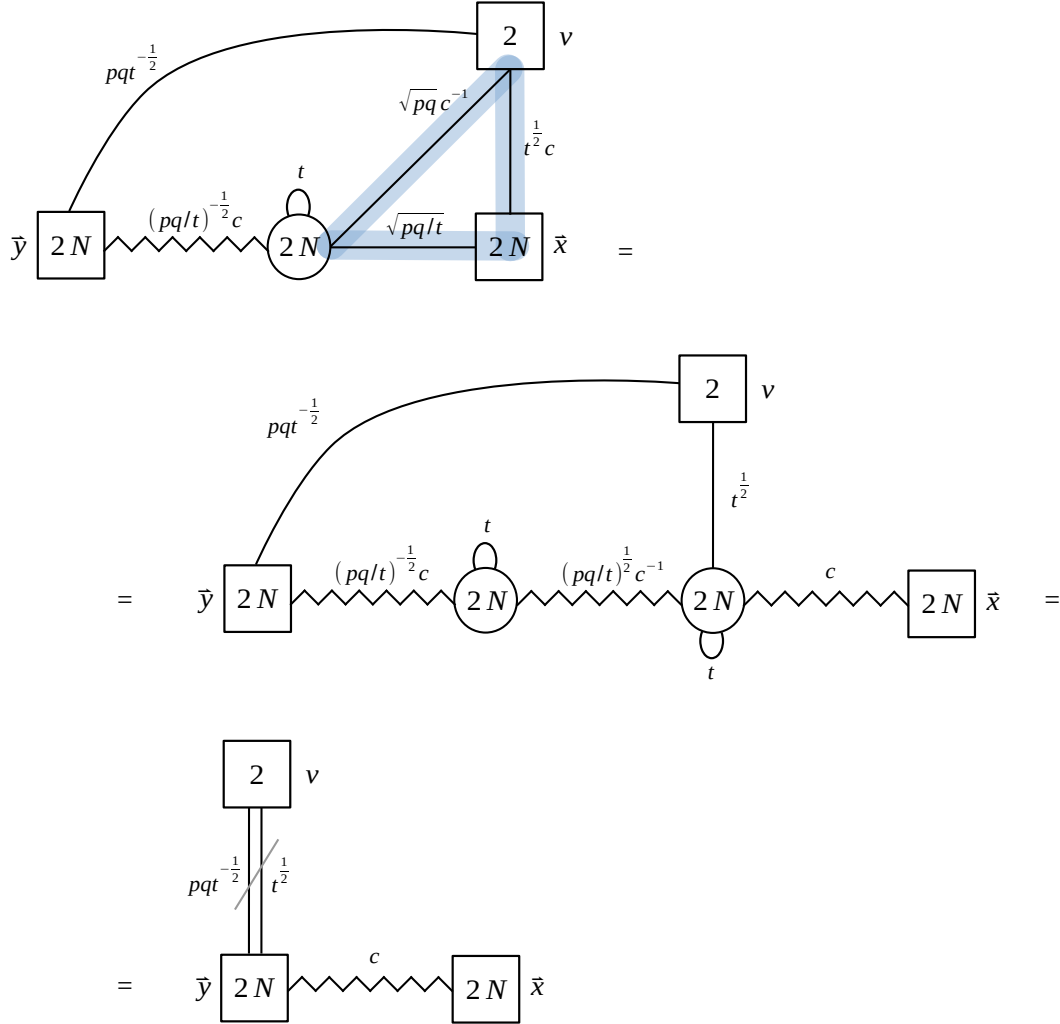


Figure 82. Starting from the asymmetric S-wall in Figure 78 for $N = M$, we apply the $B_{10} = SB_{01}S^{-1}$ move to the highlighted part of the quiver. After implementing the identifications imposed by the Identity-wall, two flavors become massive, and we obtain the symmetric S-wall.

C Derivations of basic duality moves

In this appendix we show how to derive some of the new duality moves presented in Section 2.3.

$$\mathbf{B}_{11} = \mathbf{S}\mathbf{B}_{1-1}\mathbf{S}^{-1}$$

To derive this duality we proceed as in Figure 83. In the first step we apply the duality $\mathbf{B}_{10} = \mathbf{S}\mathbf{B}_{01}\mathbf{S}^{-1}$ of Figure 21 to the blue part of the quiver. In the second step we apply the braid move of Figure 8 to the yellow and orange parts. In the third step we apply again $\mathbf{S}\mathbf{B}_{01}\mathbf{S}^{-1} = \mathbf{B}_{10}$ to the purple part.

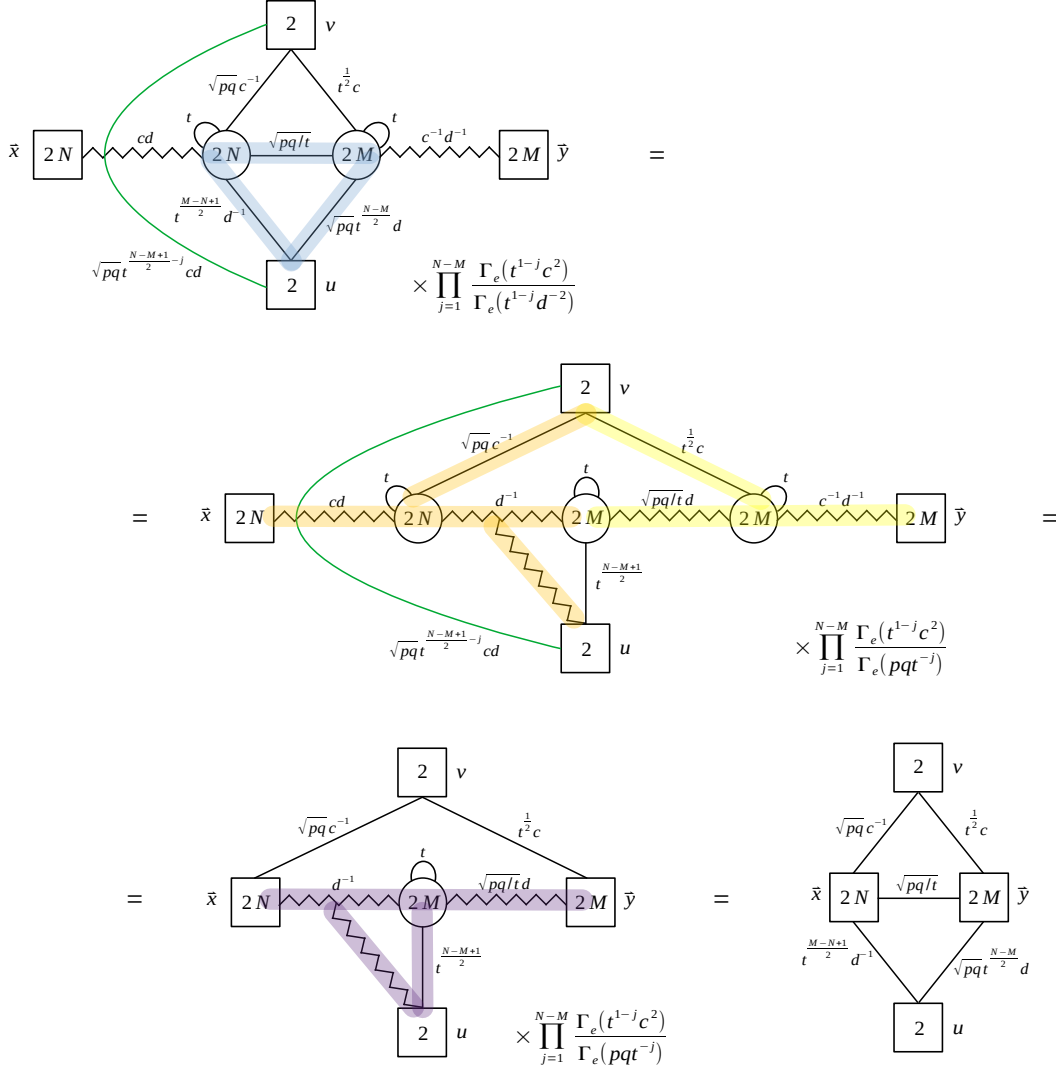


Figure 83. Derivation of the duality $\mathbf{B}_{11} = \mathbf{S}\mathbf{B}_{1-1}\mathbf{S}^{-1}$.

$$\mathbf{B}_{10} = \mathbf{T}^T \mathbf{B}_{10} (\mathbf{T}^T)^{-1}$$

To derive this duality we proceed as in Figure 84. In the first step we apply the braid move of Figure 8 to the part of the quiver highlighted in yellow. In the second step we apply the duality move $\mathbf{B}_{11} = \mathbf{S} \mathbf{B}_{1-1} \mathbf{S}^{-1}$ of Figure 24 to the blue part.

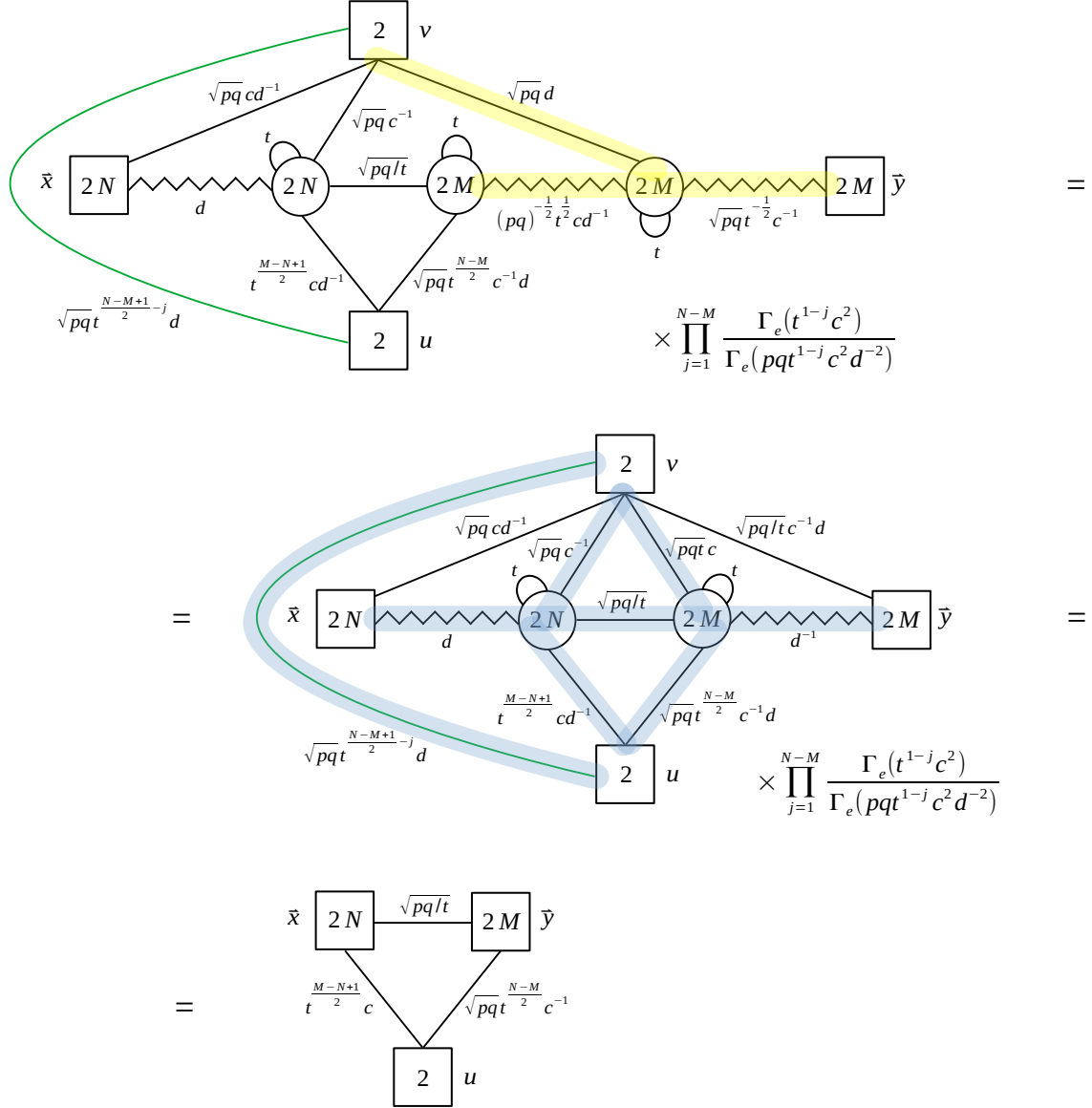


Figure 84. Derivation of the duality $\mathbf{B}_{10} = \mathbf{T}^T \mathbf{B}_{10} (\mathbf{T}^T)^{-1}$.

$$\mathbf{B}_{01} = \mathbf{T}^T \mathbf{B}_{1-1} (\mathbf{T}^T)^{-1}$$

To derive this duality we proceed as in Figure 85. In the first step we apply the braid move of Figure 8 to the part of the quiver highlighted in yellow. In the second step we apply the duality move $\mathbf{B}_{01} = \mathbf{S} \mathbf{B}_{10} \mathbf{S}^{-1}$ of Figure 22 to the blue part.

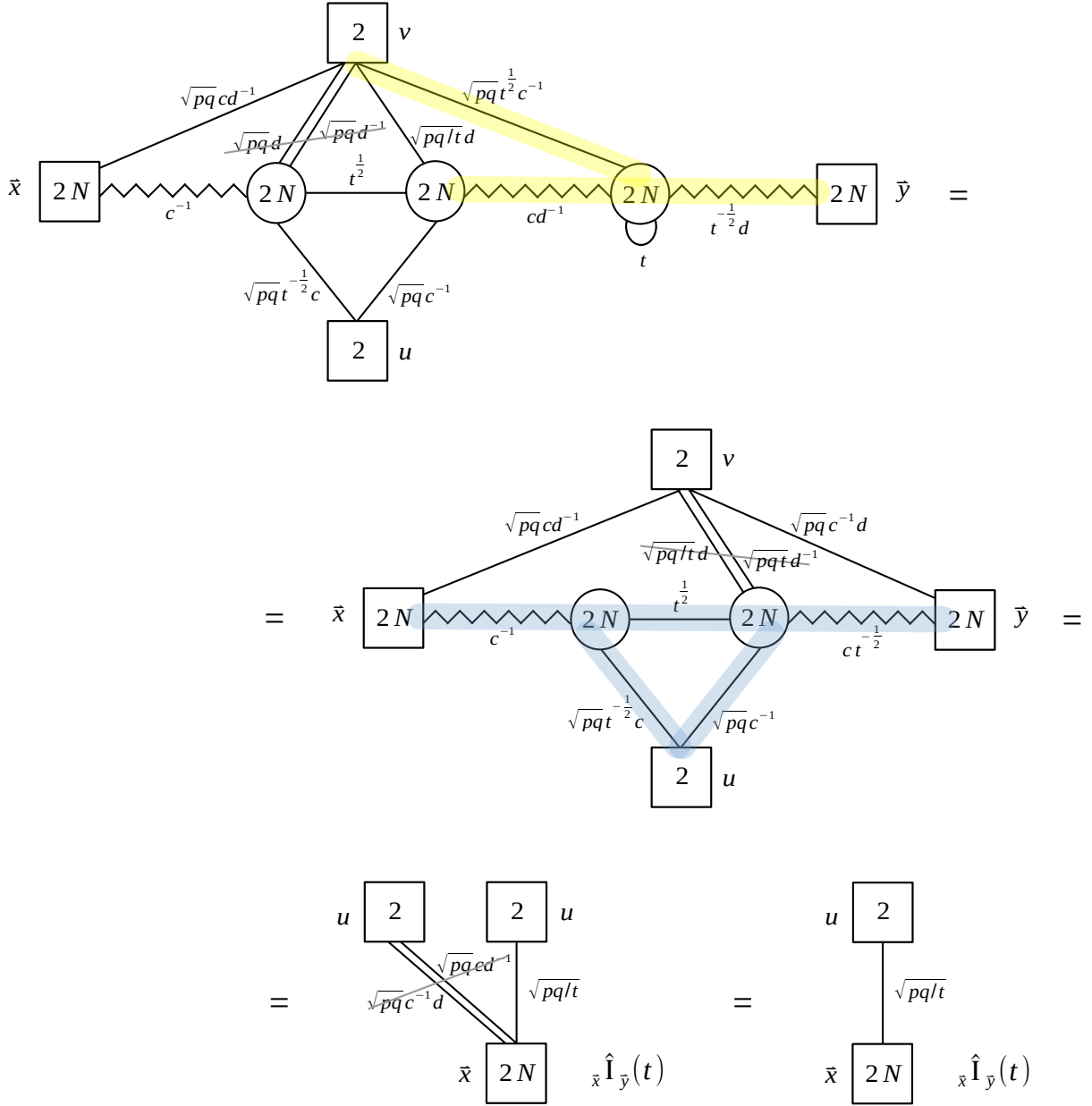


Figure 85. Derivation of the duality $\mathbf{B}_{01} = \mathbf{T}^T \mathbf{B}_{1-1} (\mathbf{T}^T)^{-1}$. The pair of lines with a bar on top denote fields that give mass to each other.

$$\mathbf{B}_{11} = \mathbf{T}^T \mathbf{B}_{01} (\mathbf{T}^T)^{-1}$$

To derive this duality we proceed as in Figure 86. In the first step we collapse the two S-walls highlighted in red. In the second step we use the braid move of Figure 8 to the yellow part. In the third step we apply the duality move $\mathbf{B}_{10} = \mathbf{S} \mathbf{B}_{01} \mathbf{S}^{-1}$ of Figure 21 to the blue part.

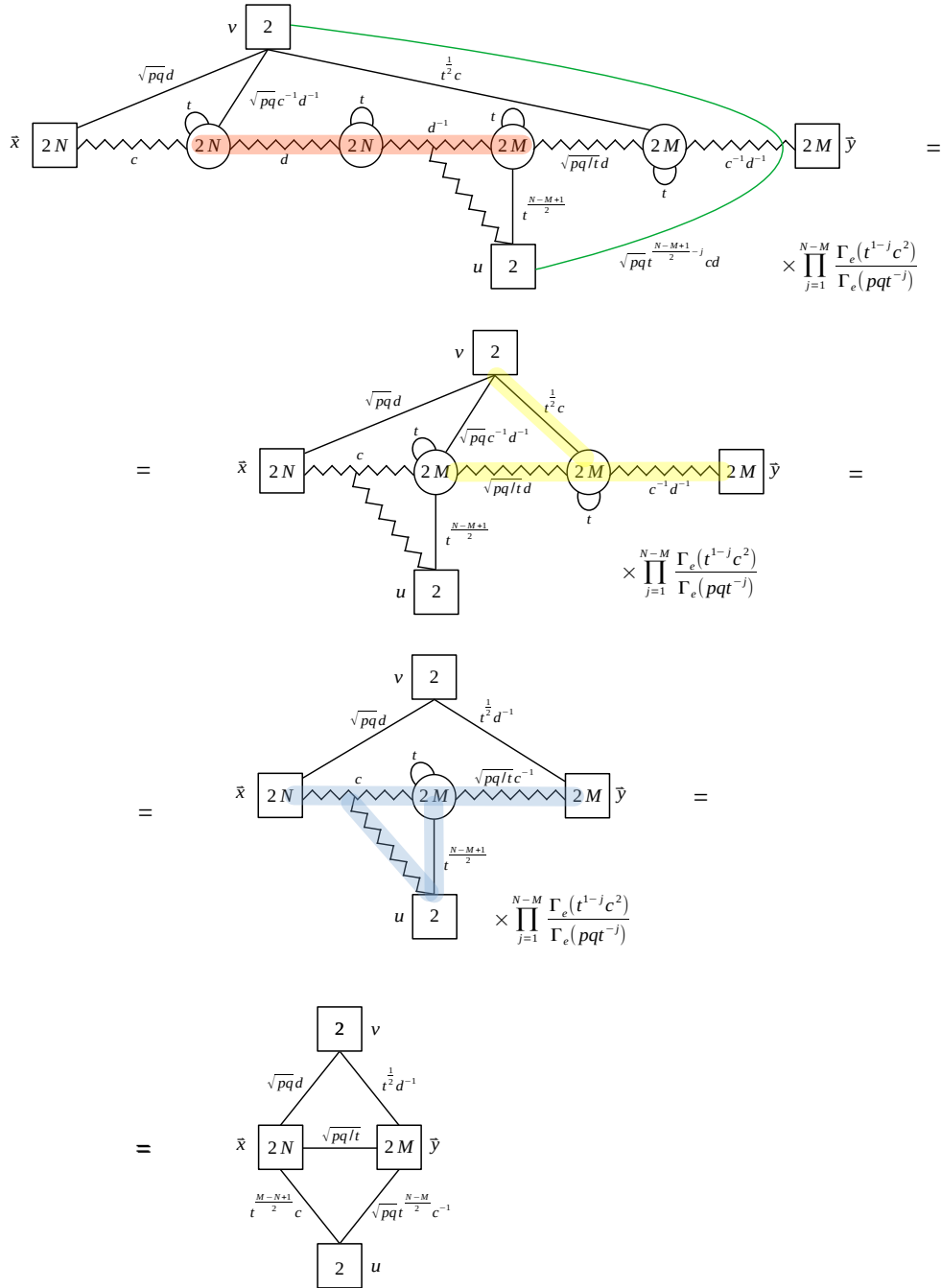


Figure 86. Derivation of the duality $\mathbf{B}_{11} = \mathbf{T}^T \mathbf{B}_{01} (\mathbf{T}^T)^{-1}$.

D Proof of the Hanany–Witten duality move

In this section we derive the Hanany–Witten (HW) move shown in Figure 87.

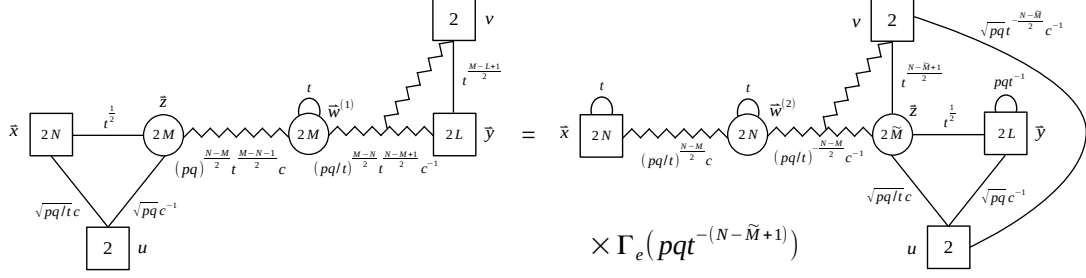


Figure 87. The Hanany–Witten duality move.

On l.h.s. of this duality, the two S-walls fuse to form an asymmetric Identity-wall. When we implement the identifications imposed by this asymmetric Identity-wall we obtain the WZ model on the l.h.s. of Figure 88. On the r.h.s. of Figure 88 we also add an Identity-wall obtained by the fusions of two S-walls.

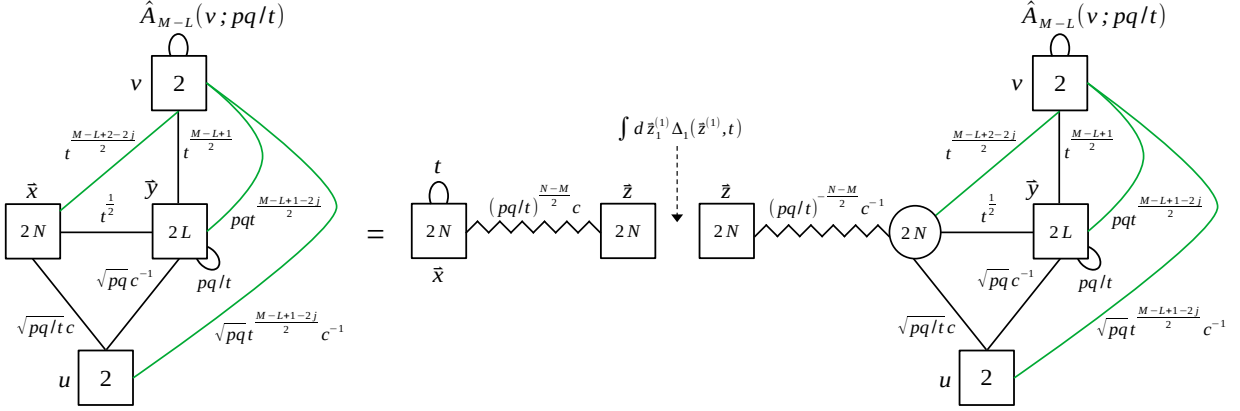


Figure 88. On the left is depicted the starting point with the asymmetric Identity-wall implemented. On the right is shown the theory with the addition of an Identity-wall written as two S-walls. The green lines denote gauge singlet fields labelled by $j = 1, \dots, M - L$.

We now focus on the part of the theory on the r.h.s. of Figure 88 that is composed by the second S-wall glued to the rightmost part of the quiver as shown on the top of Figure 89, where the S-wall is now presented with its manifest $USp(2N)$ symmetry gauged. We also define $d = (pq/t)^{\frac{M-N}{2}} c^{-1}$ to simplify the figure. Now we apply the IP duality on the first $USp(2)$ node: the rank does not change but the antisymmetric of the following $USp(4)$ becomes massive; furthermore $SU(2)_{z_1}$ is swapped with $SU(2)_{z_2}$. We then continue applying the IP duality along the tail until we dualize the $(N - 1)$ -th node to obtain the second quiver in Figure 89. We notice that here the mesons built with the green chirals connected to the $USp(2N)$ node acquire a VEV. As in the previous section, we can trade the study of the

Higgsing induced by this VEV for two IP dualizations of the same node which take us to the third quiver in Figure 89. Notice that the resulting rank of the node is $\widetilde{M} = N + L - M + 1$, as expected in the Hanany–Witten move. Now we apply the IP duality to the $(N - 1)$ -th node highlighted in red to reach the last theory in Figure 89. Notice that the rank becomes \widetilde{M} and also the $SU(2)_v$ flavor is moved to the left.

We keep applying IP dualities on the nodes moving towards the left until we reach the \widetilde{M} -th, resulting in the second theory in Figure 90. Notice that the $SU(2)_v$ flavor connected to the $USp(2\widetilde{M} - 2)$ gauge node has a charge of \sqrt{pq} , so it becomes massive. Now we continue applying the IP duality moving to the left inside the S-wall. The ranks remain unchanged while the $SU(2)_v$ flavor is no longer moving to the left. When we finally apply the IP duality on the $USp(2)$ gauge node of the S-wall we get the last quiver in Figure 90. We can recognize this as an asymmetric S-wall (with extra singlets) with specialized manifest $USp(2N)$ symmetry, which is depicted in Figure 77. Now if we glue to this the S-wall which we added in Figure 88 (and also revert the substitution $d = (pq/t)^{\frac{M-N}{2}} c^{-1}$) we obtain exactly the r.h.s. of the HW move in Figure 87, as desired.

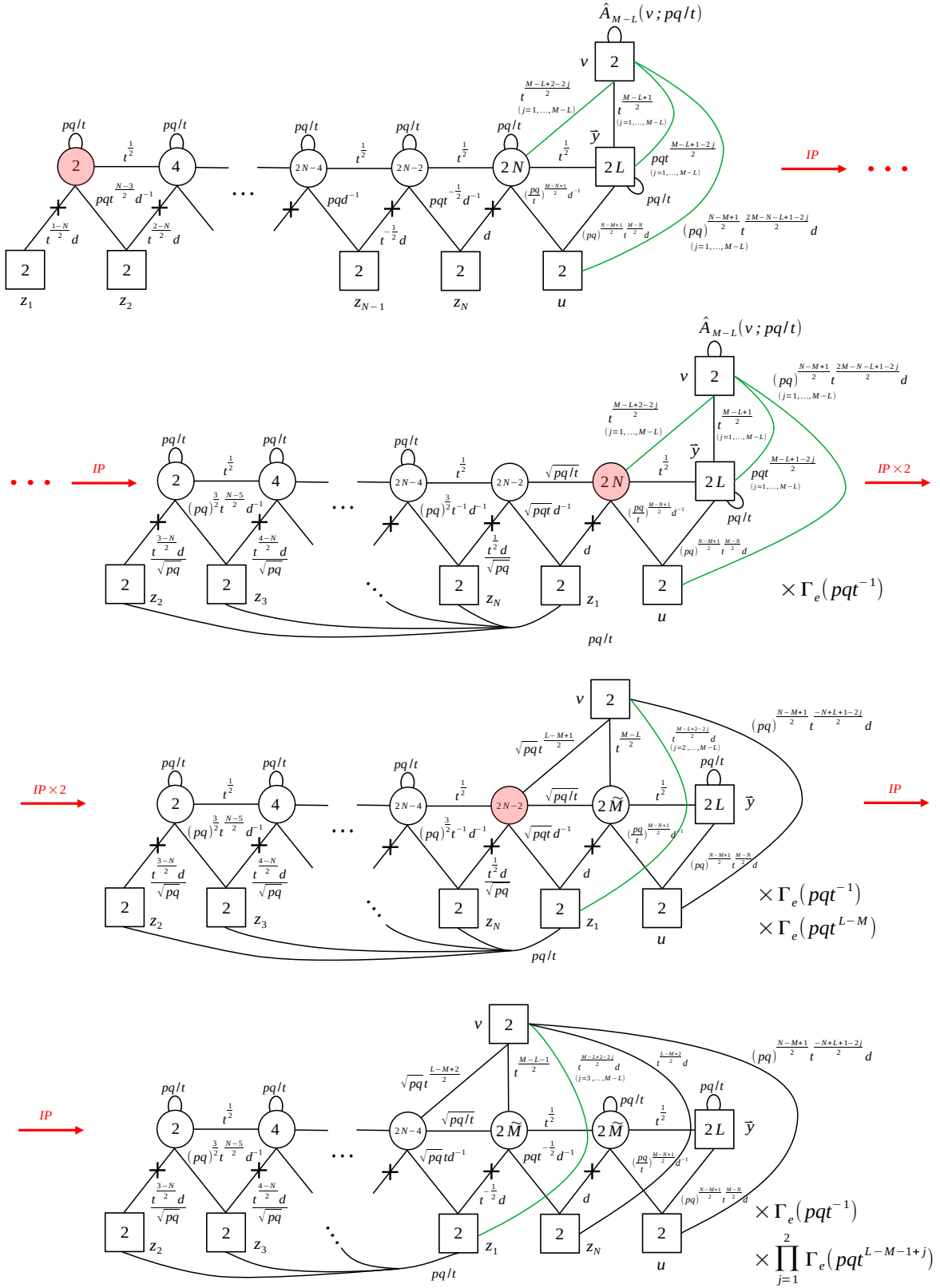


Figure 89. The first part of the proof of the Hanany–Witten move via Intriligator–Pouliot dualities.

E Limits of the $FE[USp(2N)]$ theory for $c = 1$ and $c = t^{\frac{1}{2}}$

In this section we will study two interesting deformations of the $FE[USp(2N)]$ theory. First, we consider the effect of introducing a superpotential term linear in the β_N singlet flipping the $\text{Tr}_x \text{Tr}_{y_N} D^{(N)} D^{(N)}$ meson. This deformation has the effect of giving a VEV to the meson $\text{Tr}_x \text{Tr}_{y_N} D^{(N)} D^{(N)}$. Since β_N appears linearly in the superpotential, it must have R -charge 2 and charge 0 under every other $U(1)$ symmetry, which implies that $U(1)_c$ is broken and the c fugacity is specialized to 1. In order to analyze the effect of this deformation we consider the variant of the braid duality in Figure 91 (related by flips to the braid duality in Figure 8).

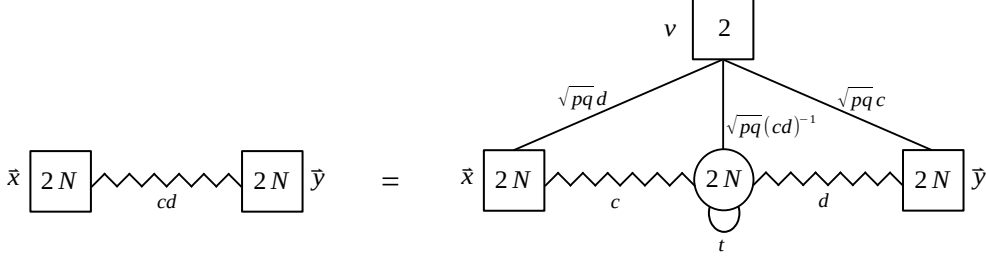


Figure 91. A flipped version of the braid duality move.

In this version of the braid, the limit we are interested in corresponds to $d = c^{-1}$. Indeed, as shown in Figure 92, on the l.h.s. we have exactly the S-walls deformed by the linear term β_N . On the r.h.s., instead, the vertical $SU(2)_v$ flavor coupled to the middle gauge node becomes massive and we are left with two S-walls giving rise to an Identity-wall. After implementing the identification of the $USp(2N)_x$ and the $USp(2N)_y$ symmetries due to the Identity-wall, we have that also the two other flavors become massive. In the end we are just left with an Identity-wall. At the level of the index this identity can be written as:

$$\mathcal{I}_{FE}^{(N,N)}(\vec{x}, \vec{y}, t, c = 1) = \frac{\prod_{j=1}^N 2\pi i y_j}{\Delta_N(\vec{y}, t)} \prod_{\sigma \in S_N} \prod_{j=1}^N \delta(x_j - y_{\sigma(j)}^{\pm}). \quad (\text{E.1})$$

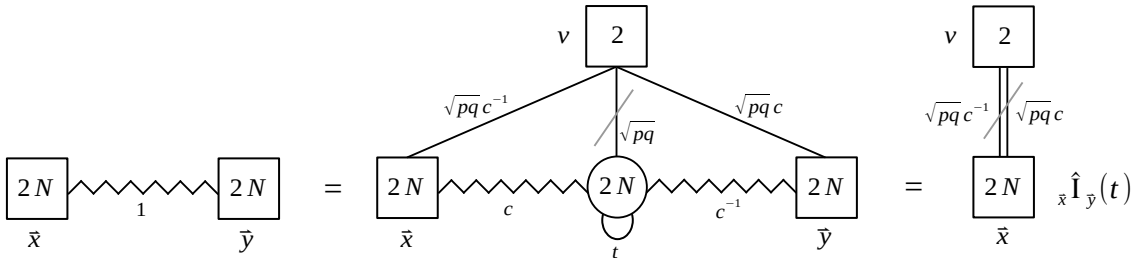


Figure 92. The result of the $c = 1$ degeneration limit of the $FE[USp(2N)]$ theory.

Another interesting deformation of the $FE[USp(2N)]$ theory corresponds to turning on a superpotential term linear in the singlet β_{N-1} which now breaks a combination of $U(1)_t \times$

$U(1)_c$, which at the level of the fugacities fixes $c = t^{\frac{1}{2}}$. This limit has already been studied in [21, 91], but here we present a new derivation of it. The effect of this deformation can indeed be easily understood considering the recursive definition of the $FE[USp(2N)]$ quiver, which can be represented as an $FE[USp(2N - 2)]$ quiver coupled to an extra block with the $USp(2N - 2)$ symmetry gauged as in Figure 93.

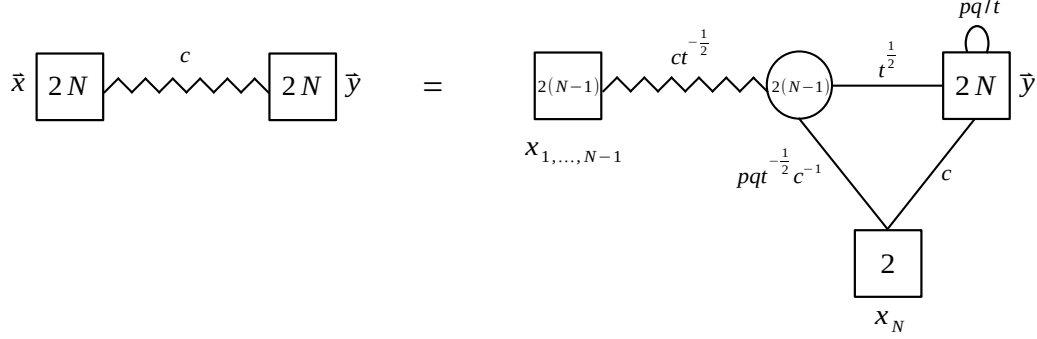


Figure 93. A quiver representation of the recursive definition of the $FE[USp(2N)]$ theory.

When we take the limit $c = t^{\frac{1}{2}}$ in Figure 93, the $FE[USp(2N - 2)]$ theory is subject to the deformation of Figure 92 and reduces to an Identity-wall, so that we obtain the result in Figure 94. At the level of the index this identity can be written as:

$$\mathcal{I}_{FE}^{(N,N)}(\vec{x}, \vec{y}, t, c = 1t^{\frac{1}{2}}) = A_N(\vec{x}; pq/t) A_N(\vec{y}; pq/t) \prod_{i,j=1}^N \Gamma_e \left(t^{\frac{1}{2}} x_i^{\pm 1} y_j^{\pm 1} \right). \quad (\text{E.2})$$

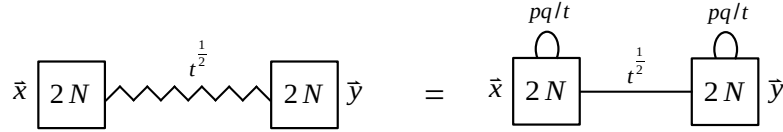


Figure 94. The result of the $c = t^{\frac{1}{2}}$ degeneration limit of the $FE[USp(2N)]$ theory.

F Derivation of a relation between WZ models

We now demonstrate the relation between WZ models in Figure 39 that we used in the main text to study the Higgsing that can occur in the dualization algorithm after applying the duality moves.

As shown in Figure 95, starting from the $FE[USp(2N)]$ theory we can first turn on the $c = t^{\frac{1}{2}}$ deformation of Figure 94 to obtain the left theory in the second line. We then turn on the deformation breaking $USp(2N)_y \rightarrow SU(2)_v$ by specializing

$$y_j = t^{\frac{N+1}{2}-j} v \quad \text{for } j = 1, \dots, N; \quad (\text{F.1})$$

to obtain the the left theory in the third line. This is a theory of N chirals in the $USp(2N)_x \times SU(2)_v$ bifundamental representation, a $USp(2N)_x$ antisymmetric of chirals and extra chirals whose index contribution is encoded in the $\hat{A}(v, pq/t)$ we defined in (3.5).

Starting again from the $FE[USp(2N)]$ theory, we can also implement the same deformations but in the reversed order. Namely, we first break $USp(2N)_y$ to $SU(2)_v$ moving to the right theory in the second line. Considering either of the lagrangian forms of the $M = 0$ asymmetric S-wall of Figures 77 or 78, it is easy to see that we are left with a $USp(2N)_x \times SU(2)_v$ bifundamental chiral plus extra chirals. Finally we take the specialization $c = \sqrt{t}$ to reach the right theory in the third line.

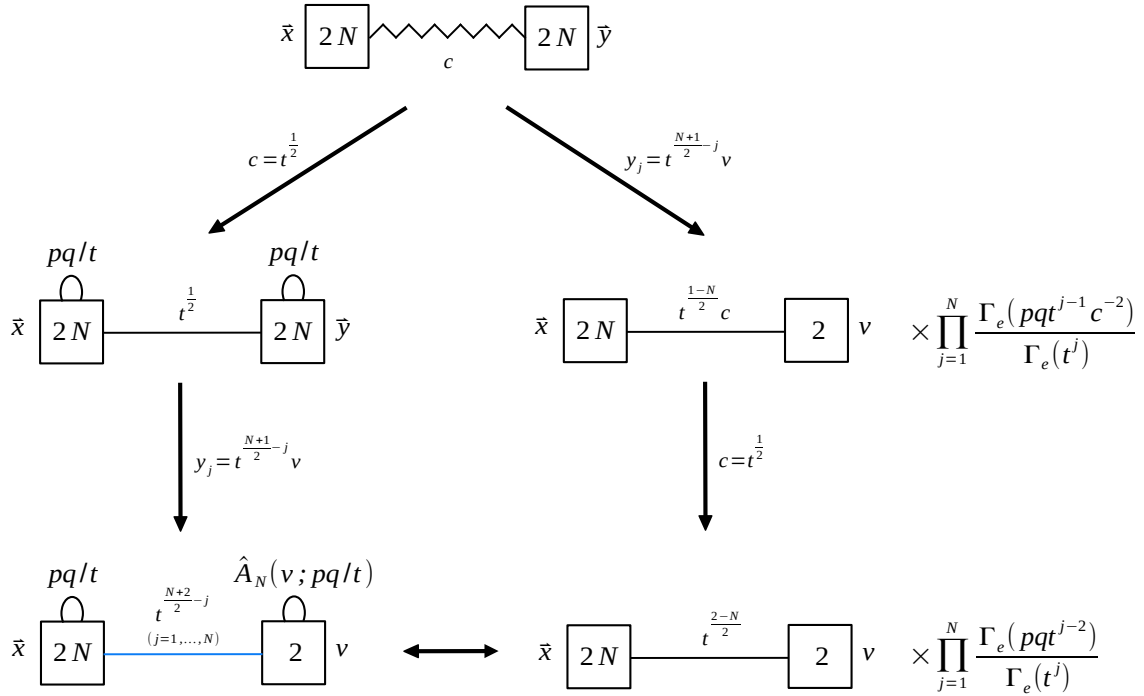


Figure 95. A relation between deformed WZ models obtained by starting from the S-wall and implementing two deformations in different orders.

$$\bar{x} \begin{array}{|c|} \hline 2N \\ \hline \end{array} \xrightarrow{t^{1+\frac{N}{2}-j}} \begin{array}{|c|} \hline \hat{A}_N(v; pq/t) \\ \hline \end{array} \begin{array}{|c|} \hline 2 \\ \hline \end{array} v = \bar{x} \begin{array}{|c|} \hline t \\ \hline \end{array} \begin{array}{|c|} \hline 2N \\ \hline \end{array} \xrightarrow{t^{1-\frac{N}{2}}} \begin{array}{|c|} \hline 2 \\ \hline \end{array} v$$

$$\times \prod_{j=1}^N \Gamma_e(pqt^{j-2}) \Gamma_e(pqt^{-j})$$

Figure 96. A relation between a theory with a set of $USp(2N)_x \times SU(2)$ bifundamentals with $j = 1, \dots, N$ and a theory with a single $USp(2N)_x \times SU(2)$ bifundamental field and a $USp(2N)_x$ antisymmetric field (plus extra singlets).

We then have the relation shown in Figure 96, where we flipped the antisymmetric of $USp(2N)_x$. The relation between the theory on the l.h.s. and the one on the r.h.s. can be neatly understood by looking at their indices which behave as singular distributions having equivalent actions on test functions. On the l.h.s. the charges of the bifundamentals are

$$t^{\frac{N}{2}}, t^{\frac{N}{2}-1}, t^{\frac{N}{2}-2}, \dots, t^{2-\frac{N}{2}}, t^{1-\frac{N}{2}}, \quad (\text{F.2})$$

and so, as we saw in Section 3.3, if we try to gauge the $USp(2N)_x$ group the mesons constructed with these bifundamentals take a VEV Higgsing the $USp(2N)_x$ group down to $USp(2)_w$. Indeed these legs produce $N - 1$ colliding poles. The residue can be taken for example at the following poles:¹³

$$x_j = t^{\frac{N}{2}-j} v \quad \text{for } j = 1, \dots, N - 1, \quad (\text{F.3})$$

where $x_N = w$ parametrizes the remaining $USp(2)_w$, while v parametrizes the other $USp(2)_v$.

On the r.h.s., instead, the meson built out of the bifundamental dressed $N - 2$ times with the antisymmetric has zero R -charge and thus takes a VEV. Hence, also on this side the $USp(2N)_x$ is Higgsed down to $USp(2)_v$, but this time it is not due to $N - 1$ mesons taking a VEV but rather a single meson dressed with $N - 2$ powers of the antisymmetric. Indeed looking at the contribution to the index of bifundamental and the antisymmetric

$$\Gamma_e(t)^N \prod_{i < j}^N \Gamma_e(tx_i^\pm x_j^\pm) \prod_{i=1}^N \Gamma_e(t^{1-\frac{N}{2}} x_i^\pm v^\pm) \quad (\text{F.4})$$

we see that there are colliding poles from

$$\prod_{i < j}^{N-1} \Gamma_e(tx_i^\pm x_j^\pm) \Gamma_e(t^{1-\frac{N}{2}} x_1 v^{-1}) \Gamma_e(t^{1-\frac{N}{2}} x_{N-1}^{-1} v) \quad (\text{F.5})$$

¹³There are also other poles that we should consider, but they are related to these by the Weyl group of $USp(2N)_x$ so they give identical contributions that cancels with part of the $1/(2^N N!)$ Weyl symmetry factor of the partially Higgsed $USp(2N)_x$ gauge group.

and the residue can be taken for example at the following poles:

$$\begin{aligned}
x_1 &= t^{\frac{N}{2}-1}v, \\
x_2 &= t^{-1}x_1 = t^{\frac{N}{2}-2}v, \\
&\vdots \\
x_{N-2} &= t^{-1}x_{N-3} = t^{2-\frac{N}{2}}v, \\
x_{N-1} &= t^{-1}x_{N-2} = t^{1-\frac{N}{2}}v,
\end{aligned}
\tag{F.6}$$

which is exactly the same specialization as (F.3). The effect of taking this residue is the Higgsing of $USp(2N)_x$ node down to $USp(2)_w$.

In conclusion, if we try to gauge their $USp(2N)$ symmetry with a test theory, we see that these two theories lead to IR dual models.

References

- [1] N. Seiberg, “Electric - magnetic duality in supersymmetric nonAbelian gauge theories,” *Nucl. Phys.* **B435** (1995) 129–146, [arXiv:hep-th/9411149](#) [[hep-th](#)].
- [2] K. A. Intriligator and N. Seiberg, “Mirror symmetry in three-dimensional gauge theories,” *Phys. Lett.* **B387** (1996) 513–519, [arXiv:hep-th/9607207](#) [[hep-th](#)].
- [3] A. Hanany and E. Witten, “Type IIB superstrings, BPS monopoles, and three-dimensional gauge dynamics,” *Nucl. Phys.* **B492** (1997) 152–190, [arXiv:hep-th/9611230](#) [[hep-th](#)].
- [4] O. Aharony, S. S. Razamat, N. Seiberg, and B. Willett, “3d dualities from 4d dualities,” *JHEP* **07** (2013) 149, [arXiv:1305.3924](#) [[hep-th](#)].
- [5] M. Aganagic, K. Hori, A. Karch, and D. Tong, “Mirror symmetry in (2+1)-dimensions and (1+1)-dimensions,” *JHEP* **07** (2001) 022, [arXiv:hep-th/0105075](#).
- [6] O. Aharony, S. S. Razamat, N. Seiberg, and B. Willett, “The long flow to freedom,” *JHEP* **02** (2017) 056, [arXiv:1611.02763](#) [[hep-th](#)].
- [7] O. Aharony, S. S. Razamat, and B. Willett, “From 3d duality to 2d duality,” *JHEP* **11** (2017) 090, [arXiv:1710.00926](#) [[hep-th](#)].
- [8] A. Gadde, S. S. Razamat, and B. Willett, “On the reduction of 4d $\mathcal{N} = 1$ theories on \mathbb{S}^2 ,” *JHEP* **11** (2015) 163, [arXiv:1506.08795](#) [[hep-th](#)].
- [9] M. Dedushenko and S. Gukov, “IR duality in 2D $N = (0, 2)$ gauge theory with noncompact dynamics,” *Phys. Rev. D* **99** no. 6, (2019) 066005, [arXiv:1712.07659](#) [[hep-th](#)].
- [10] M. Sacchi, “New 2d $\mathcal{N} = (0, 2)$ dualities from four dimensions,” *JHEP* **12** (2020) 009, [arXiv:2004.13672](#) [[hep-th](#)].
- [11] O. Aharony, S. S. Razamat, N. Seiberg, and B. Willett, “3d dualities from 4d dualities for orthogonal groups,” *JHEP* **08** (2013) 099, [arXiv:1307.0511](#) [[hep-th](#)].
- [12] C. Csáki, M. Martone, Y. Shirman, P. Tanedo, and J. Terning, “Dynamics of 3D SUSY Gauge Theories with Antisymmetric Matter,” *JHEP* **08** (2014) 141, [arXiv:1406.6684](#) [[hep-th](#)].
- [13] K. Nii, “3d duality with adjoint matter from 4d duality,” *JHEP* **02** (2015) 024, [arXiv:1409.3230](#) [[hep-th](#)].

- [14] A. Amariti, “Integral identities for 3d dualities with $SP(2N)$ gauge groups,” [arXiv:1509.02199 \[hep-th\]](#).
- [15] A. Amariti, D. Orlando, and S. Reffert, “String theory and the 4D/3D reduction of Seiberg duality. A review,” *Phys. Rept.* **705-706** (2017) 1–53, [arXiv:1611.04883 \[hep-th\]](#).
- [16] F. Benini, S. Benvenuti, and S. Pasquetti, “SUSY monopole potentials in 2+1 dimensions,” *JHEP* **08** (2017) 086, [arXiv:1703.08460 \[hep-th\]](#).
- [17] C. Hwang, H. Kim, and J. Park, “On 3d Seiberg-Like Dualities with Two Adjoints,” *Fortsch. Phys.* **66** no. 11-12, (2018) 1800064, [arXiv:1807.06198 \[hep-th\]](#).
- [18] S. Benvenuti, “A tale of exceptional 3d dualities,” *JHEP* **03** (2019) 125, [arXiv:1809.03925 \[hep-th\]](#).
- [19] A. Amariti and L. Cassia, “ $USp(2N_c)$ SQCD₃ with antisymmetric: dualities and symmetry enhancements,” *JHEP* **02** (2019) 013, [arXiv:1809.03796 \[hep-th\]](#).
- [20] K. Nii, “3d Self-dualities,” *Nucl. Phys. B* **942** (2019) 221–250, [arXiv:1811.09253 \[hep-th\]](#).
- [21] S. Pasquetti, S. S. Razamat, M. Sacchi, and G. Zafrir, “Rank Q E-string on a torus with flux,” *SciPost Phys.* **8** (2020) 014, [arXiv:1908.03278 \[hep-th\]](#).
- [22] L. E. Bottini, C. Hwang, S. Pasquetti, and M. Sacchi, “4d S-duality wall and $SL(2, \mathbb{Z})$ relations,” *JHEP* **03** (2022) 035, [arXiv:2110.08001 \[hep-th\]](#).
- [23] A. Amariti and S. Rota, “Webs of 3d $\mathcal{N} = 2$ dualities with D-type superpotentials,” [arXiv:2204.06961 \[hep-th\]](#).
- [24] C. Hwang, S. Pasquetti, and M. Sacchi, “4d mirror-like dualities,” *JHEP* **09** (2020) 047, [arXiv:2002.12897 \[hep-th\]](#).
- [25] M. Berkooz, “The Dual of supersymmetric $SU(2k)$ with an antisymmetric tensor and composite dualities,” *Nucl. Phys. B* **452** (1995) 513–525, [arXiv:hep-th/9505067](#).
- [26] P. Pouliot, “Duality in SUSY $SU(N)$ with an antisymmetric tensor,” *Phys. Lett. B* **367** (1996) 151–156, [arXiv:hep-th/9510148](#).
- [27] M. A. Luty, M. Schmaltz, and J. Terning, “A Sequence of duals for $Sp(2N)$ supersymmetric gauge theories with adjoint matter,” *Phys. Rev. D* **54** (1996) 7815–7824, [arXiv:hep-th/9603034](#).
- [28] I. Garcia-Etxebarria, B. Heidenreich, and T. Wrase, “New $N=1$ dualities from orientifold transitions. Part I. Field Theory,” *JHEP* **10** (2013) 007, [arXiv:1210.7799 \[hep-th\]](#).
- [29] I. n. Garcia-Etxebarria, B. Heidenreich, and T. Wrase, “New $N=1$ dualities from orientifold transitions - Part II: String Theory,” *JHEP* **10** (2013) 006, [arXiv:1307.1701 \[hep-th\]](#).
- [30] K. Nii, “3d Deconfinement, Product gauge group, Seiberg-Witten and New 3d dualities,” *JHEP* **08** (2016) 123, [arXiv:1603.08550 \[hep-th\]](#).
- [31] S. Pasquetti and M. Sacchi, “3d dualities from 2d free field correlators: recombination and rank stabilization,” *JHEP* **01** (2020) 061, [arXiv:1905.05807 \[hep-th\]](#).
- [32] S. Pasquetti and M. Sacchi, “From 3d dualities to 2d free field correlators and back,” *JHEP* **11** (2019) 081, [arXiv:1903.10817 \[hep-th\]](#).
- [33] S. Benvenuti, I. Garozzo, and G. Lo Monaco, “Sequential deconfinement in 3d $\mathcal{N} = 2$ gauge theories,” *JHEP* **07** (2021) 191, [arXiv:2012.09773 \[hep-th\]](#).

- [34] I. n. G. Etxebarria, B. Heidenreich, M. Lotito, and A. K. Sorout, “Deconfining $\mathcal{N} = 2$ SCFTs or the art of brane bending,” *JHEP* **03** (2022) 140, [arXiv:2111.08022 \[hep-th\]](#).
- [35] S. Benvenuti and G. Lo Monaco, “A toolkit for ortho-symplectic dualities,” [arXiv:2112.12154 \[hep-th\]](#).
- [36] L. E. Bottini, C. Hwang, S. Pasquetti, and M. Sacchi, “Dualities from dualities: the sequential deconfinement technique,” *JHEP* **05** (2022) 069, [arXiv:2201.11090 \[hep-th\]](#).
- [37] S. Bajeot and S. Benvenuti, “S-confinements from deconfinements,” [arXiv:2201.11049 \[hep-th\]](#).
- [38] S. Bajeot and S. Benvenuti, “Sequential deconfinement and self-dualities in $4d\mathcal{N} = 1$ gauge theories,” *JHEP* **10** (2022) 007, [arXiv:2206.11364 \[hep-th\]](#).
- [39] E. M. Rains, “Transformations of elliptic hypergeometric integrals,” *arXiv Mathematics e-prints* (Sept., 2003) math/0309252, [arXiv:math/0309252 \[math.QA\]](#).
- [40] V. Spiridonov, “Theta hypergeometric integrals,” *St. Petersburg Mathematical Journal* **15** no. 6, (2004) 929–967.
- [41] V. P. Spiridonov and G. S. Vartanov, “Elliptic Hypergeometry of Supersymmetric Dualities,” *Commun. Math. Phys.* **304** (2011) 797–874, [arXiv:0910.5944 \[hep-th\]](#).
- [42] V. P. Spiridonov and G. S. Vartanov, “Elliptic hypergeometry of supersymmetric dualities II. Orthogonal groups, knots, and vortices,” *Commun. Math. Phys.* **325** (2014) 421–486, [arXiv:1107.5788 \[hep-th\]](#).
- [43] C. Hwang, S. Pasquetti, and M. Sacchi, “Rethinking mirror symmetry as a local duality on fields,” [arXiv:2110.11362 \[hep-th\]](#).
- [44] O. Aharony, “IR duality in $d = 3$ $\mathcal{N}=2$ supersymmetric $USp(2N(c))$ and $U(N(c))$ gauge theories,” *Phys. Lett. B* **404** (1997) 71–76, [arXiv:hep-th/9703215](#).
- [45] K. A. Intriligator and P. Pouliot, “Exact superpotentials, quantum vacua and duality in supersymmetric $SP(N(c))$ gauge theories,” *Phys. Lett. B* **353** (1995) 471–476, [arXiv:hep-th/9505006](#).
- [46] D. Gaiotto and E. Witten, “Janus Configurations, Chern-Simons Couplings, And The theta-Angle in $\mathcal{N}=4$ Super Yang-Mills Theory,” *JHEP* **06** (2010) 097, [arXiv:0804.2907 \[hep-th\]](#).
- [47] K. Hosomichi, K.-M. Lee, S. Lee, S. Lee, and J. Park, “ $\mathcal{N}=4$ Superconformal Chern-Simons Theories with Hyper and Twisted Hyper Multiplets,” *JHEP* **07** (2008) 091, [arXiv:0805.3662 \[hep-th\]](#).
- [48] Y. Imamura and K. Kimura, “On the moduli space of elliptic Maxwell-Chern-Simons theories,” *Prog. Theor. Phys.* **120** (2008) 509–523, [arXiv:0806.3727 \[hep-th\]](#).
- [49] B. Assel, Y. Tachikawa, and A. Tomasiello, “On $\mathcal{N} = 4$ supersymmetry enhancements in three dimensions,” [arXiv:2209.13984 \[hep-th\]](#).
- [50] O. Aharony, O. Bergman, D. L. Jafferis, and J. Maldacena, “ $\mathcal{N}=6$ superconformal Chern-Simons-matter theories, M2-branes and their gravity duals,” *JHEP* **10** (2008) 091, [arXiv:0806.1218 \[hep-th\]](#).
- [51] O. Aharony, O. Bergman, and D. L. Jafferis, “Fractional M2-branes,” *JHEP* **11** (2008) 043, [arXiv:0807.4924 \[hep-th\]](#).

- [52] D. Bashkirov, “A Note on $\mathcal{N} \geq 6$ Superconformal Quantum Field Theories in three dimensions,” [arXiv:1108.4081 \[hep-th\]](#).
- [53] S. Cheon, D. Gang, C. Hwang, S. Nagaoka, and J. Park, “Duality between $N=5$ and $N=6$ Chern-Simons matter theory,” *JHEP* **11** (2012) 009, [arXiv:1208.6085 \[hep-th\]](#).
- [54] M. Evtikhiev, “Studying superconformal symmetry enhancement through indices,” *JHEP* **04** (2018) 120, [arXiv:1708.08307 \[hep-th\]](#).
- [55] D. Gang and M. Yamazaki, “Three-dimensional gauge theories with supersymmetry enhancement,” *Phys. Rev. D* **98** no. 12, (2018) 121701, [arXiv:1806.07714 \[hep-th\]](#).
- [56] I. Garozzo, G. Lo Monaco, N. Mekareeya, and M. Sacchi, “Supersymmetric Indices of 3d S -fold SCFTs,” *JHEP* **08** (2019) 008, [arXiv:1905.07183 \[hep-th\]](#).
- [57] E. Beratto, N. Mekareeya, and M. Sacchi, “Marginal operators and supersymmetry enhancement in 3d S -fold SCFTs,” *JHEP* **12** (2020) 017, [arXiv:2009.10123 \[hep-th\]](#).
- [58] E. Beratto, N. Mekareeya, and M. Sacchi, “Zero-form and one-form symmetries of the ABJ and related theories,” *JHEP* **04** (2022) 126, [arXiv:2112.09531 \[hep-th\]](#).
- [59] D. Gang, S. Kim, K. Lee, M. Shim, and M. Yamazaki, “Non-unitary TQFTs from 3D $\mathcal{N} = 4$ rank 0 SCFTs,” *JHEP* **08** (2021) 158, [arXiv:2103.09283 \[hep-th\]](#).
- [60] D. L. Jafferis and X. Yin, “Chern-Simons-Matter Theory and Mirror Symmetry,” [arXiv:0810.1243 \[hep-th\]](#).
- [61] A. Kapustin and M. J. Strassler, “On mirror symmetry in three-dimensional Abelian gauge theories,” *JHEP* **04** (1999) 021, [arXiv:hep-th/9902033 \[hep-th\]](#).
- [62] D. Gaiotto and E. Witten, “S-Duality of Boundary Conditions In $N=4$ Super Yang-Mills Theory,” *Adv. Theor. Math. Phys.* **13** no. 3, (2009) 721–896, [arXiv:0807.3720 \[hep-th\]](#).
- [63] D. R. Gulotta, C. P. Herzog, and S. S. Pufu, “From Necklace Quivers to the F-theorem, Operator Counting, and $T(U(N))$,” *JHEP* **12** (2011) 077, [arXiv:1105.2817 \[hep-th\]](#).
- [64] B. Assel, “Hanany-Witten effect and $SL(2, \mathbb{Z})$ dualities in matrix models,” *JHEP* **10** (2014) 117, [arXiv:1406.5194 \[hep-th\]](#).
- [65] I. Garozzo, N. Mekareeya, M. Sacchi, and G. Zafrir, “Symmetry enhancement and duality walls in 5d gauge theories,” *JHEP* **06** (2020) 159, [arXiv:2003.07373 \[hep-th\]](#).
- [66] C. Hwang, S. Pasquetti, and M. Sacchi, “Flips, dualities and symmetry enhancements,” *JHEP* **05** (2021) 094, [arXiv:2010.10446 \[hep-th\]](#).
- [67] C. Hwang, S. S. Razamat, E. Sabag, and M. Sacchi, “Rank Q E-string on spheres with flux,” *SciPost Phys.* **11** no. 2, (2021) 044, [arXiv:2103.09149 \[hep-th\]](#).
- [68] D. Gaiotto and H.-C. Kim, “Duality walls and defects in 5d $\mathcal{N} = 1$ theories,” *JHEP* **01** (2017) 019, [arXiv:1506.03871 \[hep-th\]](#).
- [69] H.-C. Kim, S. S. Razamat, C. Vafa, and G. Zafrir, “E-String Theory on Riemann Surfaces,” *Fortsch. Phys.* **66** no. 1, (2018) 1700074, [arXiv:1709.02496 \[hep-th\]](#).
- [70] H.-C. Kim, S. S. Razamat, C. Vafa, and G. Zafrir, “D-type Conformal Matter and SU/USp Quivers,” *JHEP* **06** (2018) 058, [arXiv:1802.00620 \[hep-th\]](#).
- [71] H.-C. Kim, S. S. Razamat, C. Vafa, and G. Zafrir, “Compactifications of ADE conformal matter on a torus,” *JHEP* **09** (2018) 110, [arXiv:1806.07620 \[hep-th\]](#).

- [72] S. S. Razamat, E. Sabag, O. Sela, and G. Zafrir, “Aspects of 4d supersymmetric dynamics and geometry,” [arXiv:2203.06880 \[hep-th\]](#).
- [73] E. Sabag and M. Sacchi, “A 5d perspective on the compactifications of 6d SCFTs to 4d $\mathcal{N} = 1$ SCFTs,” [arXiv:2208.03331 \[hep-th\]](#).
- [74] A. Dey, “Three dimensional mirror symmetry beyond ADE quivers and Argyres-Douglas theories,” *JHEP* **07** (2021) 199, [arXiv:2004.09738 \[hep-th\]](#).
- [75] A. Dey, “Higgs Branches of Argyres-Douglas theories as Quiver Varieties,” [arXiv:2109.07493 \[hep-th\]](#).
- [76] S. Giacomelli, C. Hwang, F. Marino, S. Pasquetti, and M. Sacchi, “to appear,”.
- [77] D. Nanopoulos and D. Xie, “More Three Dimensional Mirror Pairs,” *JHEP* **05** (2011) 071, [arXiv:1011.1911 \[hep-th\]](#).
- [78] H.-C. Kim, J. Kim, S. Kim, and K. Lee, “Vortices and 3 dimensional dualities,” [arXiv:1204.3895 \[hep-th\]](#).
- [79] I. Yaakov, “Redeeming Bad Theories,” *JHEP* **11** (2013) 189, [arXiv:1303.2769 \[hep-th\]](#).
- [80] D. Bashkirov, “Relations between supersymmetric structures in UV and IR for $\mathcal{N} = 4$ bad theories,” *JHEP* **07** (2013) 121, [arXiv:1304.3952 \[hep-th\]](#).
- [81] C. Hwang and J. Park, “Factorization of the 3d superconformal index with an adjoint matter,” *JHEP* **11** (2015) 028, [arXiv:1506.03951 \[hep-th\]](#).
- [82] C. Hwang, P. Yi, and Y. Yoshida, “Fundamental Vortices, Wall-Crossing, and Particle-Vortex Duality,” *JHEP* **05** (2017) 099, [arXiv:1703.00213 \[hep-th\]](#).
- [83] B. Assel and S. Cremonesi, “The Infrared Physics of Bad Theories,” *SciPost Phys.* **3** no. 3, (2017) 024, [arXiv:1707.03403 \[hep-th\]](#).
- [84] A. Dey and P. Koroteev, “Good IR Duals of Bad Quiver Theories,” *JHEP* **05** (2018) 114, [arXiv:1712.06068 \[hep-th\]](#).
- [85] B. Assel and S. Cremonesi, “The Infrared Fixed Points of 3d $\mathcal{N} = 4$ $USp(2N)$ SQCD Theories,” *SciPost Phys.* **5** no. 2, (2018) 015, [arXiv:1802.04285 \[hep-th\]](#).
- [86] S. S. Razamat and B. Willett, “Down the rabbit hole with theories of class \mathcal{S} ,” *JHEP* **10** (2014) 099, [arXiv:1403.6107 \[hep-th\]](#).
- [87] C. Closset, S. Giacomelli, S. Schafer-Nameki, and Y.-N. Wang, “5d and 4d SCFTs: Canonical Singularities, Trinions and S-Dualities,” *JHEP* **05** (2021) 274, [arXiv:2012.12827 \[hep-th\]](#).
- [88] F. Carta, S. Giacomelli, N. Mekareeya, and A. Mininno, “Dynamical consequences of 1-form symmetries and the exceptional Argyres-Douglas theories,” *JHEP* **06** (2022) 059, [arXiv:2203.16550 \[hep-th\]](#).
- [89] M. J. Kang, C. Lawrie, K.-H. Lee, M. Sacchi, and J. Song, “Higgs branch, Coulomb branch, and Hall-Littlewood index,” *Phys. Rev. D* **106** no. 10, (2022) 106021, [arXiv:2207.05764 \[hep-th\]](#).
- [90] M. Akhond, F. Carta, S. Dwivedi, H. Hayashi, S.-S. Kim, and F. Yagi, “Exploring the orthosymplectic zoo,” *JHEP* **05** (2022) 054, [arXiv:2203.01951 \[hep-th\]](#).
- [91] E. M. Rains, “Multivariate Quadratic Transformations and the Interpolation Kernel,” *SIGMA* **14** (2018) 019, [arXiv:1408.0305 \[math.CA\]](#).

- [92] N. Seiberg, “Exact results on the space of vacua of four-dimensional SUSY gauge theories,” *Phys. Rev. D* **49** (1994) 6857–6863, [arXiv:hep-th/9402044](#).
- [93] V. P. Spiridonov and G. S. Vartanov, “Vanishing superconformal indices and the chiral symmetry breaking,” *JHEP* **06** (2014) 062, [arXiv:1402.2312 \[hep-th\]](#).
- [94] S. Benvenuti, R. Comi, and S. Pasquetti, “work in progress,”.
- [95] D. Gaiotto, L. Rastelli, and S. S. Razamat, “Bootstrapping the superconformal index with surface defects,” *JHEP* **01** (2013) 022, [arXiv:1207.3577 \[hep-th\]](#).
- [96] F. Aprile, S. Pasquetti, and Y. Zenkevich, “Flipping the head of $T[SU(N)]$: mirror symmetry, spectral duality and monopoles,” *JHEP* **04** (2019) 138, [arXiv:1812.08142 \[hep-th\]](#).
- [97] A. Kapustin, B. Willett, and I. Yaakov, “Exact Results for Wilson Loops in Superconformal Chern-Simons Theories with Matter,” *JHEP* **03** (2010) 089, [arXiv:0909.4559 \[hep-th\]](#).
- [98] D. L. Jafferis, “The Exact Superconformal R-Symmetry Extremizes Z,” *JHEP* **05** (2012) 159, [arXiv:1012.3210 \[hep-th\]](#).
- [99] N. Hama, K. Hosomichi, and S. Lee, “Notes on SUSY Gauge Theories on Three-Sphere,” *JHEP* **03** (2011) 127, [arXiv:1012.3512 \[hep-th\]](#).
- [100] N. Hama, K. Hosomichi, and S. Lee, “SUSY Gauge Theories on Squashed Three-Spheres,” *JHEP* **05** (2011) 014, [arXiv:1102.4716 \[hep-th\]](#).
- [101] D. Tong, “Dynamics of $N=2$ supersymmetric Chern-Simons theories,” *JHEP* **07** (2000) 019, [arXiv:hep-th/0005186](#).
- [102] S. Benvenuti and S. Pasquetti, “3D-partition functions on the sphere: exact evaluation and mirror symmetry,” *JHEP* **05** (2012) 099, [arXiv:1105.2551 \[hep-th\]](#).
- [103] T. Nishioka, Y. Tachikawa, and M. Yamazaki, “3d Partition Function as Overlap of Wavefunctions,” *JHEP* **08** (2011) 003, [arXiv:1105.4390 \[hep-th\]](#).
- [104] A. Giveon and D. Kutasov, “Seiberg Duality in Chern-Simons Theory,” *Nucl. Phys. B* **812** (2009) 1–11, [arXiv:0808.0360 \[hep-th\]](#).
- [105] A. Kapustin, B. Willett, and I. Yaakov, “Tests of Seiberg-like dualities in three dimensions,” *JHEP* **08** (2020) 114, [arXiv:1012.4021 \[hep-th\]](#).
- [106] F. Benini, C. Closset, and S. Cremonesi, “Comments on 3d Seiberg-like dualities,” *JHEP* **10** (2011) 075, [arXiv:1108.5373 \[hep-th\]](#).
- [107] C. Closset, T. T. Dumitrescu, G. Festuccia, Z. Komargodski, and N. Seiberg, “Contact Terms, Unitarity, and F-Maximization in Three-Dimensional Superconformal Theories,” *JHEP* **10** (2012) 053, [arXiv:1205.4142 \[hep-th\]](#).
- [108] C. Closset, T. T. Dumitrescu, G. Festuccia, Z. Komargodski, and N. Seiberg, “Comments on Chern-Simons Contact Terms in Three Dimensions,” *JHEP* **09** (2012) 091, [arXiv:1206.5218 \[hep-th\]](#).